

## Functional properties of the oxygen evolving complex of photosystem II

**Promotor:**

dr. T.J. Schaafsma, hoogleraar in de moleculaire fysica.

**Co-promotor:**

dr. A.W. Rutherford, directeur de recherche CNRS, Gif-sur-Yvette.

1102701, 2062

P.H. van Vliet

# **Functional properties of the oxygen evolving complex of photosystem II**

**Proefschrift**

ter verkrijging van de graad van doctor  
in de landbouw- en milieuwetenschappen,  
op gezag van de rector magnificus,  
dr. C.M. Karssen,  
in het openbaar te verdedigen  
op maandag 15 april 1996  
des namiddags te vier uur in de Aula  
van de Landbouwuniversiteit te Wageningen.

ISBN 925137

Voor Leontine

BIBLIOTHEEK  
LANDBOUWUNIVERSITEIT  
WAGENINGEN

CIP-DATA KONINKLIJKE BIBLIOTHEEK, DEN HAAG

Vliet, P.H. van

Functional properties of the oxygen evolving complex of  
photosystem II / P.H. van Vliet. - [S.l. : s.n.], - III.

Thesis Landbouwwuniversiteit Wageningen. - With ref. -

With summary in Dutch.

ISBN 90-5485-532-0

Subject headings: photosynthesis / oxygen evolution.

## Stellingen

- 1 It can not be excluded that some of the changes in the  $S_2$  minus  $S_1$  FTIR spectrum observed by Noguchi *et al.* in Photosystem II after  $Ca^{2+}$  depletion by low pH treatment in the presence of citrate, originate from binding of citrate to PS-II (Noguchi, T., Ono, T. & Inoue, Y. (1995) *Biochim. Biophys. Acta* 1228, 189-200).
- 2 The conclusion by Kusunoki that the EPR signal from the  $S_3$  state in  $Ca^{2+}$ -depleted PS-II originates from a peroxide radical is not sufficiently supported by experimental data (Kusunoki, M. (1995) *Chem. Phys. Letters* 239, 148-157).
- 3 In view of the report by Deligiannakis *et al.*, it is most straightforward to consider the acceptor component "D<sub>480</sub>" in Photosystem II described by Stemler and Jursinic as the non-heme iron to which formate is bound (Deligiannakis, Y., Petrouleas, V. & Diner, B. A. (1994) *Biochim. Biophys. Acta* 1188, 260-270; Stemler, A. & Jursinic, P. A. (1993) *Biochim. Biophys. Acta* 1183, 269-280).
- 4 In contrast to what is generally thought, the  $F^-$  anion can functionally occupy the  $Cl^-$ -site in Photosystem II essential for oxygen evolving activity (*this Thesis*, Chapter 4).
- 5 The electron microscopy study of two-dimensional crystals of Photosystem II by Ford *et al.* does not sufficiently rule out the possibility that the region in Tris-washed Photosystem II which is assigned to a micro-cavity, is unstained protein (Ford, R. C., Rosenberg, M. F., Shepherd, F. H., McPhie, P. & Holzenburg, A. (1995) *Micron* 26, 133-140).
- 6 The observation by Lindberg *et al.* of a residual oxygen evolving activity in Photosystem II after release of all exchangeable  $Cl^-$  following long incubation in a  $Cl^-$ -free buffer-solution at pH 6.3, is consistent with their earlier report which indicated the presence of a fraction of centers containing  $Cl^-$  which is not exchangeable under these conditions (Lindberg, K., Wydrzynski, T., Vänngård, T., & Andréasson, L-E. (1990) *FEBS Lett.* 264, 153-155; Lindberg, K., Vänngård, T., & Andréasson, L-E. (1993) *Photosynth. Res.* 38, 401-408).
- 7 The assumption by Roberts and Lindahl that a significant fraction of the purified nickel-iron hydrogenase contains a nickel ion which is EPR silent under all conditions and does not change its oxidation state upon lowering of the redoxpotential, implies that this fraction exhibits no hydrogenase activity (Roberts, L. M., & Lindahl, P. A. (1994) *Biochemistry* 33, 14339-14350).
- 8 Measurements of the light-intensity dependent 820 nm absorbance changes in leaves may yield information on electron donor events to the reaction center of Photosystem I *in vivo*.
- 9 Extensive publicity given to possible negative climatic effects caused by earth atmospheric pollution, will continue until all terrestrial oil sources have been exhausted.

## Preface

I would like to thank all the people who directly or indirectly contributed to this Thesis. It was a great pleasure to work in the group of Bill Rutherford. Bill's support and enthusiasm were enormous. The discussions that we had of experiments, editorial aspects and about many other subjects, I enjoyed very much.

Tjeerd Schaafsma gave a great deal of support by constructive discussions and very useful advice on editorial aspects. The visits to the Department of Molecular Physics I enjoyed very much and I experienced them as a confirmation of the fruitful link between Saclay and Wageningen.

Paul Mathis gave me the important support that I required to work in the Section de Bioénergétique in Saclay and he always showed his interest in my work.

Significant contributions to this Thesis came also from Alain Boussac, Sun Un and Andreas Seidler. The many discussions with them were quite useful.

Although I spent most of my time in Saclay in complete darkness, working there was big fun at least in part due to the music parties at Bill's place and the playing biljart after work now and then with (among others) Klaus Brettel, Andreas Seidler and Winfried Leibl. I never figured out, though, how Andreas was able on certain evenings to, besides playing very well, systematically leave me the most unfavourable ball positions imaginable.

Significant support I received from Jacintha who decided to join me and to work in France. Family and friends showed continuous interest in us and visited us frequently in France. From Marry and Dick van Vliet, and Miep and Ton Verdu we received significant and special support in many different ways. This included designing the image on the cover of this Thesis by Ton Verdu.

# Contents

	page
<b>Abbreviations</b>	1
<b>1</b> Introduction	2
<b>2</b> Overview and rationale of methods and techniques used.	11
<b>3</b> Chloride-depletion effects in the Calcium-deficient Oxygen Evolving Complex of Photosystem II (Van Vliet, P., Boussac, A., & Rutherford A.W. (1994) <i>Biochemistry</i> 33, 12998-13004).	16
<b>4</b> Properties of the Chloride-Depleted Oxygen Evolving Complex of Photosystem II studied by EPR (Van Vliet, P. & Rutherford A.W. (1996) <i>Biochemistry</i> , in press).	32
<b>5</b> Properties of the Iodide-Reconstituted Oxygen Evolving Complex of Photosystem II studied by EPR (Van Vliet, P., Homann, P.H. & Rutherford A. W., in preparation).	58
<b>6</b> On the magnetic properties Oxygen Evolving Complex of Photosystem II studied by EPR (Van Vliet, P. & Rutherford A.W. (1996), in preparation).	71
<b>7</b> On the magnetic properties of the Chloride-Depleted Oxygen Evolving Complex of Photosystem II studied by EPR (Van Vliet, P., Un, S. & Rutherford A.W. (1996), in preparation).	85
<b>Summary</b>	95
<b>Samenvatting</b>	98

## Abbreviations

ATP	adenosine triphosphate
CW	continuous wave
EPR	electron paramagnetic resonance
Mn	manganese
NADP	nicotinamide adenine dinucleotide phosphate
P	primary electron donor
P <sub>680</sub>	primary electron donor of photosystem II
P <sub>700</sub>	primary electron donor of photosystem I
PPBQ	phenyl-p-benzoquinone
PS	photosystem
Q <sub>A</sub> , Q <sub>B</sub>	primary and secondary quinone electron acceptors of photosystem II
S <sub>0</sub> ..S <sub>4</sub>	redox states of the donor side of photosystem II
Tyr <sub>D</sub>	side-path electron donor of photosystem II
Tyr <sub>Z</sub>	secondary electron donor of photosystem II



## Chapter 1

### Introduction

The membrane spanning protein complexes Photosystem I (PS-I) and Photosystem II (PS-II) in the photosynthetic membrane of green plants and cyanobacteria, use light as an energy source to drive a chain of redox reactions mediating electron transfer from water to NADP<sup>+</sup>.

PS-I and PS-II function as follows; their light-harvesting components (the antenna) contain chlorophyll molecules that absorb incident light. After light absorption, the excitation energy is rapidly transferred between the antenna chlorophylls. After excitation of special chlorophylls in the reaction center, closely connected to the antenna, a primary radical pair is formed denoted P<sup>+</sup>I<sup>-</sup>, where P is the primary electron donor and I is the primary electron acceptor. The primary charge separation is followed by electron transfer steps that further separate the charges across the membrane. The components in PS-I and PS-II, essential for this electron transfer, are depicted in Figure 1. Electron transfer events occurring in PS-II are reviewed in Refs. 1-4 and those occurring in PS-I are reviewed in Refs. 5 and 6. Detailed information on photosynthetic electron transport in green plants and cyanobacteria can be found in [7]. Photosynthetic systems also are found in purple bacteria, green sulphur bacteria and heliobacteria. These are reviewed in Refs. 8 and 9.

Figure 1 shows a schematic view on photosynthetic electron transport in green plants and cyanobacteria. The oxygen evolving complex (OEC) of PS-II catalyzes the oxidation of water, resulting in the formation of molecular oxygen as a by-product and the release of protons into an enclosed compartment, called the lumen. At the stromal side of the photosynthetic membrane, PS-II reduces bound plastoquinone (Q<sub>B</sub>) to plastoquinol (PQH<sub>2</sub>) accompanied by proton uptake. PQH<sub>2</sub> then dissociates from its site and is replaced by an other plastoquinone (PQ) molecule from the PQ-pool. At the luminal side of the membrane, PQH<sub>2</sub> is re-oxidized by the Rieske-cytochrome b/f complex (reviewed in Ref. 10) accompanied by additional release of protons into the lumen. A water soluble copper protein, plastocyanin (PC), shuttles the electrons from cytochrome f to the photo-oxidized primary electron donor (P<sub>700</sub>) in PS-I. The electron on the photo-reduced primary electron acceptor chlorophyll (A<sub>0</sub>)

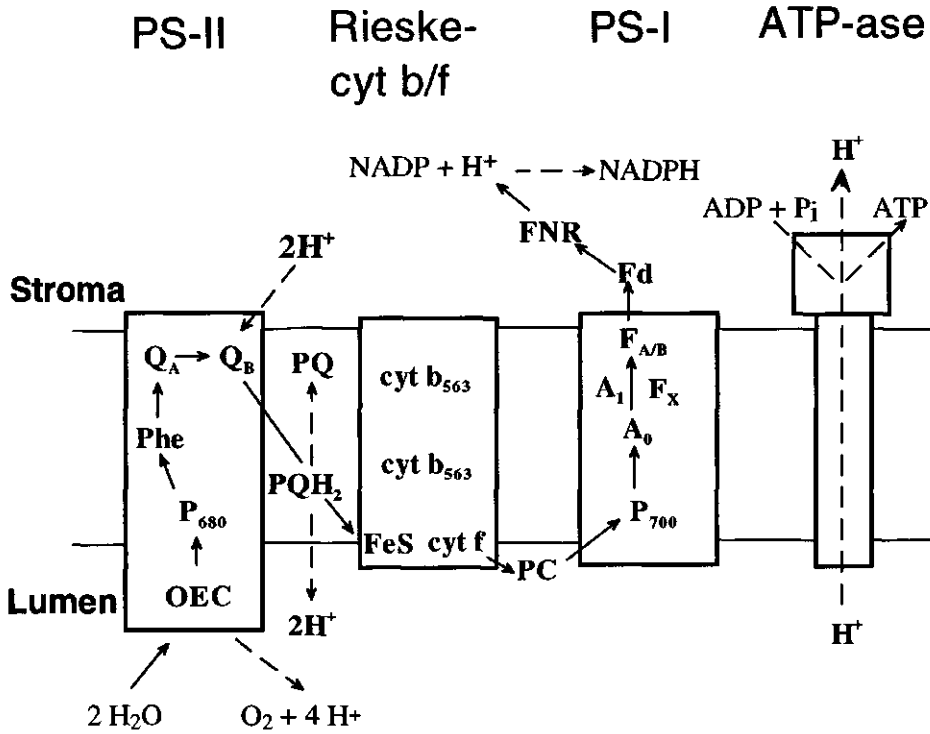


Figure 1. Schematic representation of photosynthetic electron transport in green plants and cyanobacteria. OEC, oxygen evolving complex; P<sub>680</sub>, primary electron donor; Phe, pheophytin primary electron acceptor; Q<sub>A</sub>, Q<sub>B</sub>, primary and secondary quinone electron acceptors; PQ, plastoquinone pool; PQH<sub>2</sub>, plastoquinol; FeS, Rieske-iron; cyt f, cytochrome f; PC, plastocyanin; P<sub>700</sub>, primary electron donor; A<sub>0</sub>, chlrophyll primary electron acceptor; A<sub>1</sub>, phylloquinone; F<sub>A/B</sub>, F<sub>X</sub>, iron sulphur clusters; Fd, ferredoxin; FNR, ferredoxin-NADP<sup>+</sup>-reductase. Electron transfer steps are marked by continuous arrows. Cyclic electron transport via PS-I and cytochrome b/f occurring under certain conditions is not indicated in the scheme.

in PS-I, is transferred to iron-sulphur centers (F<sub>A/B</sub>) present at the stromal side of PS-I. In this electron transfer, one of the two phylloquinones (A<sub>1</sub>) and an iron-sulphur center (F<sub>X</sub>) present between A<sub>0</sub> and F<sub>A/B</sub>, are thought to be important (discussed in Refs. 5 and 11). The iron cluster F<sub>A</sub> or F<sub>B</sub> reduces water-soluble ferredoxin (Fd) which then donates electrons to ferredoxin-NADP<sup>+</sup>-reductase (FNR), the enzyme that reduces NADP<sup>+</sup> to NADPH.

The spatial separation of the electrochemical reactions described above, results in the acidification of the lumen. The proton motive force and the transmembrane electric potential drive the membrane spanning ATP-ase in the photosynthetic membrane to phosphorylate ADP

to ATP. The resulting energy carriers ATP and NADPH are used in the Calvin cycle for CO<sub>2</sub> fixation which takes place in the chloroplast stroma.

Figure 2 shows a structural cartoon of PS-II which is designed on the basis of the many similarities between the reaction center of PS-II and that of purple bacteria, the crystal structure of which has been resolved [12]. For reviews on structural and functional aspects of PS-II see [2,3,13-15]. The PS-II reaction center is composed of a heterodimer of membrane spanning proteins, denoted D<sub>1</sub> and D<sub>2</sub>, that exhibit significant sequence homologies with the L and M subunits in the bacterial reaction center. The heterodimer contains the primary electron donor chlorophyll, P<sub>680</sub>, the primary

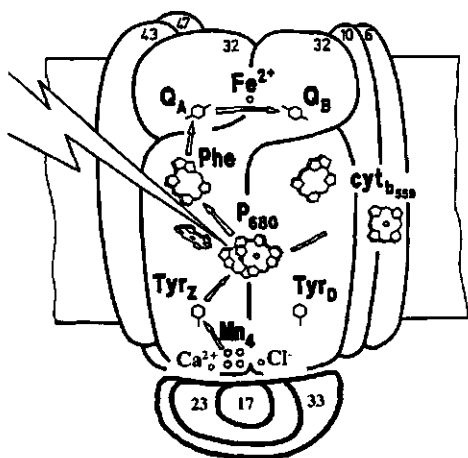


Figure 2. A cartoon of PS-II. Abbreviations are explained in the caption of Figure 1 or in the text.

electron acceptor, pheophytin a, two quinone acceptors, Q<sub>A</sub> and Q<sub>B</sub>, as well as a non-heme iron. All of these components have analogy to those in the bacterial reaction center. The primary electron donor in the bacterial reaction center corresponds to a dimer of bacterial chlorophyll. The identity of that in PS-II, however, is not yet clear (reviewed in Refs. 15 and 16).

The donor side of PS-II is quite different from that of other known photosystems and is unique in its ability to oxidize water which requires the building up of a high degree of oxidizing power ( $E_m \geq 0.815$  V). For a discussion of the thermodynamics of intermediate steps that could be involved in water oxidation, see Refs. 17 and 18.

Catalysis of water oxidation occurs in a charge accumulating enzyme cycle consisting of five intermediate oxidation states designated S<sub>0</sub> to S<sub>4</sub>, where the subscript is the number of oxidizing equivalents stored [19]. This cycle is depicted in Figure 3. S<sub>4</sub> is considered a

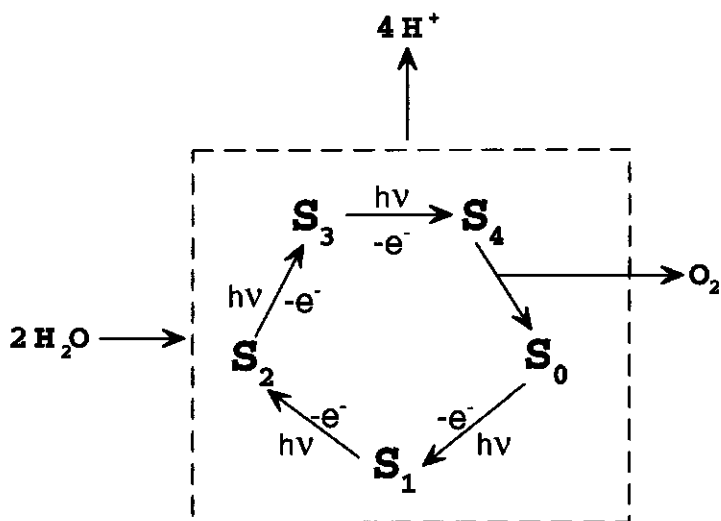


Figure 3. A scheme of the enzyme cycle of water oxidation (see text).

transient state that spontaneously converts to  $S_0$ , accompanied by the release of molecular oxygen.  $S_0$  and  $S_1$  are stable in the dark. Under normal conditions, dark-adapted PS-II is mainly present in the  $S_1$  state. The light-generated  $S_2$  and  $S_3$  states are unstable and decay in darkness to  $S_1$ . The  $S_3$  state decays via  $S_2$  to  $S_1$ . The kinetic properties of the charge accumulation states under different experimental conditions have been characterized in detail (reviewed in Refs. 3 and 20). It has been suggested that water does not bind to the catalytic site before formation of the  $S_4$  oxidation state (reviewed in Ref. 20). However, from recent  $H_2^{16}O/H_2^{18}O$  exchange experiments, using mass spectrometry with a relatively high time resolution, a relatively slowly exchanging substrate water molecule was observed in the  $S_3$  state, suggesting that water may functionally bind in the  $S_3$  state [21,22]. Proton release from the oxygen evolving complex into the bulk can occur at each S-state transition. The stoichiometry of proton release induced by the S-state transitions depends on the type of PS-II material (membranes or cores) and in membranes is also dependent on the pH. For a review on proton release during charge accumulation see Ref. 23.

The oxidizing equivalents enter into the charge storage device via a redox active tyrosine residue of the  $D_1$  subunit,  $Tyr_Z$ , which is the direct electron donor to  $P_{680}^+$ . A tyrosine residue of  $D_2$ ,  $Tyr_D$ , is also redox active. However,  $Tyr_D^+$ , which is stable, does not

change its oxidation state during enzyme turnover and is thought not to participate in steady-state electron transfer from water to P<sub>680</sub><sup>+</sup>.

A cluster of probably four manganese ions, present at the luminal side of PS-II, plays a central role in the charge accumulation cycle (reviewed in Refs. 3 and 20). In addition to the Mn cluster, the ions Ca<sup>2+</sup> and Cl<sup>-</sup> are essential for oxygen evolving activity. On the basis of extended X-ray absorption fine structure (EXAFS) studies it has been suggested that Ca<sup>2+</sup> and Cl<sup>-</sup> may bind to the Mn cluster [24,25]. Several suggestions in the literature on the role(s) of these ions, are summarized in Refs. 3 and 20. Three extrinsic polypeptides of 33, 23 and 17 kDa, present at the luminal side of PS-II contribute to the stability of the oxygen evolving enzyme but are not essential for oxygen evolving activity (reviewed in Ref. 26). The 33 kDa polypeptide stabilizes the Mn cluster. The 17- and 23 kDa polypeptides play a role in retention of functional Ca<sup>2+</sup> and Cl<sup>-</sup> [26,27].

There is no consensus on the location of the Mn cluster relative to the reaction center of PS-II. Nevertheless, the idea that the Mn cluster is asymmetrically positioned in PS-II being significantly closer to Tyr<sub>Z</sub> than to Tyr<sub>D</sub> seems to be favoured (reviewed in e.g. Ref. 28 and see also Ref. 29) (however see Ref. 30). With respect to the structure of the Mn cluster, a model has been proposed based on EXAFS studies. This model consists of a pair of di- $\mu$ -oxo-bridged Mn dimers linked by a mono- $\mu$ -oxo bridge and carboxylate ligands [24,31]. The arrangement of the two dimers relative to each other is, however, uncertain [24,31].

Many studies on the charge accumulation properties of the oxygen evolving complex have been done using CW EPR spectroscopy (for reviews see Refs. 3, 20 and 32). In untreated PS-II, the EPR spectrum of the S<sub>2</sub> state is dominated by a characteristic multiline EPR signal at  $g = 2$  [33]. This signal is attributed to a ground state spin  $S = 1/2$  probably arising from a mixed valence tetrameric Mn cluster (see Ref. 34 and references therein). The S<sub>2</sub> multiline signal appeared to be modified following the removal of Ca<sup>2+</sup> from PS-II [35] (see also Ref. 36). Although this modification was shown to be induced by the chelator present during Ca<sup>2+</sup>-depletion treatments, the origin of the chelator-induced modification of S<sub>2</sub> remained uncertain (see introduction Chapter 3; reviewed in Ref. 37).

In Chapter 3 of this Thesis, experimental evidence is presented indicating that the modification of S<sub>2</sub> originates from chelator-binding to PS-II occurring when Ca<sup>2+</sup> is absent and that the chelator-binding affinity is lowered by Cl<sup>-</sup> depletion [38]. These and further Cl<sup>-</sup>-

depletion effects in  $\text{Ca}^{2+}$ -deficient PS-II described in this study, are discussed in relation to possible role(s) of  $\text{Ca}^{2+}$  and  $\text{Cl}^-$  in the mechanism of water oxidation.

Depending on the conditions, the  $S_2$  state also exhibits an EPR signal around  $g = 4$  [reviewed in Refs. 3 and 20]. The  $S_2$   $g = 4$  and  $S_2$  multiline EPR signals probably originate from two different structural states of the oxygen evolving complex with different magnetic properties of the Mn cluster [39-42]. The spin state responsible for the  $S_2$   $g = 4$  signal may yield significant information on the topology of the Mn cluster [43]. However, the  $S_2$   $g = 4$  signal is less well characterized than the  $S_2$  multiline signal and may arise either from a spin  $S = 3/2$  or  $S = 5/2$  ground or excited state of the mixed valence Mn cluster (see e.g. Refs. 44 and 45). One important problem in the study on the magnetic origin of the  $S_2$   $g = 4$  signal is that the relationship between the appearance of the  $S_2$   $g = 4$  EPR signal from the Mn cluster and the functional and biochemical properties of the oxygen evolving complex is poorly understood (discussed in Ref. 20).

In Chapter 4 of this Thesis, this problem is tackled by the study of the functional and EPR spectroscopic properties of  $\text{Cl}^-$ -depleted PS-II under a range of well defined experimental conditions. The results from this study indicate that besides a  $\text{Cl}^-$ -site essential for oxygen evolution, equivalent to that studied in previous work, a second  $\text{Cl}^-$ -site is present in PS-II which is not essential for oxygen evolution. In addition,  $\text{SO}_4^{2-}$  and  $\text{F}^-$ , which are often used to displace the  $\text{Cl}^-$  essential for oxygen evolution, appear to have specific effects on the properties of PS-II. These include the striking observation that addition of  $\text{F}^-$  to  $\text{Cl}^-$ -depleted PS-II results in reconstitution of oxygen evolution in a significant fraction (~50%) of centers in which, however, the enzyme turnover is slowed down.

It has been previously shown that the halide  $\text{I}^-$  also reconstitutes oxygen evolving activity [46,47]. Chapter 5 of this Thesis presents an EPR study of  $\text{I}^-$ -activated PS-II.

In untreated PS-II, no signals from states other than the  $S_2$  state have been detected by conventional CW-EPR. Nevertheless, since the Mn cluster is thought to be the dominant paramagnetic relaxation center of  $\text{Tyr}_D^\bullet$ , Mn redox chemistry during S-state transitions has been studied by a range of different EPR techniques using  $\text{Tyr}_D^\bullet$  as a magnetic probe (see Refs. 48-51). Investigations on the relaxation properties of  $\text{Tyr}_D^\bullet$  using CW EPR and pulsed EPR, in samples of well-defined S-state composition using flash-illumination, indicated that the  $\text{Tyr}_D^\bullet$  in  $S_1$  was significantly slower relaxing than in the other S-states (see Refs. 49 and

50). Those studies suggested that the Mn cluster is paramagnetic in  $S_2$ ,  $S_3$  and  $S_0$  and diamagnetic in  $S_1$ . This also was indicated from a study on the flash-dependent magnetic susceptibility in PS-II [52].

Koulouglotis *et al.* [53] observed by pulsed EPR that the  $\text{Tyr}_D^\bullet$  spin-lattice relaxation rate ( $T_1^{-1}$ ) decreased during dark-incubation with a half-time of  $t_{1/2} \approx 3.5$  h. These authors interpreted their results as indicating that the  $S_1$  state slowly converts in darkness from a paramagnetic to a diamagnetic form and related these forms to the so-called "active" and "resting" states, respectively, of the enzyme as proposed earlier [54].

In Chapter 6 of this Thesis the microwave power saturation properties of  $\text{Tyr}_D^\bullet$  of the oxygen evolving complex are studied by CW EPR. This study is focussed on the interconversion between the two forms of  $S_1$  and their influence on the other S-states. The results indicate the presence of a fast-relaxing  $S_1\text{Tyr}_D^\bullet$  which converts in the dark to a slow relaxing  $S_1\text{Tyr}_D^\bullet$  upon long dark-adaptation, in agreement with the work of Koulouglotis *et al.* [53]. This conversion is accelerated by addition of PPBQ (1 mM), presumably originating from the reduced form of PPBQ. Flash-experiments show that the event responsible for the conversion of the slow relaxing to the fast relaxing form of  $S_1$  occurs in the first enzyme cycle at the  $S_3$  to  $S_0$  or the  $S_0$  to  $S_1$  transition. The fast- and slow-relaxing forms of  $S_1$  may correspond to a paramagnetic and diamagnetic  $S_1$  state reflecting structurally different Mn clusters, as was previously proposed [53]. Alternatively, in view of the results from this work, it may be considered that the Mn cluster in  $S_1$  is diamagnetic and that the fast-relaxing  $\text{Tyr}_D^\bullet$  in  $S_1$  is due to a nearby paramagnetic species different from the Mn cluster.

Until now, the influence of the state giving rise to the  $S_2$   $g = 4$  on the microwave power saturation properties of  $\text{Tyr}_D^\bullet$  has not been addressed. Chapter 7 of this Thesis describes the microwave power saturation of  $\text{Tyr}_D^\bullet$  in Cl<sup>-</sup>-depleted PS-II which exhibits an intense  $S_2$   $g = 4$  signal, as described in Chapter 4 [55]. It is shown that the spin state of the Mn cluster giving rise to an  $S_2$   $g = 4$  signal enhances the relaxation of  $\text{Tyr}_D^\bullet$ . However, on the basis of a mathematical model describing the dipolar interaction between two paramagnets, the spins contributing to the  $S_2$   $g = 4$  signal are expected to be magnetically decoupled from  $\text{Tyr}_D^\bullet$  due to the mismatch between the  $g$ -values of the two spin systems. The results are discussed in relation to the possible spin state responsible for the  $S_2$   $g = 4$  signal.

## References

- 1 Babcock, G. T., Barry, B. A., Debus, R. J., Hoganson, C. W., Atamian, M., McIntosh, L., Sithole, I., & Yocum, C. F. (1989) *Biochemistry* 28, 9557-9565.
- 2 Andersson, B. & Styring, S. (1991) In *Current Topics in Bioenergetics* (Lee, C. P., ed.) Vol. 16, pp 2-81, Academic Press Inc., San Diego, California.
- 3 Debus, R. J. (1992) *Biochim. Biophys. Acta* 1102, 269-352.
- 4 Rutherford, A. W. (1989) *Trends Biochem. Sci.* 16, 227-232.
- 5 Golbeck, J. H. (1992) *Ann. Rev. Plant Physiol. Mol. Biol.* 43, 293-324.
- 6 Golbeck, J. H., & Bryant, D. A. (1991) in *Current Topics in Bioenergetics* (Lee, C. P., ed.) Vol. 16, pp 83-177, Academic Press Inc., San Diego, California.
- 7 Lee, C. P., (ed.) *Current Topics in Bioenergetics* (1991), Academic Press Inc., San Diego, California.
- 8 Deisenhofer, J., & Norris, J. R., (eds.) *The Photosynthetic Reaction center*, Vol.1, Vol. 2, (1993), Academic Press, inc., San Diego, California.
- 9 Blankenship, R. E., Madigan, M. T., & Bauer, C. E., (eds.) *Anoxygenic Photosynthetic Bacteria*, (1995), Kluwer Dordrecht, The Netherlands.
- 10 Bendall, D. S. (1982) *Biochim. Biophys. Acta* 683, 119-151.
- 11 Evans, M. C. W. & Nugent, J. H. A. (1993) in *The Photosynthetic Reaction center* (Deisenhofer, J., & Norris, J. R., eds.), Vol. 2, pp 391-415, Academic Press, inc., San Diego, California.
- 12 Deisenhofer, J., Epp, O., Miki, K., Huber, R., & Michel, H. (1985) *Nature* 318, 618-624.
- 13 Barber, J. (ed.) *The Photosystems: Structure, Function and Molecular Biology* (1992), Elsevier Science Publishers, New York.
- 14 Vermaas, W. F. J., Styring, S., Schröder, W. P., & Andersson, B. (1993) *Photosynth. Res.* 38, 249-263.
- 15 Van Mieghem, F. J. E. (1994) *Ph. D. Thesis*, Agricultural University of Wageningen, The Netherlands.
- 16 Van Gorkom H. J., & Schelvis, J. P. M. (1993) *Photosynth. Res.* 38, 297-301.
- 17 Krishtalik, L. I. (1986) *Biochim. Biophys. Acta* 849, 162-171.
- 18 Krishtalik, L. I. (1990) *Bioelectrochem. and Bioenerg.* 23, 249-263.
- 19 Kok, B., Forbush, B., & McGloin, M. (1970) *Photochem. Photobiol.* 11, 457-475.
- 20 Rutherford, A. W., Zimmermann, J-L., & Boussac, A. (1992) in *The Photosystems: Structure, Function and Molecular Biology* (Barber, J., ed.) Chapter 5, pp 179-229, Elsevier Science Publishers, New York.
- 21 Messinger, J., Badger, M., & Wydrzynski, T. (1995) *Proc. Natl. Acad. Sci.* 92, 3209-3213.
- 22 Bader, K. P., Renger, G., & Schmidt, G. H. (1993) *Photosynth. Res.* 38, 355-361.
- 23 Lavergne, J., & Junge, W. (1993) *Photosynth. Res.* 38, 279-296.
- 24 Yachandra, V. K., DeRose, V. J., Latimer, M. J., Mukerji, I., Sauer, K., & Klein, M. P. (1993) *Science* 260, 675-679.
- 25 Latimer, M. J., DeRose, V. J., Mukerji, I., Yachandra, V. K., Sauer, K., & Klein, M. P. (1995) *Biochemistry* 34, 10898-10909.
- 26 Murata, N., & Miyao, M. (1985) *Trends Biochem. Sci.* 10, 122-124.
- 27 Homann, P. H. (1988) *Photosynth. Res.* 15, 205-220.



- 28 Hoganson, C. W., & Babcock, G. T. (1994) in *Metal Ions in Biological Systems* (Sigel, H., & Sigel, A., eds.), Vol. 30, pp 66-100, Marcel Dekker Inc., New York, Basel, Hongkong.
- 29 Gilchrist, M. L., Ball, Jr. A., Randall, D. W. & Britt, R. D. (1995) *Proc. Natl. Acad. Sci.* (in press).
- 30 Un, S., Brunel, L-C, Brill, T. M., Zimmermann, J-L., & Rutherford, A. W. (1994) *Proc. Natl. Acad. Sci.* 91, 5262-5266.
- 31 Sauer, K., Yachandra, V. K., Britt, R. D., & Klein, M. P. (1992) in *Manganese Redox Enzymes* (Pecoraro, V. L., ed.), pp 141-175, VCH, New York.
- 32 Rutherford, A. W., Zimmermann, J-L., & Boussac, A. (1991) *New J. Chem.* 15, 491-500.
- 33 Dismukes, G. C., & Siderer, Y. (1981) *Proc. Natl. Acad. Sci.* 78, 274-278.
- 34 Britt, R. D., Lorigan, G. A., Sauer, K., Klein, M. P. & Zimmermann, J-L. (1992) *Biochim. Biophys. Acta* 1040, 95-101.
- 35 Boussac, A., Zimmermann, J-L., & Rutherford, A. W. (1989) *Biochemistry* 28, 8984-8989.
- 36 Sivaraja, M., Tso, J., & Dismukes, G. C. (1989) *Biochemistry* 28, 9459-9464.
- 37 Boussac, A., & Rutherford, A. W. (1994) *Biochem. Soc. Trans.* 22, 352-358.
- 38 Van Vliet, P., Boussac, A., & Rutherford A.W. (1994) *Biochemistry* 33, 12998-13004.
- 39 dePaula, J. C., Innes, J. B., & Brudvig, G. W. (1985) *Biochemistry* 24, 8114-8120.
- 40 Zimmermann, J-L., & Rutherford A. W. (1986) *Biochemistry* 25, 4609-46154
- 41 Hansson, Ö., Aasa, R., & Vänngård, T. (1987) *Biophys. J.* 51, 825-832.
- 42 Kim, D. H., Britt, R. D., Klein, M. P., & Sauer, K. (1992) *Biochemistry* 31, 541-547.
- 43 Philouze, C., Blondin, G., Girerd, J-J., Guilhem, J., Pascard, C., & Lexa, D. (1994) *J. Am. Chem. Soc.* 116, 8557-8565.
- 44 Astashkin, A. V., Kodera, Y., & Kawamori, A. (1994) *J. Magn. Res. B* 105, 113-119.
- 45 Smith, P. J., Åhring, K. A. & Pace, R. J. (1993) *J. Chem. Soc. Faraday Trans.* 89, 2863-2868.
- 46 Rashid, A., & Homann, P. H. (1992) *Biochim. Biophys. Acta* 1101, 303-310.
- 47 Homann, P. H. (1993) *Photosynth. Res.* 38, 395-400.
- 48 De Groot, A., Plijter, J. J., Evelo, R., Babcock, G. T. & Hoff, A. J. (1986) *Biochim. Biophys. Acta* 848, 8-15.
- 49 Styring, S., & Rutherford, A. W. (1988) *Biochemistry* 27, 4915-4923.
- 50 Evelo, R. G., Styring, S., Rutherford, A. W., & Hoff, A. J. (1989) *Biochim. Biophys. Acta* 973, 428-442.
- 51 Kodera, Y., Takura, K., & Kawamori, A. (1992) *Biochim. Biophys. Acta* 1101, 23-32.
- 52 Sivaraja, M., Philo, J. S., Lary, J., & Dismukes, G. C. (1989) *J. Am. Chem. Soc.* 111, 3221-3225.
- 53 Koulouglotis, D., Hirsh, D. J., & Brudvig, G. W., (1992) *J. Am. Chem. Soc.* 114, 8322-8323.
- 54 Beck, W. F., dePaula, J. C., & Brudvig, G. W. (1985) *Biochemistry* 24, 3035-3043.
- 55 Van Vliet, P., & Rutherford, A. W. (1995) *Biochemistry* (in press).

## Chapter 2

### Overview and rationale of methods and techniques used

#### *Biochemical methods*

PS-II enriched membranes were isolated (from spinach) according to the method of Berthold *et al.* [1] with the modifications of Ford and Evans [2]. The principle of the isolation procedure is based on the chloroplast membrane organization consisting of stroma-exposed membrane regions and stacked membrane regions (grana) which contain most PS-II. The key factors in the isolation of the PS-II containing grana partition regions are (1) The presence of  $Mg^{2+}$  (5 mM) during breaking of the chloroplast envelope which presumably conserves the chloroplast membrane organization and (2) Treatment of broken chloroplasts (in the presence of  $Mg^{2+}$ ) with the detergent Triton X-100 which presumably solubilizes the stroma-exposed membrane regions while the grana partition regions remain essentially unaffected.

Depletion of the ions  $Ca^{2+}$  or  $Cl^-$  in PS-II essential for oxygen evolution, included treatments that affect the association of the 17- and 23 kDa extrinsic polypeptides. These polypeptides play a role in retention of functional  $Ca^{2+}$  and  $Cl^-$  (reviewed in Refs. 3 and 4). The following treatments were used.

- (1) Unless stated otherwise,  $Ca^{2+}$  was depleted (Chapter 3) using the method described by Boussac *et al.* [5]. This method includes incubation of PS-II membranes in the presence of 1.2 M NaCl, resulting in the dissociation of the 17- and 23 kDa extrinsic polypeptides, and in the presence of the chelator EGTA (5 mM) to trap free  $Ca^{2+}$  in the buffer solution. The incubation was done under room light since functional  $Ca^{2+}$  in PS-II is released most easily in  $S_3$  [6,7].
- (2)  $Cl^-$  was depleted in salt-washed/ $Ca^{2+}$ -depleted PS-II (Chapter 3) by washing (resuspension, dilution and centrifugation) in  $Cl^-$ -free buffer solutions (pH 6.5). The rationale behind this treatment was that the 17- and 23 kDa polypeptides, which are important for retaining  $Cl^-$  in its site [4], are removed by the salt-treatment. Therefore,  $Cl^-$  depletion in salt-washed PS-II is considered to occur

simply by subsequent washes in Cl<sup>-</sup>-free solutions. The Cl<sup>-</sup> depletion is done in the presence of EGTA ( $\geq 50 \mu\text{M}$ ) to avoid inadvertent Ca<sup>2+</sup> contamination.

- (3) Depletion of Cl<sup>-</sup> in PS-II, while Ca<sup>2+</sup> remains present, was done in two steps (Chapters 4, 5 and 7). Firstly, untreated PS-II membranes were washed in Cl<sup>-</sup>-free buffer solutions (pH 6.3-6.5). This pretreatment is generally done to minimize Cl<sup>-</sup> contamination during subsequent Cl<sup>-</sup>-depletion treatments. Secondly, following the Cl<sup>-</sup>-free washes, the PS-II membranes were treated at high pH (pH 10) for a short period (~30 s) according to the method of Homann [8,9]. This high pH-treatment presumably results in a more labile binding or dissociation of the 17- and 23 kDa extrinsic polypeptides resulting in the release of Cl<sup>-</sup> from the site essential for oxygen evolution. Subsequent lowering of the pH is then thought to result in the rebinding of the extrinsic polypeptides to PS-II. Protein analysis of pH 10/Cl<sup>-</sup>-depleted PS-II by SDS-gel electrophoresis and subsequent Western blotting gel electrophoresis confirmed that the extrinsic polypeptides were associated to nearly all the centers after Cl<sup>-</sup>-depletion (Chapter 4).
- (4) Unless stated otherwise, replacement of the Cl<sup>-</sup> essential for oxygen evolution by other anions was done as follows [9]: Firstly, Cl<sup>-</sup> was depleted in PS-II as described above, i.e. by Cl<sup>-</sup>-free washes and subsequent pH 10/Cl<sup>-</sup>-depletion. Secondly, anions (as their sodium salt) were added following pH 10/Cl<sup>-</sup>-depletion at pH 7.3 which is suboptimal for oxygen evolution and then the pH was lowered to pH 6.3. The idea behind this treatment is that at pH 7.3, inadvertent irreversible inhibition of oxygen evolution is minimized and yet access to the Cl<sup>-</sup>-site essential for oxygen evolution is increased due to relatively labile association at this pH of the 17- and 23 kDa extrinsic polypeptides to PS-II which are thought to shield the essential Cl<sup>-</sup>-site [9,10].

#### *Measurements of oxygen evolution*

Oxygen evolving activity was systematically measured in Ca<sup>2+</sup>/Cl<sup>-</sup>-depleted PS-II before and after Ca<sup>2+</sup>/Cl<sup>-</sup> reconstitution to monitor the degree of Ca<sup>2+</sup>/Cl<sup>-</sup> depletion and its reversibility. Ca<sup>2+</sup> and Cl<sup>-</sup> were reconstituted in PS-II either as described above

or by adding these ions to the  $\text{Ca}^{2+}/\text{Cl}^-$ -depleted PS-II membranes in the measuring cuvette prior to the measurement of oxygen evolution. In some experiments, the light-dependence of oxygen evolution was measured to investigate enzyme kinetics (Chapter 4). These measurements yield information on the fraction of inhibited centers, the quantum yield of water oxidation and the enzyme turnover rate.

### *Illumination treatments*

The  $\text{S}_2$  state in concentrated EPR samples (2.5-15 mg chlorophyll/ml) of dark-adapted PS-II membranes, was generated by continuous illumination of the samples cooled to 200 K [11] (Chapters 3-7). This method allows the accumulation of  $\text{S}_2\text{Q}_\text{A}^-$  in essentially all the centers since at this temperature (1) only the  $\text{S}_1$  to  $\text{S}_2$  transition is allowed, (2)  $\text{S}_2\text{Q}_\text{A}^-$  is stable and (3) the electron transfer from  $\text{Q}_\text{A}$  to  $\text{Q}_\text{B}$  is blocked.

In EPR samples of PS-II depleted of  $\text{Ca}^{2+}$  and/or  $\text{Cl}^-$ , the  $\text{S}_3$  state was generated by continuous illumination at 0 °C in the presence of the electron acceptor PPBQ followed by rapid freezing (Chapters 3 and 4). The idea behind this method is that in these preparations the  $\text{S}_3$  to  $\text{S}_0$  transition is thought to be inhibited and that the  $\text{S}_3$  state under these conditions is relatively stable (on the minutes time scale) [12]. PPBQ was added to efficiently remove the electron from  $\text{Q}_\text{A}^-$  to prevent relatively rapid (seconds) recombination reactions of  $\text{Q}_\text{A}^-$  with the  $\text{S}_2$  or  $\text{S}_3$  oxidation states. For reviews on the kinetic properties of the charge accumulation states under different experimental conditions see Refs. 13 and 14.

Besides the use of continuous illumination treatments described above, the charge accumulation states in EPR samples of PS-II were selectively generated by flash-illumination at room temperature (Chapters 4-6). The EPR samples contained 2-3 mg chlorophyll/ml and were illuminated with green, single-turnover laser flashes (15 ns, 532 nm, 300 mJ), i.e. under conditions that the flashes were saturating and yet a relatively good signal to noise was obtained. The extent to which the flashes were saturating was probed by the flash-induced  $\text{S}_2$  multiline signal intensity in untreated PS-II.

Under normal conditions, dark-adapted PS-II centers are mostly present in  $S_1\text{Tyr}_D^\bullet$ . Nevertheless, some dark-adapted PS-II can be present in  $S_0\text{Tyr}_D^\bullet$  or  $S_1\text{Tyr}_D$  [15,16]. Where indicated, these centers were converted to  $S_1\text{Tyr}_D^\bullet$  resulting in  $S_1\text{Tyr}_D^\bullet$  in virtually all the centers, using a preflash treatment described in Refs. 16 and 17 by illumination of the dark-adapted samples with a single flash in the absence of PPBQ, followed by dark-adaptation for 10-15 min. at room temperature. After this preflash treatment PPBQ was added and the samples were further illuminated with a given number of flashes followed by rapid ( $\sim 1$  s) freezing in darkness.

In general, PPBQ is added at a concentration of  $\sim 1$  mM. However, during some experiments described in the Chapters 4 and 6, secondary effects of PPBQ were observed presumably induced by a fraction of reduced PPBQ ( $\text{PPBQH}_2$ ). To avoid these effects, relatively low concentrations of PPBQ were added ( $50\text{-}100 \mu\text{M}$ ) to samples that had ferricyanide ( $50\text{-}100 \mu\text{M}$ ) present to maintain PPBQ in the oxidized form.

### *Measuring techniques*

For continuous illumination of the EPR samples in a non-silvered dewar flask containing ethanol cooled to 198 K with solid  $\text{CO}_2$  or cooled to  $0^\circ\text{C}$  with liquid nitrogen, an 800 W projector was used and the light passing through 2 cm water and an infrared filter. Flash illumination at room temperature was provided from an Nd-Yag laser (15 ns, 300 mJ, 532 nm).

EPR spectra were recorded at liquid helium temperatures using a Bruker ER 200 or ER 300 X-band spectrometer equipped with an Oxford Instruments cryostat and temperature control system.

Oxygen evolution was measured using an oxygen sensitive Clark-type electrode, at  $25^\circ\text{C}$  under continuous light. Unless stated otherwise, the measurements were done under near saturating light at a chlorophyll concentration of  $20 \mu\text{g/ml}$  in the presence of  $0.5$  mM PPBQ as an external electron acceptor. The light intensity was varied using calibrated neutral grey (Balzers) filters. The Clark electrode was calibrated using an air-saturated buffer solution (containing  $\sim 266 \mu\text{M O}_2$ ) followed by

removal of molecular oxygen from the buffer solution either by subsequent addition of dithionite or by bubbling the solution with nitrogen gas. No differences between the two methods of molecular oxygen removal were observed. The detected changes of the molecular oxygen concentration in the cuvette were recorded on a mV recorder.

## References

- 1 Berthold, D. A., Babcock, G. T., & Yocum, C. F. (1981) *FEBS Lett.* 134, 231-234.
- 2 Ford, R. C., & Evans, M. C. W. (1983) *FEBS* 160, 159-164.
- 3 Murata, N., & Miyao, M. (1985) *Trends Biochem. Sci.* 10, 122-124.
- 4 Homann, P. H. (1988) *Photosynth. Res.* 15, 205-220.
- 5 Boussac, A., Zimmermann, J-L., & Rutherford, A. W. (1990) *FEBS* 277, 69-74.
- 6 Boussac, A., & Rutherford, A. W. (1988) *FEBS Lett.* 236, 432-436.
- 7 Ädelroth, P., Lindberg, K., & Andréasson, L-E (1995), 9021-9027.
- 8 Homann, P.H. (1985) *Biochim. Biophys. Acta* 809, 311-319.
- 9 Homann, P. H. (1993) *Photosynth. Res.* 38, 395-400.
- 10 Rashid, A., & Homann, P. H. (1992) *Biochim. Biophys. Acta* 1101, 303-310.
- 11 Brudvig, G. W., Casey, J. L., & Sauer, K. (1983) *Biochim. Biophys. Acta* 723, 366-371.
- 12 Boussac, A., Zimmermann, J-L., & Rutherford, A. W. (1989) *Biochemistry* 28, 8984-8989.
- 13 Debus, R. J. (1992) *Biochim. Biophys. Acta* 1102, 269-352.
- 14 Rutherford, A. W., Zimmermann, J-L., & Boussac, A. (1992) in *The Photosystems: Structure, Function and Molecular Biology* (Barber, J., ed.) Chapter 5, pp 179-229, Elsevier Science Publishers, New York.
- 15 Styring, S., & Rutherford, A. W. (1987) *Biochim. Biophys. Acta* 993, 378-387.
- 16 Vermaas, W. F. T., Renger, G., & Dohnt, G. (1984) *Biochim. Biophys. Acta* 764, 194-202.
- 17 Styring, S., & Rutherford, A. W. (1988) *Biochemistry* 27, 4915-4923.

## Chloride-depletion effects in the Calcium-deficient Oxygen Evolving Complex of Photosystem II

Pieter van Vliet<sup>\*</sup>, Alain Boussac and A. William Rutherford

*Section de Bioénergétique (URA CNRS 1290), Département de Biologie Cellulaire et Moléculaire, CEA Saclay, 91191 Gif-sur-Yvette, France, and Department of Molecular Physics, Agricultural University, Wageningen, The Netherlands.*

**Key Words:** photosynthesis, oxygen evolution, charge accumulation states, Cl<sup>-</sup>, electron paramagnetic resonance.

The effects of Cl<sup>-</sup> depletion in Photosystem II (PS-II)-enriched membranes have been investigated by electron paramagnetic resonance (EPR) spectroscopy after removal of the 17- and 23 kDa polypeptides and depletion of Ca<sup>2+</sup> by NaCl treatment. When the salt-treatment was done in the presence of a high concentration (5 mM) of the chelator ethylene glycol bis ( $\beta$ -aminoethyl ether)-N,N,N',N'-tetraacetic acid (EGTA), a modified multiline signal stable in the dark was observed from the S<sub>2</sub> state and a 13 mT wide S<sub>3</sub> signal could be generated by illumination at 0°C as reported previously under these conditions [Boussac, A., Zimmermann, J-L., & Rutherford, A. W. (1990) *FEBS Lett.* 277, 69-74]. The modified S<sub>2</sub> multiline signal was lost after a further Cl<sup>-</sup> depletion in the presence of a low EGTA concentration (50  $\mu$ M). Upon Cl<sup>-</sup> reconstitution, a normal S<sub>2</sub> multiline signal could be generated by continuous illumination at 200 K. In contrast, a lowering of the EGTA concentration (50  $\mu$ M) alone, in the presence of Cl<sup>-</sup> (30 mM), had no effect on the modified S<sub>2</sub> multiline signal. These results indicate that the modification of S<sub>2</sub> is due to binding of the chelator to PS-II and that Cl<sup>-</sup> stabilizes the chelator binding. When Cl<sup>-</sup> depletion in Ca<sup>2+</sup>-depleted PS-II was done in the

---

<sup>\*</sup>To whom correspondence should be addressed. CEA Saclay. Telephone: 33-1-6908 2940. Fax: 33-1-6908 8717.

presence of a high concentration of EGTA (5 mM), the modified  $S_2$  multiline signal disappeared but was regenerated by  $Cl^-$  reconstitution in darkness. These results indicate that when  $Cl^-$  depletion is done to the EGTA-modified PS-II, the  $S_2$  multiline signal disappears but the  $S_2$  state remains stable in the dark. Thus, EGTA binding and  $Cl^-$  depletion appear to be additive phenomena.  $Cl^-$  depletion also modified the  $S_3$  EPR signal showing a narrow signal ( $<10$  mT) around  $g = 2$ . This modification of the  $S_3$  signal was reversed by  $Cl^-$  reconstitution resulting in the re-appearance of the 13 mT wide  $S_3$  signal. The modifications of  $S_2$  and  $S_3$  due to  $Cl^-$  depletion observed in  $Ca^{2+}$ -depleted membranes are similar to those observed following  $Cl^-$  depletion in regular PS-II membranes, in which functional  $Ca^{2+}$  is thought to be present. These results, therefore, indicate that the modifications of the  $S_2$  and  $S_3$  EPR signals due to  $Cl^-$  depletion are independent of  $Ca^{2+}$ . Investigations of PS-II membranes which were salt-treated without EGTA revealed that the chemical 4-(*N*-morpholino)ethanesulphonic acid (MES), generally used as a pH buffer, was able to modify the  $S_2$  state, in a similar fashion to EGTA. In consideration of the components that are known to modify  $S_2$  [EGTA, (ethylenedinitrilo)tetraacetic acid (EDTA), citrate, pyrophosphate and MES], the results indicate that the modification of  $S_2$  is due binding of these components by their anionic groups containing oxygen, nearby or to the Mn cluster itself. The observed effects of  $Ca^{2+}$  and  $Cl^-$  depletion in PS-II may be relevant to the proposed role(s) of  $Ca^{2+}$  and  $Cl^-$  in controlling substrate binding in the functional charge accumulation cycle.

## Introduction

Photosynthetic water-photolysis is catalyzed by the photosystem II protein complex (PS-II)<sup>1</sup> and is thought to occur upon accumulation of four positive charges in a cycle, consisting of five intermediate states designated  $S_0$  to  $S_4$ , where the subscript is the number of charges stored [1]. The kinetic properties of the charge accumulation states under different experimental conditions have been characterized in detail (reviewed in Refs. 2 and 3). A

---

<sup>1</sup> Abbreviations: PS-II, the photosystem II protein complex; Tyr<sub>D</sub>, side-path electron donor of PS-II responsible for EPR signal  $\Pi_{slow}$ ; Q<sub>A</sub>, primary quinone electron acceptor of PS-II; CW, continuous wave; EPR, electron paramagnetic resonance; ESEEM, electron spin echo envelope modulation; EDTA, (ethylenedinitrilo) tetraacetic acid; EGTA, ethylene glycol bis ( $\beta$ -aminoethyl ether)-*N,N,N',N'*-tetraacetic acid; MES, 4-(*N*-morpholino) ethanesulphonic acid; PPBQ, phenyl-*p*-benzoquinone.



manganese cluster, which is thought to consist of four manganese ions, plays a central role in the charge accumulation cycle. Also  $\text{Ca}^{2+}$  and  $\text{Cl}^-$  are essential in the mechanism of water oxidation (for reviews see Refs. 2 and 3). Three extrinsic proteins of 33, 23 and 17 kDa, present at the luminal side of PS-II, contribute to the stability of the oxygen evolving enzyme but are not essential for oxygen evolution (reviewed in Ref. 4). The 33 kDa polypeptide stabilizes the manganese cluster. The 17 and 23 kDa extrinsic polypeptides play a role in retention of functional  $\text{Ca}^{2+}$  and  $\text{Cl}^-$  [4,5].

In the study on the role(s) of  $\text{Ca}^{2+}$  and  $\text{Cl}^-$  in the mechanism of water oxidation, a number of methods have been developed to deplete these ions, inducing reversible inhibition of oxygen evolution and keeping the manganese cluster in its site [2,5,6].

Several studies, using different techniques, have indicated that  $\text{Cl}^-$  depletion leads to inhibition of the  $\text{S}_3$  to  $\text{S}_0$  transition (reviewed in Ref. 3). Depletion of  $\text{Ca}^{2+}$  involves dissociation of the 17- and 23 kDa proteins by washing PS-II membranes in NaCl [7] or treatment at low pH [8]. In salt-washed PS-II,  $\text{Ca}^{2+}$  is released most easily in  $\text{S}_3$  [9] and for this reason  $\text{Ca}^{2+}$  release is greatly enhanced when the treatments are done in the light [9-13]. Following  $\text{Ca}^{2+}$  depletion in PS-II, the  $\text{S}_3$  to  $\text{S}_0$  transition in the charge accumulation cycle is inhibited [11,13]. Under physiological conditions, light-dependent  $\text{Ca}^{2+}$  release from the donor-side of PS-II may be involved in regulation of the balance between photosynthetic electron transport and dark reactions [14].

Many studies on the charge accumulation cycle have been done using EPR spectroscopy. In untreated PS-II membranes, a multiline EPR signal at  $g = 2$  is observed in the  $\text{S}_2$  state [15]. This signal can be generated by illumination treatments allowing for a single stable charge separation, e.g. single flash illumination at room temperature, or continuous illumination at 200 K [15-17]. Under some conditions, the  $\text{S}_2$  state exhibits also an EPR signal at  $g = 4.1$  (reviewed in Ref. 3). Following inhibition of oxygen evolution by treatment with  $\text{SO}_4^{2-}$  at pH 7.5, no  $\text{S}_2$  multiline EPR signal was detected after a single flash or illumination at 200 K and little [18] or no [19]  $g = 4.1$  EPR signal appeared. However, the multiline EPR signal was restored by addition of  $\text{Cl}^-$  in the dark, following the illumination [18] (see also Refs. 19 and 20). From these observations it was concluded that  $\text{Cl}^-$  depletion results in a modification of the  $\text{S}_2$  state, resulting in the loss of its characteristic EPR signal, and which is reversed to the normal  $\text{S}_2$  state by  $\text{Cl}^-$  reconstitution [18,20].

In functional PS-II, no signals from states other than the  $S_2$  state have been detected by conventional CW-EPR. However, in  $Ca^{2+}$ -depleted PS-II, an EPR signal around  $g = 2$  was observed corresponding to the formal  $S_3$  state with a peak-to-trough width of 16.4 mT when the 17 and 23 kDa extrinsic polypeptides were reconstituted [21] or a 13 mT wide EPR signal in the absence of these polypeptides [22]. Upon generation of this signal from  $S_2$ , the multiline EPR signal was completely suppressed. Boussac *et al.* [23] proposed that upon formation of  $S_3$  from  $S_2$ , the oxidation state of the manganese cluster remains unchanged and that a nearby amino acid is oxidized instead. In this model, the organic radical formed with  $S = 1/2$ , interacts with the  $S = 1/2$  manganese cluster [23]. The radical species was proposed to be an oxidized histidine on the basis of its absorption spectrum in the ultraviolet [23], although alternative explanations were not excluded (discussed in Ref. 24). Besides  $Ca^{2+}$ -depleted PS-II,  $S_3$  signals were also observed following inhibition of oxygen evolution by treatments with  $F^-$  [25],  $SO_4^{2-}$  [19],  $NH_3$  [26, 27] or acetate [28].

In  $Ca^{2+}$ -depleted PS-II following a salt-wash with millimolar amounts of the chelators EGTA [21] or EDTA [29] a dark-stable  $S_2$  modified multiline EPR signal was observed, indicating a perturbation of the manganese cluster due to the treatment. This modification was eliminated by reconstitution of  $Ca^{2+}$  [21]. A modified multiline EPR signal was also observed following a low pH treatment in the presence of citrate [30]. It was shown that the modification of  $S_2$  was induced by millimolar concentrations of the chelator and required light [22]. The chelator-induced modification was discussed as being due to either additional removal of  $Ca^{2+}$  by the chelator or direct binding of the chelator to the manganese cluster [22]. The second possibility was favoured.

Subsequently, ESEEM spectra were obtained from the modified  $S_2$  state [31]. An ESEEM frequency, probably arising from  $^{14}N$ , was present in  $^{15}N$  labeled PS-II. This frequency was proposed to arise from the coupling between the manganese cluster and the  $^{14}N$  nucleus from EGTA. This was supported by the observation that this frequency was absent when pyrophosphate was used to induce the modification of  $S_2$ . These data were taken as further support for the idea that direct binding of the chelator to PS-II is responsible for the modification of  $S_2$ .

Nevertheless, despite these indications, the modification of the multiline EPR signal is frequently considered to be due to  $Ca^{2+}$  release. At least in part, this is due to the fact that the evidence and arguments for chelator binding to PS-II are far from conclusive. Thus, the

question whether the chelator-induced modification is due to  $\text{Ca}^{2+}$  removal or to binding of the chelator itself warrants further investigation.

This report deals with the effects of  $\text{Cl}^-$  depletion on the  $\text{S}_2$  and  $\text{S}_3$  state in  $\text{Ca}^{2+}$ -depleted PS-II membranes. It has been suggested that  $\text{Ca}^{2+}$  and  $\text{Cl}^-$  may play role(s) in controlling functional association of the substrate to the active site (reviewed in Ref. 3). Experimental evidence is presented indicating that chelator-binding to PS-II occurs when  $\text{Ca}^{2+}$  is absent. In addition,  $\text{Cl}^-$  influences the chelator-binding.

### Materials and methods

Photosystem II-enriched membranes were prepared according to the method of Berthold *et al.* [32] with the modifications of Ford and Evans [33] and were stored at  $-80^\circ\text{C}$  until use. The activity of these membranes was  $\approx 500 \mu\text{M O}_2/\text{mg}$  of chlorophyll/h.

Salt treatment of PS-II membranes was done as described by Boussac *et al.* [22] by incubation of PS-II membranes (0.5 mg chlorophyll/mL) for 30 minutes in 1.2 M NaCl, 0.3 M Sucrose and 25 mM MES (pH 6.5) under room light at  $5^\circ\text{C}$ . This was done either in the presence of EGTA (5 mM) or in the absence of EGTA (see below).

The salt-washed PS-II membranes were spun down, followed by a range of different washing procedures on ice under room light as described in the Results. Unless stated otherwise the solutions were buffered with 10 mM MES (pH 6.5).  $\text{Ca}^{2+}$ -free buffer solutions were prepared by putting them through a CHELEX-100 column.

$\text{Cl}^-$  depletion in salt-washed PS-II was done by three washes (resuspension, dilution and centrifugation) in  $\text{Cl}^-$ -free solutions at pH 6.5. The rationale behind this treatment was that the 17- and 23 kDa polypeptides, which are important for retaining  $\text{Cl}^-$  in its functional site [5], are absent following the salt-treatment and  $\text{Cl}^-$  depletion in this preparation is, therefore, considered to occur by additional washes in  $\text{Cl}^-$ -free solutions.

The membranes were resuspended at 8-12 mg chlorophyll/mL in the final solution used in the washing procedure described in the results and put in calibrated quartz EPR tubes, dark-adapted on ice for  $\approx 1$  h, frozen in the dark and stored in liquid nitrogen until use for EPR measurements. Further additions to these membranes were done in the EPR tube in the dark after thawing. Illumination of the samples was done in the presence of PPBQ dissolved in dimethyl sulphoxide, added as an external electron acceptor to a final concentration of 1 mM.

The samples were illuminated in a non-silvered Dewar flask containing ethanol cooled to 198 K with solid CO<sub>2</sub> or cooled to 0 °C with liquid nitrogen. After the illumination at 0 °C, the samples were rapidly frozen (<1 sec.) to 198 K and stored in liquid nitrogen. Illumination was done with a 800 W projector through 2 cm water and an infrared filter.

EPR spectra were recorded at liquid helium temperatures with a Bruker ER 200 D X-band spectrometer equipped with an Oxford Instruments cryostat.

Differences in signal intensity of the EPR spectra, due to variable chlorophyll concentrations in the EPR tubes, were eliminated by scaling relative to the amplitude of Tyr<sub>D</sub>• measured at an unsaturating microwave power (80 μW) at 20 K. No significant differences were observed in the amplitude of Tyr<sub>D</sub>• in these preparations before and after illumination procedures.

Salt-treated membranes not used for EPR measurements were stored in aliquots at -80 °C and were used afterwards for measurements of oxygen evolving activity. For these measurements, the membranes were thawed out and resuspended in 30 mM NaCl, 0.5 M sucrose and 25 mM MES (pH 6.5) to a chlorophyll concentration of ~2.5 mg/mL and stored on ice in darkness. The measurements were done in the buffer solution used for resuspension, using a Clark type electrode, at 20 °C under continuous saturating light. The chlorophyll concentration was 20 μg/ml and 0.5 mM PPBQ was added as an external electron acceptor.

The oxygen evolving activity of Ca<sup>2+</sup>-depleted PS-II membranes used in this study, was largely inhibited. The residual activity of the different preparations was lost relatively rapidly with a half inhibition time of 20 s during the measurement and showed an initial rate of about 30 % of that when 6 mM Ca<sup>2+</sup> was present during the measurement. In the presence of 6 mM Ca<sup>2+</sup> the loss of activity during the measurement was comparable to that of the intact starting material with a half inhibition time of 80 s and the initial rate was about 65 % of the control, indicating a fraction of damaged centers of about 35 % following washing and reconstitution treatments.

## Results

*Effects of Cl<sup>-</sup> Depletion in salt-washed/EGTA-Treated PS-II: The S<sub>2</sub> state.* The effects of depleting Cl<sup>-</sup> and lowering the EGTA concentration in Ca<sup>2+</sup>-depleted/EGTA-treated PS-II membranes were investigated. Figure 1a-d shows EPR spectra of dark-adapted PS-II

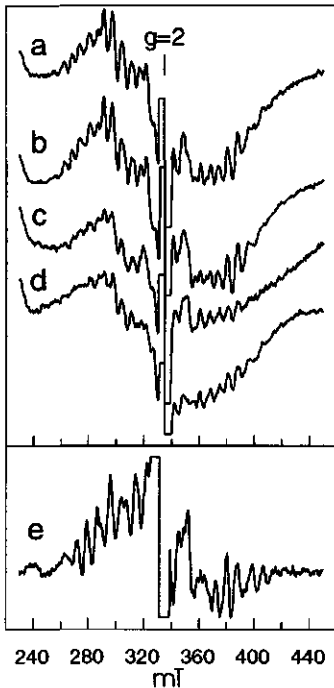


Figure 1. EPR spectra of dark-adapted, salt-washed/EGTA-treated PS-II membranes were washed once in (a) 30 mM  $\text{Cl}^-$  and 5 mM EGTA, or three times in (b) 30 mM  $\text{Cl}^-$  and 50  $\mu\text{M}$  EGTA, (c) 50  $\mu\text{M}$  EGTA, (d) 50  $\mu\text{M}$  EGTA followed by one wash in 30 mM  $\text{Cl}^-$  and 50  $\mu\text{M}$  EGTA. (e) Light minus dark spectrum of the sample from spectrum d after addition of PPBQ followed by illumination at 200 K. Instrument settings: 9.44 GHz; modulation amplitude 2.2 mT; temperature 10 K. Spectrum a-d were measured at a microwave power of 20 mW, and spectrum e, at 31 mW.

detected by EPR, as was observed following  $\text{Cl}^-$  depletion in functional PS-II [18,19]. Another possibility is that the  $\text{Cl}^-$ -depleted  $\text{S}_2$  state is not stable in the dark. To investigate the origin of the decrease in the multiline signal, the  $\text{Cl}^-$ -free washed PS-II membranes were reconstituted with 30 mM  $\text{Cl}^-$  in the presence of 50  $\mu\text{M}$  EGTA and dark-adapted. The  $\text{Cl}^-$ -reconstituted membranes showed the same residual amount of dark-stable modified multiline signal (Figure 1d) as the  $\text{Cl}^-$ -free washed membranes (Figure 1c). In addition, a normal multiline signal was formed after illumination at 200 K (Figure 1e). This indicates that most of the centers lost the

membranes which were salt-washed/EGTA-treated, followed by a range of different washing procedures as described below.

Following a wash in 5 mM EGTA and 30 mM  $\text{Cl}^-$ , a dark-stable  $\text{S}_2$  modified multiline signal was present (Figure 1a) as characterized by Boussac *et al.* [21]. Since the spectra in Figure 1a-d were recorded in dark-adapted samples, baseline signals (e.g., cyt b559, the Rieske center) underly the Mn multiline signal. In these membranes, no additional multiline signal could be generated by illumination at 200 K (not shown), indicating that most of the centers were modified after the treatment. Lowering the EGTA concentration to 50  $\mu\text{M}$  in these membranes in the presence of  $\text{Cl}^-$  (30 mM), did not affect the dark-stable modified multiline signal (Figure 1b). However, when the EGTA concentration was lowered in the absence of  $\text{Cl}^-$ , only a residual modified multiline signal was present (Figure 1c) with an intensity of about 15 % compared to that of the control (Figure 1a). It is possible that upon  $\text{Cl}^-$  depletion, the  $\text{S}_2$  state is not

chelator-induced modification during the Cl<sup>-</sup>-free washes at a low concentration of EGTA, and that the centers were in S<sub>1</sub> following Cl<sup>-</sup> reconstitution and dark adaptation. A small amount of S<sub>3</sub> signal was generated by the illumination at 200 K due to turnover from S<sub>2</sub> to S<sub>3</sub> in a small fraction of centers present in the dark-stable S<sub>2</sub> state as indicated by the residual modified multiline signal in the dark spectrum. The light-induced signal around 354 mT ( $g = 1.90$ ) corresponds to Q<sub>A</sub><sup>-</sup>-Fe<sup>2+</sup>.

As expected, a normal S<sub>2</sub> multiline signal similar to that in Figure 1e also was observed after Ca<sup>2+</sup> reconstitution, with 5 mM Ca<sup>2+</sup>, of salt-washed/EGTA-treated PS-II with 30 mM Cl<sup>-</sup> present (not shown). The possibility that the observed loss of the EGTA-induced modification of S<sub>2</sub> after Cl<sup>-</sup>-free washes followed by Cl<sup>-</sup> reconstitution (Figure 1e) was due to contamination with Ca<sup>2+</sup> can be ruled out for the following reasons. (1) There was very little variability from experiment to experiment in the extents of the effects of Cl<sup>-</sup> depletion on the EPR signals. (2) The presence of 50 μM EGTA during the experiment is far beyond the threshold for Ca<sup>2+</sup> contamination and residual amounts of contaminating Ca<sup>2+</sup> were, therefore, trapped by EGTA. (3) The membranes following the different treatments, including the Cl<sup>-</sup>-reconstituted membranes, described above, were equally inhibited in terms of oxygen evolution and showed the same extent of reconstituted oxygen evolving activity when 6 mM Ca<sup>2+</sup> was present. Thus, the observation that the EGTA-induced modification in the salt-washed/EGTA-treated membranes was reversed by Cl<sup>-</sup> depletion in the presence of a low concentration of EGTA (50 μM) in the absence of Ca<sup>2+</sup> (Figure 1) strongly indicates that the modification of S<sub>2</sub> is due to binding of the chelator to PS-II. This conclusion and further conclusions from this work (see below) are summarized in Figure 5.

In a further investigation of the relationship between the chelator-induced modification of S<sub>2</sub> and Cl<sup>-</sup> depletion, salt-washed/EGTA-treated PS-II membranes were washed in a Cl<sup>-</sup>-free solution in the presence of a high EGTA concentration (5 mM). Following this washing procedure, a small amount of dark-stable modified multiline signal was present (Figure 2a; thin line) with an intensity of approximately 15 % compared to that of a control sample washed in 5 mM EGTA and 30 mM Cl<sup>-</sup> (see e.g. Figure 1a). Addition of Cl<sup>-</sup> to this sample in complete darkness resulted in an increased intensity of the dark-stable modified multiline signal (Figure 2a; thick line). The intensity of the Cl<sup>-</sup>-induced multiline signal (Figure 2b) was about 50 % of that of the control (Figure 1a).

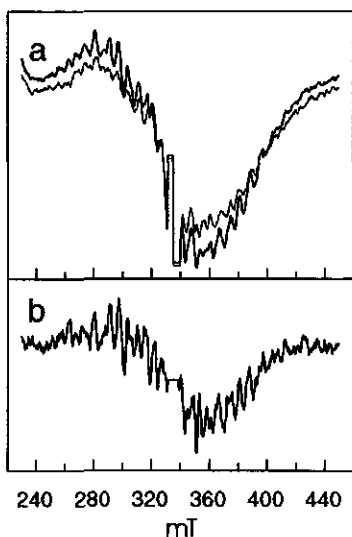


Figure 2. EPR spectra of salt-washed/EGTA-treated PS-II membranes, washed afterwards three times with 5 mM EGTA. (a) Dark spectra before (thin) and after (thick) addition of  $\text{Cl}^-$  (100 mM) in the dark, followed by 30 min incubation in darkness on ice. (b)  $\text{Cl}^-$ -induced spectrum from (a) (thick minus thin). The intensity of spectrum b was multiplied by 2 in comparison to spectrum a. Instrument settings as in Figure 1; microwave power 20 mW.

by rapid addition of  $\text{Cl}^-$  in darkness following dark-adaptation. The results were not very reproducible in that the addition of  $\text{Cl}^-$  resulted in the appearance of variable amounts of normal multiline signal (not shown). This problem probably originates from the decay of the normal  $\text{S}_2$  state that is formed during  $\text{Cl}^-$  addition and mixing. Nevertheless, these results indicate that the  $\text{S}_2$  state after  $\text{Cl}^-$  depletion in  $\text{Ca}^{2+}$ -depleted PS-II, does not exhibit a multiline signal and is probably more stable in the dark than the normal  $\text{S}_2$  state (Figure 5).

Figure 1 showed that the EGTA-induced modification in salt-washed/EGTA-treated PS-II, was reversed by lowering the chelator concentration in the absence of  $\text{Cl}^-$ . However, Figure 2 shows that this effect was largely overruled when the chelator concentration was kept at 5 mM. Nevertheless, the chelator-modified  $\text{S}_2$  which is stable in the dark, was not detected by EPR after  $\text{Cl}^-$  depletion, indicating that the  $\text{Cl}^-$  depletion treatment prevented the detection of the chelator-modification. Thus,  $\text{Cl}^-$  depletion modified the  $\text{S}_2$  state to a state which is not detected by EPR. Moreover, provided that the EGTA concentration was sufficiently high (5 mM), the EGTA and  $\text{Cl}^-$  depletion treatments that modify  $\text{S}_2$  in  $\text{Ca}^{2+}$ -depleted PS-II, were additive (see Figure 5).

The state that is present in salt-washed/EGTA-treated PS-II after  $\text{Cl}^-$  depletion in the presence of a low EGTA concentration (see Figure 1c), resulting in the loss of the EGTA-induced modification, was further investigated

*Effects of Cl<sup>-</sup> Depletion in Salt-washed/EGTA-Treated PS-II: The S<sub>3</sub> state.* Figure 3 shows light-induced EPR signals from salt-washed/EGTA-treated membranes following continuous illumination at 0 °C. In membranes washed in 30 mM Cl<sup>-</sup> and 5 mM EGTA a light-induced signal around g = 2 is observed

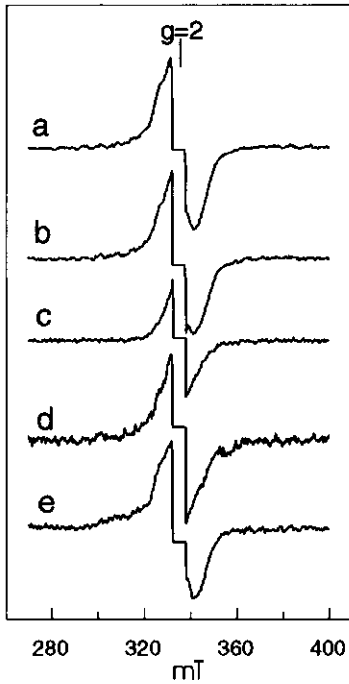


Figure 3. Light minus dark spectra of salt-washed/EGTA-treated PS-II membranes that were illuminated for 3 min at 0 °C in the presence of PPBQ and rapidly frozen afterwards. The membranes were washed once in (a) 30 mM Cl<sup>-</sup> and 5mM EGTA, or three times in (b) 30 mM Cl<sup>-</sup> and 50 μM EGTA, (c) 50 μM EGTA, (d) 5 mM EGTA, (e) 50 μM EGTA, followed by one wash in 30 mM Cl<sup>-</sup> and 50 μM EGTA. Instrument settings were as in Figure 1 except that the modulation amplitude was 0.22 mT and microwave power 2 mW. No (negative) contribution from the S<sub>2</sub> multiline signal intensity is present in the difference spectra.

with a peak-to-trough width of about 13 mT (Figure 3a). This signal is observed in Ca<sup>2+</sup>-depleted membranes lacking the extrinsic 17- and 23 kDa polypeptides and corresponds to the formal S<sub>3</sub> state [22]. Lowering the EGTA concentration to 50 μM in these membranes in the presence of Cl<sup>-</sup> (30 mM) did not affect the properties of the S<sub>3</sub> signal (Figure 3b). However, after washes without Cl<sup>-</sup> in 50 μM EGTA (Figure 3c) or 5 mM EGTA (Figure 3d), the light-induced S<sub>3</sub> signal was narrower (<10 mT) and unresolved due to the overlap with the stable tyrosine radical. The narrow S<sub>3</sub> signal is typically observed in untreated PS-II membranes following Cl<sup>-</sup> depletion [19,25]. Thus, Cl<sup>-</sup> depletion in Ca<sup>2+</sup>-depleted PS-II not only modifies the S<sub>2</sub> state (see above) but also modifies the S<sub>3</sub> state, resulting in a narrower S<sub>3</sub> signal (see Figure 5). This modification was completely reversed by Cl<sup>-</sup> reconstitution in 30 mM Cl<sup>-</sup> and 50 μM EGTA, resulting in the 13 mT wide S<sub>3</sub>-signal (Figure 3e).

*A MES-Induced S<sub>2</sub> Dark-Stable Modified Multiline signal.* It was shown above that chelator binding is responsible for the modification of the S<sub>2</sub> multiline



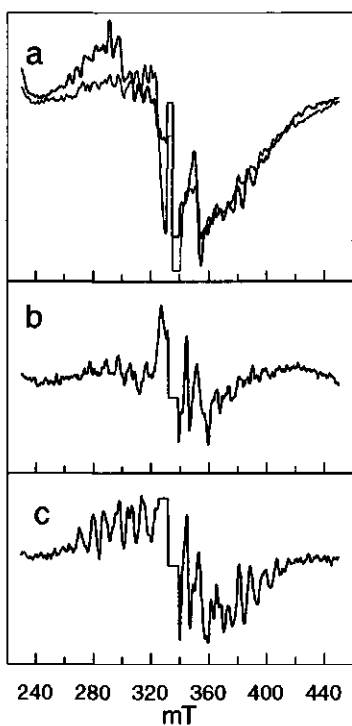


Figure 4. Dark spectra of salt-washed PS-II followed by three washes in  $\text{Ca}^{2+}$ -free solutions containing 30 mM  $\text{Cl}^-$  and (a) (thin) 5 mM MES (pH 6.5) or (thick) 500 mM MES (pH 6.5). Spectra b and c are light minus dark spectra of the samples from (a) containing 500 mM and 5 mM MES, respectively, after addition of PPBQ followed by illumination at 200 K. Instrument settings were as in Figure 2.

shown). Control samples in which 500 mM NaCl was added to salt-washed PS-II already containing 25 mM MES showed no additional modified multiline signal.

Note that this particular preparation is contaminated with the Rieske-iron sulphur center in the reduced form as indicated by the dark-stable signal around 350 mT ( $g = 1.9$ ) in Figure 4a. There is also contamination with PSI manifest as the light-induced signals at 346 mT ( $g$

signal in  $\text{Ca}^{2+}$ -depleted PS-II. Nevertheless, the salt-treatment without a chelator, followed by washes in  $\text{Ca}^{2+}$ -free buffer solutions resulted in a small amount of dark-stable modified multiline signal. Since the  $\text{Ca}^{2+}$ -free solutions contained only  $\text{Cl}^-$ , and MES as a pH buffer, we investigated the possibility that the modification was due to the presence of MES. This was done by washing the salt-treated membranes (without a chelator) in a  $\text{Ca}^{2+}$ -free solution containing 5, 25 or 500 mM of MES and 30 mM  $\text{Cl}^-$ .

Following washes in 500 mM MES, a dark-stable modified multiline signal was observed (Figure 4a; thick line) similar to that observed using a chelator (see above). In this sample only a small amount of normal multiline signal was formed after illumination at 200 K (Figure 4b), indicating that most of the centers were present in a dark-stable  $S_2$  state. In 5 mM MES, the modified multiline signal was nearly absent (Figure 4a; thin line) and a normal multiline signal was generated instead following 200 K illumination (Figure 4c), indicating that in 5 mM MES most of the centers were present in the  $S_1$  state. In 25 mM MES an intermediate amount of dark-stable modified multiline was present (not

-1.95) and 357 mT (g ~1.89) in Figure 4b, c corresponding to iron-sulphur centers which are electron acceptors in PSI and are stably photo-reduced after continuous illumination at 200 K.

The concentration of MES necessary for complete modification was much larger (hundreds of millimolar) than that of the chelators EGTA and EDTA (millimolar), indicating that the binding affinity of MES is much lower than that of the chelators.

## Discussion

The effects of the various  $\text{Cl}^-$  and  $\text{Ca}^{2+}$ -depletion and reconstitution treatments in PS-II relevant to this work are shown schematically in Figure 5.

In this study, experimental conditions were obtained which reversed the chelator modification in salt-washed/EGTA-treated PS-II, without  $\text{Ca}^{2+}$  reconstitution. Thus, it seems very unlikely that the modification of  $\text{S}_2$ , resulting in a dark-stable modified  $\text{S}_2$  multiline signal, is due to removal of  $\text{Ca}^{2+}$  and the results, therefore, indicate that the modification is due to binding of the chelator to PS-II. Chelator binding to PS-II occurs upon release of  $\text{Ca}^{2+}$  and, in addition, both events occur most easily in  $\text{S}_3$  [9,11,22]. Upon  $\text{Ca}^{2+}$  reconstitution, the modification of  $\text{S}_2$  is eliminated [21] and it is shown above that this is likely to be due to dissociation of the chelator from PS-II. From these observations it seems clear that the access of the chelators to PS-II is greatly enhanced in  $\text{S}_3$  when  $\text{Ca}^{2+}$  is released from the functional site. This may have some relevance to the role(s) of  $\text{Ca}^{2+}$  in functional oxygen evolving PS-II (discussed in Ref. 3). It has been suggested that  $\text{Ca}^{2+}$  may play a role in controlling substrate access to the active site of the oxygen evolving enzyme (reviewed in Ref. 3).

Components that modify  $\text{S}_2$ , resulting in a modified multiline signal, include citrate, EGTA, EDTA [21,22] (see also Refs. 29 and 30), pyrophosphate [31], and MES (this work). The questions which arise are (1) Where do the components that modify  $\text{S}_2$  bind? and (2) How do they interact with the manganese cluster? That the components mentioned above modify  $\text{S}_2$  in the same way, resulting in a characteristic dark-stable modified multiline signal, indicates that a specific binding site is involved. Observations using ESEEM suggested that the chelator EGTA was close to the manganese cluster [31]. A common chemical feature of the components that modify  $\text{S}_2$  is the presence of anionic groups containing oxygen — carboxylic acid (EGTA, EDTA, citrate), pyrophosphate, and sulphonic acid (MES) — indicating that modification of

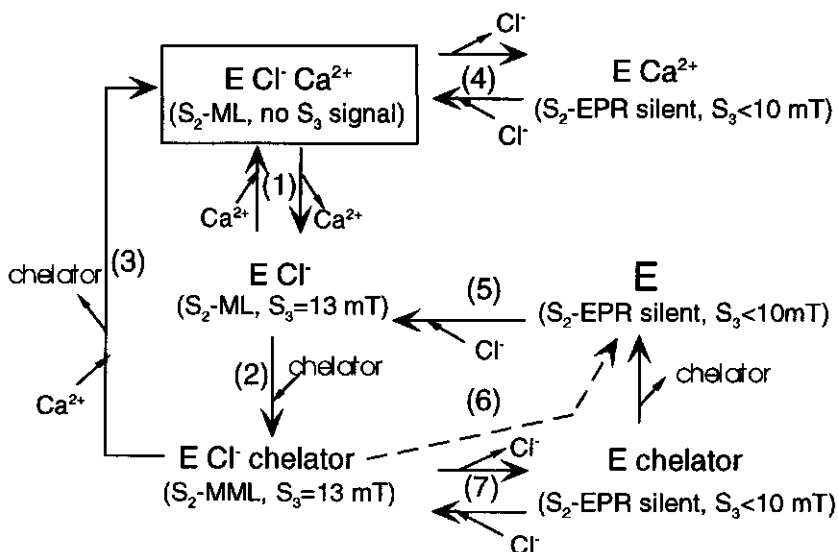


Figure 5. A schematic representation of the effects of  $\text{Ca}^{2+}$  and  $\text{Cl}^-$  depletion in the oxygen evolving enzyme (E) on the EPR properties of  $\text{S}_2$  and  $\text{S}_3$  (see results and discussion). Functional PS-II (E Cl-  $\text{Ca}^{2+}$ ) is indicated in the box. ML= regular multiline signal. MML= chelator-modified multiline signal. Steps: (1)  $\text{Ca}^{2+}$  depletion by salt-treatment in a low concentration (50  $\mu\text{M}$ ) of EGTA followed by  $\text{Ca}^{2+}$  reconstitution [9,13,22]. (2) Modification of  $\text{S}_2$  by the chelator in salt-washed PS-II [22] (see also Figure 4). (3)  $\text{Ca}^{2+}$  reconstitution in salt-washed/EGTA-treated PS-II [21]. (4)  $\text{Cl}^-$  depletion in functional PS-II followed by  $\text{Cl}^-$  reconstitution [18,19,25]. (6)  $\text{Cl}^-$  depletion in salt-washed/EGTA-treated PS-II in the presence of a low concentration (50  $\mu\text{M}$ ) of EGTA (Figure 1c and 3c) followed by (5)  $\text{Cl}^-$  reconstitution (Figure 1d,e and 3e). (7)  $\text{Cl}^-$  depletion in salt-washed/EGTA-treated PS-II in the presence of a high concentration (5 mM) of EGTA [Figure 2a (thin) and 3d] followed by  $\text{Cl}^-$  reconstitution (Figure 2a (thick), b).

the manganese cluster includes an interaction with the anionic oxygens. Further information about the characteristics of the chelator binding in  $\text{Ca}^{2+}$ -depleted PS-II comes from the observation that treatment with phthalic or terephthalic acid (10 mM), at pH 6.5 in the presence of  $\text{Cl}^-$  (30 mM), does not result in the generation of a modified stable multiline signal [22]. This may indicate that chelator binding requires an interaction with poly-anionic groups of a given configuration that is obtained with flexible molecules (see Ref. 22). This may further suggest that the modification of  $\text{S}_2$  by MES, containing a single sulphonic acid group per molecule, occurs upon binding of more than one molecule per PS-II.

The key factor in the experiment that reversed the chelator-induced modification in the absence of  $\text{Ca}^{2+}$ , was the removal of  $\text{Cl}^-$  in the presence of a low concentration of EGTA (50  $\mu\text{M}$ ). Thus,  $\text{Cl}^-$  appears to support the binding of the chelator to PS-II and  $\text{Cl}^-$  depletion

lowers significantly the binding affinity of the chelator. This phenomenon is quite surprising since the anionic chelators may have been expected to compete with  $\text{Cl}^-$  for a common binding site. Many inhibitors of oxygen evolution (e.g.  $\text{OH}^-$ ,  $\text{NH}_3$ , amines,  $\text{SO}_4^{2-}$ ,  $\text{F}^-$ ) seem to be competitive with  $\text{Cl}^-$ -binding (reviewed in Ref. 3). Earlier attempts made in our laboratory to reverse the effect of the chelator in increasing concentrations of  $\text{Cl}^-$  in the absence of  $\text{Ca}^{2+}$ , were unsuccessful (G. N. Johnson and A.W.R., unpublished). Yachandra *et al.* [34] have suggested that  $\text{Cl}^-$  is a ligand to the Mn cluster. It can be speculated that ligation of  $\text{Cl}^-$  to the manganese cluster induces an enhanced affinity of the anionic groups of the chelator to the manganese cluster e.g. due to a changed redox distribution between the Mn ions. It is also possible that chelator binding is stabilized by protonation events occurring in parallel to  $\text{Cl}^-$ -reconstitution. The pH dependence of  $\text{Cl}^-$ -reconstituted oxygen evolution in PS-II indicated that one protonation event occurs per reconstituted  $\text{Cl}^-$  [6]. The observed  $\text{Cl}^-$ -stimulated chelator binding may have some relevance to the role(s) of  $\text{Cl}^-$  in the mechanism of oxygen evolution, in that  $\text{Cl}^-$  controls functional association of the substrate to PS-II. Several suggestions on the role(s) of  $\text{Cl}^-$ , found in the literature, are summarized in Ref. 3.

It was shown in the Results that  $\text{Cl}^-$  depletion of  $\text{Ca}^{2+}$ -depleted/EGTA-treated PS-II modified the EPR spectroscopic properties of both the  $S_2$  and  $S_3$  state. The chelator-modified  $S_2$  state, present when  $\text{Cl}^-$  depletion is done in a high concentration of EGTA (5 mM), is not detected by EPR and the modified  $S_3$  signal is narrow, having a width  $<10$  mT. These modifications were completely reversed by reconstitution with  $\text{Cl}^-$ , resulting in the appearance of the chelator-modified  $S_2$  multiline signal and a 13 mT wide  $S_3$  signal (Figure 3e). The  $\text{Cl}^-$ -dependent behaviour of  $S_2$  that was observed in  $\text{Ca}^{2+}$ -depleted PS-II is similar to that following  $\text{Cl}^-$  depletion in functional PS-II [18,20]. In addition, the type of  $S_3$  signal that was observed in  $\text{Ca}^{2+}$ -depleted,  $\text{Cl}^-$ -depleted PS-II is similar to that observed following  $\text{Cl}^-$  depletion in functional PS-II after treatment with  $\text{SO}_4^{2-}$  [19] or  $\text{F}^-$  [25], also having a width smaller than 10 mT. Thus, the effects of  $\text{Cl}^-$  depletion on the EPR properties of  $S_2$  and  $S_3$  in  $\text{Ca}^{2+}$ -depleted PS-II appear to be similar to those observed following  $\text{Cl}^-$  depletion in regular PS-II membranes in which the functional  $\text{Ca}^{2+}$  is thought to be present: the formation of an  $S_2$  state not detected by EPR and a narrower  $S_3$  signal ( $<10$  mT). These results indicate that the  $\text{Cl}^-$ -related EPR properties of  $S_2$  and  $S_3$  described above are  $\text{Ca}^{2+}$ -independent.

On the basis of an enzymological study in PS-II depleted of Cl<sup>-</sup> and Ca<sup>2+</sup>, Waggoner and Yocum [35] concluded that activation of oxygen evolution in PS-II requires binding of Cl<sup>-</sup> after binding of Ca<sup>2+</sup>. This is in apparent contradiction with our conclusion based on the EPR phenomena described above. The conclusions may be reconciled by suggesting that different Cl<sup>-</sup>-binding sites are involved which would imply that the Cl<sup>-</sup>-binding site in Ca<sup>2+</sup>-depleted PS-II probed by EPR, is not related to oxygen evolving activity. The very different experimental conditions used in the two studies could make direct comparison of the EPR and enzymological studies unreliable. Nevertheless, the data points of Waggoner and Yocum [35], although clearly showing a requirement of both Ca<sup>2+</sup> and Cl<sup>-</sup> for oxygen evolving activity, are not as clear in indicating an ordered binding requirement. A more precise enzymological study is required to resolve this point. Thus that Cl<sup>-</sup>, essential in the charge accumulation cycle, remains bound when Ca<sup>2+</sup> is removed, is the most straightforward explanation and remains the most favoured interpretation of our data.

#### Acknowledgment

We thank T. J. Schaafsma for critically reading the manuscript.

#### References

- 1 Kok, B., Forbush, B., & McGloin, M. (1970) *Photochem. Photobiol.* 11, 457-475.
- 2 Debus, R. J. (1992) *Biochim. Biophys. Acta* 1102, 269-352.
- 3 Rutherford, A. W., Zimmermann, J-L., & Boussac, A. (1992) in *The Photosystems: Structure, Function and Molecular Biology* (Barber, J., ed.) Chapter 5, pp 179-229, Elsevier Science Publishers, New York.
- 4 Murata, N., & Miyao, M. (1985) *Trends Biochem. Sci.* 10, 122-124.
- 5 Homann, P. H. (1988) *Photosynth. Res.* 15, 205-220.
- 6 Homann, P. H. (1988) *Biochim. Biophys. Acta* 934, 1-13.
- 7 Ghanotakis, D. F., Topper, J. N., Babcock, G. T., & Yocum, C. F. (1984) *FEBS Lett.* 170, 169-173.
- 8 Ono, T., & Inoue, Y. (1988) *FEBS Lett.* 227, 147-152.
- 9 Boussac, A., & Rutherford, A. W. (1988) *FEBS Lett.* 236, 432-436.
- 10 Dekker, J. P., van Gorkom, H. J., Wensink, J., & Ouweland, L. (1984) *Biochim. Biophys. Acta* 767, 1-9.
- 11 Boussac, A., Maisson-Peteri, B., Verotte, C., & Etienne, A-L. (1985) *Biochim. Biophys. Acta* 808, 225-230.
- 12 Miyao, M., & Murata, N. (1986) *Photosynth. Res.* 10, 498-496.

- 13 Boussac, A., & Rutherford, A. W. (1988) *Biochemistry* 27, 3476-3483.
- 14 Krieger, A., & Weis, E. (1992) *Photosynthetica* 27, 89-98.
- 15 Dismukes, G. C., & Siderer, Y (1981) *Proc. Natl. Acad. Sci. USA* 78, 274-278.
- 16 Hansson, Ö., & Andréasson, L-E. (1982) *Biochim. Biophys. Acta* 679, 261-268.
- 17 Brudvig, G. W., Casey, J. L., & Sauer, K. (1983) *Biochim. Biophys. Acta* 723, 366-371.
- 18 Ono, T., Zimmermann, J-L., Inoue, Y., & Rutherford, A. W. (1986) *Biochim. Biophys. Acta* 851, 193-201.
- 19 Boussac, A., Sétif, P., & Rutherford, A. W. (1992) *Biochemistry* 31, 1224-1234.
- 20 Boussac, A., & Rutherford, A. W. (1994) *J. Biol. Chem.* 269, 12462-12467.
- 21 Boussac, A., Zimmermann, J-L., & Rutherford, A. W. (1989) *Biochemistry* 28, 8984-8989.
- 22 Boussac, A., Zimmermann, J-L., & Rutherford, A. W. (1990) *FEBS* 277, 69-74.
- 23 Boussac, A., Zimmermann, J-L., Rutherford, A. W., & Lavergne, J. (1990) *Nature* 347, 303-306.
- 24 Rutherford, A. W., & Boussac, A. (1992) In *Research in Photosynthesis* (Murata, N., ed.) Vol II, pp 21-27, Kluwer Academic Publishers, Dordrecht.
- 25 Baumgarten, J., Philo, J. S., & Dismukes, G. C. (1990) *Biochemistry* 29, 10814-10822.
- 26 Andréasson, L.-E., & Lindberg, K. (1992) *Biochim. Biophys. Acta* 1100, 177-183.
- 27 Hallahan, B. J., Nugent, J. H. A., Warden, J. T., & Evans, M. C. W. (1992) *Biochemistry* 31, 4652-4573
- 28 MacLachlan, D. J., & Nugent, J. H. A. (1993) *Biochemistry* 32, 9772-9780.
- 29 Ono, T., & Inoue, Y. (1990) *Biochim. Biophys. Acta* 1020, 269-277.
- 30 Sivaraja, M., Tso, J., & Dismukes, G. C. (1989) *Biochemistry* 28, 9459-9464.
- 31 Zimmermann, J-L., Boussac, A., & Rutherford, A. W. (1993) *Biochemistry* 32, 4831-4841.
- 32 Berthold, D. A., Babcock, G. T., & Yocum, C. F. (1981) *FEBS Lett.* 134, 231-234.
- 33 Ford, R. C., & Evans, M. C. W. (1983) *FEBS* 160, 159-164.
- 34 Yachandra, V. K., DeRose, V. J., Latimer, M. J., Mukerji, I., Sauer, K., & Klein, M. P. (1993) *Science* 260, 675-679.
- 35 Waggoner, C. M., & Yocum, C. F. (1990) In *Current Research in Photosynthesis* (Baltscheffsky M., ed.) Vol I, pp 733-736, Kluwer, Dordrecht.

## Properties of the Chloride-Depleted Oxygen Evolving Complex of Photosystem II studied by EPR

Pieter van Vliet\* and A. William Rutherford

*Section de Bioénergétique (URA CNRS 1290), Département de Biologie Cellulaire et Moléculaire, CEA Saclay, 91191 Gif-sur-Yvette, France, and Department of Molecular Physics, Agricultural University, Wageningen, The Netherlands.*

**Key Words:** photosynthesis, oxygen evolution, charge accumulation states,  $\text{Cl}^-$ , electron paramagnetic resonance.

The effects of different  $\text{Cl}^-$  depletion treatments in photosystem II (PS-II)-enriched membranes have been investigated by electron paramagnetic resonance spectroscopy (EPR) and by measurements of oxygen evolving activity. The results indicated that the oxygen evolving complex of PS-II exhibits two distinct  $\text{Cl}^-$ -dependent properties. (1) After  $\text{Cl}^-$ -free washes at pH 6.3, a reversibly altered distribution of structural states of PS-II was observed, manifest as the appearance of a  $g = 4$  EPR signal from the  $\text{S}_2$  state in a significant fraction of centers (20-40 %) at the expense of the  $\text{S}_2$  multiline signal. In addition, small but significant changes were observed in the shape of the  $\text{S}_2$  multiline EPR signal. Reconstitution of  $\text{Cl}^-$  to  $\text{Cl}^-$ -free washed PS-II rapidly reversed the observed effects of the  $\text{Cl}^-$ -free washing. The anions,  $\text{SO}_4^{2-}$  and  $\text{F}^-$ , which are often used during  $\text{Cl}^-$  depletion treatments, had no effect on the  $\text{S}_2$  EPR properties of PS-II under these conditions in the absence or presence of  $\text{Cl}^-$ . Flash experiments and measurements of oxygen evolution versus light intensity indicated that the two structural states observed after the removal of  $\text{Cl}^-$  at pH 6.3, originated from oxygen evolving centers exhibiting a lowered quantum yield of water oxidation. (2) Depletion of  $\text{Cl}^-$  in PS-II by pH 10 treatment, reversibly inhibited the oxygen evolving activity to ~15 %. The pH 10 treatment depleted the  $\text{Cl}^-$  from a site which is considered to be equivalent to that

---

\* To whom correspondence should be addressed. CEA Saclay, Tel: 33-1-69-08-29-40; Fax: 33-1-69-08-87-17.

studied in most earlier work on Cl<sup>-</sup>-depleted PS-II. The S<sub>2</sub> state in pH 10/Cl<sup>-</sup>-depleted PS-II was reversibly modified to a state from which no S<sub>2</sub> multiline EPR signal was generated and which exhibited an intense S<sub>2</sub> g = 4 EPR signal corresponding to at least 40 % but possibly a much larger fraction of centers. The state responsible for the intense S<sub>2</sub> g = 4 signal generated under these conditions is unlike that observed after removal of Cl<sup>-</sup> from PS-II at pH 6.3, in that this state was more stable in the dark showing a half-decay time of ≈1.5 h at 0 °C, and was unable to undergo further charge accumulation. Nevertheless, a fraction of centers, probably different from those exhibiting the S<sub>2</sub> g = 4 signal, was able to advance to the formal S<sub>3</sub> state giving rise to a narrow EPR signal at g = 2. Addition of the anions SO<sub>4</sub><sup>2-</sup> or F<sup>-</sup> to pH 10/Cl<sup>-</sup>-depleted PS-II affected the properties of PS-II, resulting in EPR properties of the S<sub>2</sub> state similar to those reported earlier following Cl<sup>-</sup> depletion treatment of PS-II in the presence of these anions. Surprisingly, after addition of F<sup>-</sup>, the g = 4 EPR signal showed a damped, flash-dependent oscillation. In addition, a narrow signal around g = 2, corresponding to the formal S<sub>3</sub> state, also showed a damped flash-dependent oscillation pattern. The presence of oscillating EPR signals (albeit damped) in F<sup>-</sup>-treated pH 10/Cl<sup>-</sup>-depleted PS-II indicate functional enzyme turnover. This was confirmed by measurements of the oxygen evolving activity versus light intensity which indicated ~45 % of oxygen evolving centers in which the enzyme turnover was slowed down by a factor of 2. The distinct Cl<sup>-</sup>-depletion effects in PS-II observed under the two different Cl<sup>-</sup> depletion treatments are considered to reflect the presence of two distinct Cl<sup>-</sup>-binding sites in PS-II.

## Introduction

Photosynthetic water oxidation, resulting in the formation of molecular oxygen and proton release, is thought to occur upon photo-accumulation of four positive charges in an enzyme cycle consisting of five intermediate states designated S<sub>0</sub> to S<sub>4</sub>, where the subscript is the number of charges stored [1]. A cluster of four manganese ions, which is thought to be present at the luminal side of the membrane-spanning photosystem II protein complex (PS-II)<sup>1</sup>, plays a central role in the charge accumulation cycle. The kinetic properties of the Mn

---

<sup>1</sup>Abbreviations: PS-II, the photosystem II protein complex; Tyr<sub>D</sub>, side-path electron donor of PS-II responsible for EPR signal II<sub>slow</sub>; Q<sub>A</sub>, Q<sub>B</sub>, primary and secondary quinone electron acceptors of PS-II; CW, continuous wave; EPR, electron paramagnetic resonance; FTIR, Fourier transform infrared; CAPS, 3-(cyclohexylamino)-



oxidation states under different experimental conditions have been characterized in detail (reviewed in Refs. 2 and 3). In addition to the Mn cluster, the ions  $\text{Ca}^{2+}$  and  $\text{Cl}^-$  are essential for oxygen evolving activity. Three extrinsic polypeptides of 33, 23 and 17 kDa, present at the luminal side of PS-II contribute to the stability of the oxygen evolving enzyme but are not essential for oxygen evolving activity (reviewed in Ref. 4). The 33 kDa polypeptide stabilizes the Mn cluster. The 17- and 23 kDa polypeptides play a role in retention of functional  $\text{Ca}^{2+}$  and  $\text{Cl}^-$  [4,5]. In the study of the roles of  $\text{Ca}^{2+}$  and  $\text{Cl}^-$  in the charge accumulation cycle, a number of methods have been developed to specifically deplete these anions from PS-II, resulting in reversible inhibition of oxygen evolution while the Mn cluster is retained in its site [2,6]. Depletion of  $\text{Ca}^{2+}$  involves dissociation of the 17- and 23 kDa proteins by washing of the PS-II membranes in a high concentration of NaCl [7] or treatment at a low pH [8]. Methods for depletion of  $\text{Cl}^-$  from PS-II include a short treatment at a high pH (pH 10) or treatments at slightly elevated pH (pH 7.5) in the presence of the inhibitory counter anions  $\text{SO}_4^{2-}$  or  $\text{F}^-$  [6]. Several lines of evidence indicate that depletion of functional  $\text{Ca}^{2+}$  or  $\text{Cl}^-$  from PS-II results in inhibition of the  $\text{S}_3$  to  $\text{S}_0$  transition of the charge accumulation cycle (reviewed in Refs. 3 and 9).

Several suggestions have been made for the roles of  $\text{Ca}^{2+}$  and  $\text{Cl}^-$  in the mechanism of photosynthetic water oxidation (reviewed in Refs. 2 and 3) including that these anions may regulate protonation/deprotonation events [10-13]. Furthermore, it has been suggested that these anions play a role in controlling the access and binding of the substrate (reviewed in Ref. 3) (see also [14]). With respect to the role of  $\text{Cl}^-$ , the latter suggestion was partly based on observations that  $\text{Cl}^-$  protects against reductive attack by a range of substrate-like inhibitors (see e.g. [15-17]). The extrinsic polypeptides themselves also protect against reductive attack [18,19]. Since  $\text{Cl}^-$  seems to enhance the association of the 17- and 23- kDa extrinsic polypeptides to PS-II [5,19], some of the protective effects of  $\text{Cl}^-$  may result from its stabilizing effect on protein associations.

Many studies on the magnetic properties of the oxygen evolving complex have been done using EPR spectroscopy. In untreated PS-II, no signals from states other than the  $\text{S}_2$  state have been detected by conventional CW-EPR. However, after  $\text{Ca}^{2+}$  depletion an EPR signal around  $g = 2$  with a width of 16.4 mT was observed, corresponding to the formal  $\text{S}_3$

---

1-propane sulphonic acid; HEPES, 4-(2-hydroxyethyl)-1-piperazineethane sulphonic acid; MES, 4-(N-morpholino)ethane sulphonic acid; PPBQ, phenyl-p-benzoquinone.

state [20] (see also [21]). Boussac *et al.* [20,22] have proposed that upon the  $S_2$  to  $S_3$  transition in  $Ca^{2+}$ -depleted PS-II, the oxidation state of the Mn cluster remains unchanged and that an organic species is oxidized instead giving rise to an  $S = 1/2$  radical magnetically interacting with the  $S = 1/2$  Mn cluster. The radical species was proposed to be an oxidized histidine on the basis of its absorption spectrum in the ultraviolet [22]. Although this assignment has received further support from a study by FTIR difference spectroscopy [23], it is not definitive (discussed in Refs. 2 and 24). Recently, Gilchrist *et al.* [25] have proposed on the basis of an ESE-ENDOR investigation in  $Ca^{2+}$ -depleted PS-II, that the radical signal originates from oxidized Tyr<sub>Z</sub>, the electron transfer intermediate between the Mn cluster and the primary electron donor P<sub>680</sub>.

Besides their formation in  $Ca^{2+}$ -depleted PS-II,  $S_3$  signals also were observed after inhibition of oxygen evolution by treatments in the presence of  $F^-$  [26],  $SO_4^{2-}$  [12],  $NH_3$  [27,28], or acetate [29] which are thought to displace the functional  $Cl^-$  in PS-II.

In untreated PS-II, the EPR spectrum of the  $S_2$  state is dominated by a characteristic multiline EPR signal at  $g = 2$  [30]. This signal can be generated by illumination treatments allowing for a single stable charge separation, e.g., illumination with a single flash at room temperature [30], or with continuous illumination at 200 K [31]. The  $S_2$  multiline signal is attributed to a ground state spin  $S = 1/2$  probably arising from a mixed valence Mn tetramer (see Ref. 32 and references therein). Depending on the conditions, the  $S_2$  state also exhibits a signal around  $g = 4$  (reviewed in Ref. 3). This signal is less well characterized than the  $S_2$  multiline signal but is thought to arise from a spin  $S = 3/2$  or  $S = 5/2$  ground or excited state of the mixed valence Mn cluster (see e.g. Refs. 33 and 34). The nature of the  $S_2$   $g = 4$  signal may depend on the pretreatment of the enzyme [35]. The  $S_2$   $g = 4$  and  $S_2$  multiline signal probably originate from two different structural states of the oxygen evolving complex with different magnetic properties of the Mn cluster [36-38].

The multiline EPR signal from  $S_2$  seems to be related to functional binding of  $Cl^-$  to PS-II as indicated by the loss of the ability to generate the  $S_2$  multiline signal following inhibition of oxygen evolution by  $Cl^-$  depletion in the presence of  $SO_4^{2-}$  [12,39-41] or  $F^-$  [26,42,43]. After inhibition of oxygen evolution by  $Cl^-$  depletion in the presence of  $SO_4^{2-}$ , a modified  $S_2$  state was generated which was not detected by EPR and was converted to the normal  $S_2$  state by rapid addition of  $Cl^-$  in darkness, resulting in the reconstitution of the  $S_2$  multiline EPR

signal [39]. A similar Cl<sup>-</sup> depletion effect on the EPR properties of S<sub>2</sub> was observed in Ca<sup>2+</sup>-depleted PS-II, indicating that this Cl<sup>-</sup> depletion effect was independent of Ca<sup>2+</sup> [14].

The relationship between the appearance of the S<sub>2</sub> g = 4 EPR signal from the Mn cluster and the functional and biochemical properties of the oxygen evolving complex is poorly understood (discussed in Ref. 3). The S<sub>2</sub> g = 4 signal, observed in untreated PS-II resuspended in sucrose buffer, seems to be suppressed in favour of the S<sub>2</sub> multiline signal by the presence of glycerol, ethylene glycol and ethanol which are used as cryoprotectants or solvents [37]. However, these effects seem to vary depending on the experimental conditions (see e.g. Ref. 44 and 45). The S<sub>2</sub> g = 4 signal in untreated PS-II was shown to originate from the functional charge accumulation cycle [37,46]. Even so, it has also been suggested that the appearance of the S<sub>2</sub> g = 4 signal is related to inhibition of oxygen evolution due to the release of Cl<sup>-</sup> [44] on the basis of the observation that the S<sub>2</sub> g = 4 signal was enhanced after treatment of PS-II with F<sup>-</sup> (e.g. [45]) or NH<sub>3</sub> (e.g. [47]) which were thought to displace the functional Cl<sup>-</sup>. However, the S<sub>2</sub> g = 4 signal intensities generated following displacement of the functional Cl<sup>-</sup> in PS-II by various counter-anions did not correlate to the extent of inhibited oxygen evolving activity [40].

In this report the properties of Cl<sup>-</sup>-depleted PS-II were investigated under various experimental conditions, with the aim of relating the biochemical status of Cl<sup>-</sup>-depleted PS-II to the observed EPR properties.

### **Materials and methods**

Photosystem II-enriched membranes were prepared according to the method of Berthold *et al.* [48] with the modifications of Ford and Evans [49]. The oxygen evolving activity of these membranes was ≈500 μM O<sub>2</sub>/mg chlorophyll/h. Prior to use for further treatments (see below), the PS-II membranes were stored at -80 °C in a buffer solution containing 25 mM MES (pH 6.5), 0.3 M sucrose and 10 mM NaCl.

Cl<sup>-</sup> depletion in PS-II was done by a short treatment at pH 10 (see below) as described by Homann [50]. The principle of the Cl<sup>-</sup> depletion treatment is based on the idea that the 17- and 23 kDa extrinsic polypeptides are involved in retention of Cl<sup>-</sup> in the functional site [5,51]. The short treatment at pH 10 is thought to induce a transient dissociation of the 17- and 23 kDa extrinsic polypeptides resulting in the release of Cl<sup>-</sup> from its site [5,51]. Prior to the pH

10 treatment, the Cl<sup>-</sup> concentration in untreated PS-II membranes was lowered by three washes (resuspension, dilution and centrifugation) in a Cl<sup>-</sup>-free buffer solution containing 5 mM MES (pH 6.3) and 0.5 M sucrose.

In some experiments, where indicated, PS-II membranes were washed in a Cl<sup>-</sup>-free buffer solution as described above except that the pH was adjusted to pH 6.5. No differences were observed between the effects of the washes at pH 6.3 or the washes at pH 6.5. The PS-II membranes that were repetitively washed in Cl<sup>-</sup>-free buffer solutions at pH 6.3 or pH 6.5, will be referred to as Cl<sup>-</sup>-free washed PS-II.

Following resuspension and dilution of the Cl<sup>-</sup>-free washed PS-II membranes to a chlorophyll concentration of 125 µg/ml in a buffer-free solution containing 0.4 M sucrose, the pH was increased to pH 10 by addition of 15 mM (15 µl/ml of 1.0 M) CAPS (pH 10). After 10-35 sec. of incubation at pH 10, the pH was lowered to pH 7.3 by adding 45 mM (45 µl/ml of 1.0 M) HEPES (pH 7.3) and, unless stated otherwise, directly followed by lowering the pH to pH 6.3 by adding 45 mM (45 µl/ml of 1.0 M) of unneutralized MES followed by 10 min. incubation. Addition of anions (as their sodium salt) to pH 10/Cl<sup>-</sup>-depleted PS-II was done at pH 7.3, i.e. under conditions in which irreversible inhibition of oxygen evolution is minimized and yet PS-II is still sensitive to treatments that affect Cl<sup>-</sup>-dependent oxygen evolving activity [50,52]. Following 10-20 min. incubation the pH was lowered to pH 6.3 as described above. The pH 10 treatment and addition of anions was done while stirring at 4 °C under dim room light. To minimize possible Cl<sup>-</sup> contamination, the experiments were done using sucrose BDH ARISTAR (<0.5 ppm Cl<sup>-</sup>).

Following the treatments described above, the content of the 17-, 23- and 33 kDa extrinsic polypeptides in the PS-II membrane preparations was determined by SDS-gel electrophoresis and subsequent Western blotting. SDS-gel electrophoresis was carried out as described in Ref. 53, except that 750 mM instead of 375 mM Tris (pH 8.8) was present in the resolving gel, and 6 M urea was added to both gel and sample buffer. Western blotting was carried out as described in Ref. 54, except that the tank blot device used for protein transfer onto the PVDF membrane, was from Biorad. Furthermore, the PVDF membrane was simultaneously incubated with the antibodies against the three extrinsic polypeptides. The antibodies were kindly provided by Dr. C. Jansson, Stockholm.

The membranes were resuspended at 2.5-15 mg chlorophyll/ml, put in calibrated quartz EPR tubes, dark-adapted, frozen in the dark and stored in liquid nitrogen until used for EPR

measurements. Further additions to these membranes were done in the EPR tube in the dark after thawing. Where indicated, illumination of the samples was done following addition in darkness of the external electron acceptor PPBQ dissolved in dimethyl sulphoxide.

Continuous illumination of the samples was done, using an 800 W projector through 2 cm water and an infrared filter, in a non-silvered dewar flask containing ethanol cooled to 198 K with solid CO<sub>2</sub> or cooled to 0 °C with liquid nitrogen. Flash illumination at room temperature was provided from an Nd-Yag laser (15 ns, 300 mJ, 532 nm).

EPR spectra were recorded at liquid helium temperatures with a Bruker ER 200 X-band spectrometer equipped with an Oxford Instruments cryostat.

Measurements of oxygen evolving activity were done using a Clark-type electrode, at 25 °C under continuous light. The measurements were done under near saturating light at a chlorophyll concentration of 20 µg/ml or under non-saturating light at a chlorophyll concentration of 40 µg/ml and 0.5 mM PPBQ was added as an external electron acceptor. The light intensity was varied using calibrated neutral gray (Balzers) filters.

## Results

*The effects of Cl<sup>-</sup>-free washes at pH 6.5.* After Cl<sup>-</sup>-free washes at pH 6.5, prior to pH 10/Cl<sup>-</sup> depletion treatment, the oxygen evolving activity of the PS-II membranes measured in the presence of Cl<sup>-</sup> (10 mM) was about 85 % relative to that in untreated PS-II indicating a fraction (15 %) of irreversible inhibition after the Cl<sup>-</sup>-free washes, probably due to Mn release from the functional site of PS-II as indicated by the appearance of a small 6-line signal around  $g = 2$  in the EPR spectrum originating from hexaquomanganese (II) (not shown).

In the absence of Cl<sup>-</sup>, the oxygen evolving activity of Cl<sup>-</sup>-free washed PS-II membranes was about 80 % of that after reconstitution of Cl<sup>-</sup>. Thus the Cl<sup>-</sup>-free washes resulted in a partial (20 %) reversibly inhibited oxygen evolving activity. The apparent Cl<sup>-</sup> affinity for reconstitution of oxygen evolution from 80 % to 100 % in Cl<sup>-</sup>-free washed PS-II was about 0.4 mM (not shown). The level of inhibition of oxygen evolution was dependent on the light-intensity and increased at lower light intensities (Figure 1). The oxygen evolving activity in Cl<sup>-</sup>-free washed PS-II, when extrapolated to full light saturation, was similar to that after reconstitution of Cl<sup>-</sup> (10 mM) (Figure 1) indicating that apart from the fraction (15 %) of irreversibly inhibited oxygen evolution, the removal of Cl<sup>-</sup> did not affect the number of oxygen

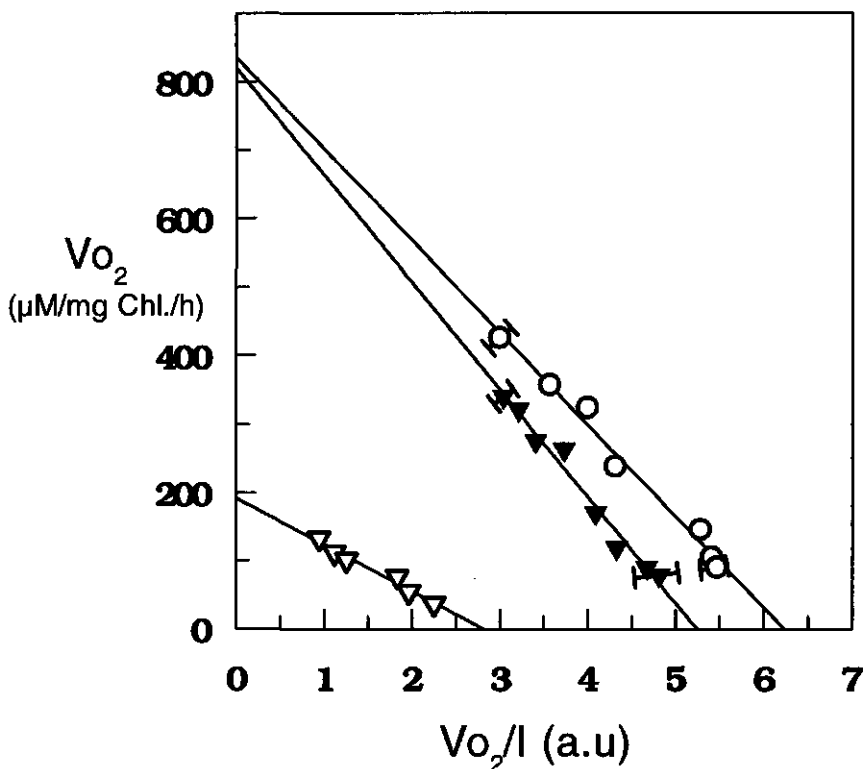


Figure 1. Plot of oxygen evolution ( $V_{O_2}$ ) versus oxygen evolution over light-intensity ( $V_{O_2}/I$ ). The measurements were done either following three washes of PS-II membranes in a  $\text{Cl}^-$ -free buffer solution containing 5 mM MES (pH 6.3) and 0.5 M sucrose and resuspension in the same buffer ( $\blacktriangledown$ , O), or after subsequent pH 10/ $\text{Cl}^-$  depletion treatment following the  $\text{Cl}^-$ -free washes and followed by reconstitution with  $\text{F}^-$  (25 mM) and resuspension in 10 mM MES (pH 6.3), 0.5 M sucrose and 25 mM  $\text{F}^-$  ( $\blacktriangledown$ ). The measurements were done in a buffer solution containing 10 mM MES (pH 6.3) and 0.5 M sucrose in the absence ( $\blacktriangledown$ , $\blacktriangledown$ ) or presence of 10 mM  $\text{Cl}^-$  (O). Each data point is the average of at least six measurements. The error in the data-points from the  $\text{F}^-$ -reconstituted PS-II membranes matched or was smaller than the symbol size.

evolving centers but rather influenced the enzyme kinetics. Since the EPR studies shown below indicate specific  $\text{Cl}^-$ -dependent modifications at the electron donor side of PS-II while no  $\text{Cl}^-$ -dependent effects were observed at the electron acceptor side, it is most likely that the observed changes in the enzyme kinetics are related to donor side phenomena.

In control samples which were washed in the presence of  $\text{Cl}^-$  (10 mM) without sucrose (see below), the  $S_2$  state exhibited a characteristic multiline EPR signal and no  $g = 4$  EPR signal was observed (Figure 2a). However, after  $\text{Cl}^-$ -free washes (pH 6.5) without sucrose, a  $g = 4$  signal was observed from  $S_2$  (Figure 2b). The  $S_2$   $g = 4$  signal exhibited a peak to trough

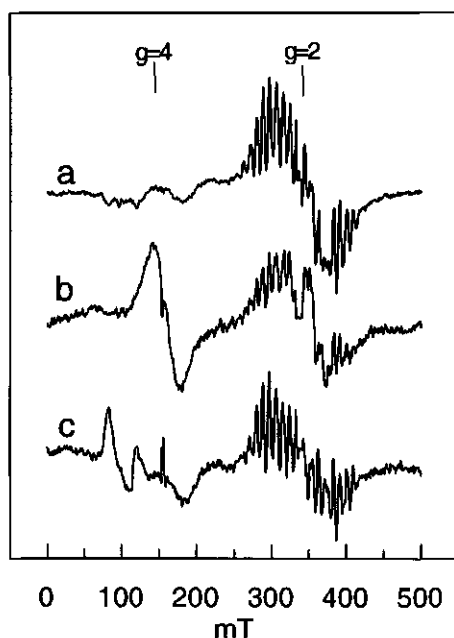


Figure 2. Light minus dark EPR spectra of PS-II membranes that were illuminated for 3 min. at 200 K in the presence of PPBQ (1 mM). The PS-II membranes were (a) washed three times in 5 mM MES (pH 6.5) and 10 mM  $\text{Cl}^-$  and resuspended in the same buffer solution, or (b) washed twice in 5 mM MES (pH 6.5) and 0.1 M sucrose followed by two washes and resuspension in 5 mM MES (pH 6.5) (i.e. in the absence of sucrose). (c) The  $\text{Cl}^-$ -free washed sample used for spectrum b was thawed and  $\text{Cl}^-$  (50 mM) was added rapidly (30 s) in darkness and refrozen. Instrument settings: 9.42 GHz; modulation amplitude, 2.2 mT; temperature, 10 K; microwave power, 31 mW.

width of 34.2 mT and a turning point at  $g = 4.2$ , showing EPR properties similar to the  $S_2$   $g = 4$  signal observed in untreated PS-II in the presence of sucrose [37,55]. In addition, the intensity of the  $S_2$  multiline signal was significantly lowered (see also Figure 4). This was mainly due to a decreased intensity of the hyperfine lines which was 30 % relative to the control while a broad signal underlying the  $S_2$  multiline signal (e.g. [56]) was apparently unaffected by the  $\text{Cl}^-$ -free washes. Furthermore, in most cases (8 from 12 PS-II preparations used), the  $\text{Cl}^-$ -free washes resulted in some minor changes in of the hyperfine structure of the  $S_2$  multiline signal (Figure 2b). Although we cannot rule out that a fraction of centers remains unaffected by the  $\text{Cl}^-$ -free washes, the nature of the changes in the multiline signal lead us to consider that the majority of centers is modified (i.e. >70 % of the centers does not exhibit an  $S_2$  multiline signal after  $\text{Cl}^-$ -free washes).

The  $S_2$   $g = 4$  and  $S_2$  multiline signal in  $\text{Cl}^-$ -free washed PS-II showed a half-decay time of 4-5 min. at room temperature (in the presence of 1 mM PPBQ) similar to that observed from  $S_2$  in untreated PS-II under similar conditions (see also Refs. 31 and 57). Rapid addition of  $\text{Cl}^-$  (50 mM) in darkness to the  $S_2$  state (Figure 2b), a method that has been used to investigate the  $S_2$  state in  $\text{Cl}^-$ -depleted PS-II [39], reversed the effects of  $\text{Cl}^-$ -free washes (Figure 2c) resulting in the suppression of the  $g = 4$  signal and reconstitution of the multiline

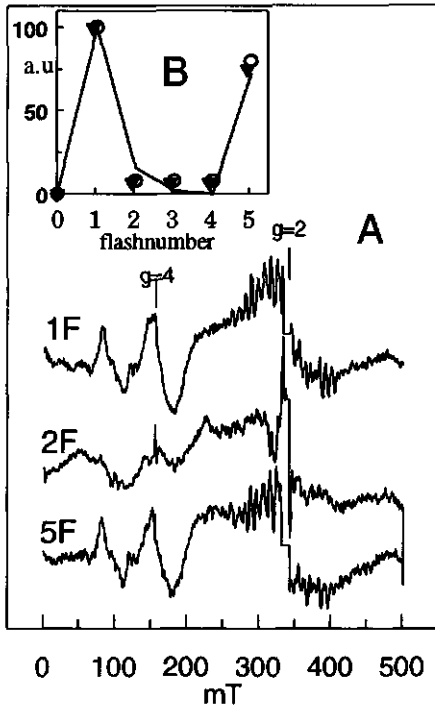


Figure 3. (A) Light minus dark EPR spectra of Cl<sup>-</sup>-free washed PS-II membranes in 5 mM MES (pH 6.5) and 0.3 M sucrose, after illumination with single flashes at room temperature in the presence of PPBQ (1 mM), followed by rapid (1s) freezing in darkness. (B) The intensities of (▼) the signal at  $g = 4$  and (○) the multiline signal plotted relative to the number of flashes. The  $g = 4$  signal intensity was determined from the peak to trough amplitude and the multiline signal intensity was determined as the sum of the resolved hyperfine line amplitudes. The continuous line was fitted to the data points assuming 100 %  $S_1$  before illumination, 8 % misses and no double hits. Before addition of PPBQ (1 mM) and flash illumination, the dark-adapted samples were synchronized as described in [57] by illumination with a preflash followed by dark-adaptation for 10 min. at room temperature. Instrument settings were as in Figure 2.

signal. The  $Q_A^-Fe^{2+}$  EPR signal at  $g = 1.90$  (350 mT), detected after generation of  $S_2Q_A^-$  by illumination at 200 K (Figure 2a, b), disappeared following thawing of the sample for the addition of Cl<sup>-</sup> in darkness (Figure 2c), due to electron transfer from  $Q_A^-$  to PPBQ resulting in the formation of the semiquinone form of PPBQ. This semiquinone, which is a good oxidant, oxidizes the non-heme iron giving rise to an EPR signal at  $g = 8$  (82 mT) and  $g = 6$  (120 mT) (Figure 3c) from  $Fe^{3+}$  [58,59].

As reported earlier [37,55], when sucrose-containing (0.3-0.5 M) buffers were used, continuous illumination at 200 K of untreated PS-II in the presence of Cl<sup>-</sup> (10 mM) resulted in the formation of an  $S_2$   $g = 4$  signal in a fraction of centers (not shown). The intensity of this signal was doubled after Cl<sup>-</sup>-free washes of those samples (not shown). The resulting  $S_2$   $g = 4$  EPR signal was similar to that shown in Figure 2b which was recorded in Cl<sup>-</sup>-free washed PS-II in the absence of sucrose. The increase of the  $S_2$   $g = 4$  signal intensity was reversed by addition of Cl<sup>-</sup>. Occasionally, Cl<sup>-</sup>-free washed PS-II in the absence of sucrose did not exhibit an  $S_2$   $g = 4$  signal, showing otherwise properties identical to those described above. When sucrose was added, the  $S_2$   $g = 4$  signal was observed exhibiting the Cl<sup>-</sup>-dependent behaviour



as described above. These effects of sucrose are not understood but may be related to the binding properties of the extrinsic polypeptides.

Flash illumination of Cl<sup>-</sup>-free washed PS-II resulted in a flash-dependent oscillation of the S<sub>2</sub> g = 4 and multiline signals (Figure 3). The signals from the S<sub>2</sub> state oscillated in parallel with maximal intensities on the first and fifth flash. Furthermore, the signal at g = 8 originating from the oxidized non-heme iron showed a flash-dependent binary oscillation and with maximal intensities on odd numbered flashes. These results indicate that both the S<sub>2</sub> multiline signal and the S<sub>2</sub> g = 4 signal in Cl<sup>-</sup>-free washed PS-II originate from the functional charge accumulation cycle. A flash-dependent oscillation of the g = 4 signal was observed previously in untreated PS-II [37]. The results indicate that the Cl<sup>-</sup> removed at pH 6.3 and affects the S<sub>2</sub> EPR properties as described above, is not obligatory for oxygen evolving activity.

The quantitative relationship between the Cl<sup>-</sup> dependent intensity of the S<sub>2</sub> g = 4 signal and that of the S<sub>2</sub> multiline signal was studied after reconstitution of increasing Cl<sup>-</sup> concentrations following the Cl<sup>-</sup>-free washes. The results are shown in Figure 4. We determined the fraction of centers contributing to the EPR signal at g = 2, by the sum of hyperfine line intensities and the intensity of the broad signal underlying the multiline signal. The EPR signal intensity at g = 2 in Cl<sup>-</sup>-free washed PS-II was about 65 % of that observed at a Cl<sup>-</sup> concentration (5 mM) which is sufficient to completely suppress the g = 4 signal. The addition of a small amount of Cl<sup>-</sup> (0.2 mM), resulted in an increased intensity of both the signal at g = 4, from 94 % to maximal (100 %), and the signal at g = 2, from 65 % to 80 %. The origin of this increase of both S<sub>2</sub> EPR signals is unknown. It could reflect a small fraction of centers in Cl<sup>-</sup>-free washed PS-II in which the S<sub>2</sub> state was not formed. Alternatively, it is possible that in a fraction of centers the S<sub>2</sub> state was reversibly modified by the Cl<sup>-</sup>-free washes and did not exhibit an S<sub>2</sub> EPR signal, as is the case after inhibition of oxygen evolution by Cl<sup>-</sup> depletion of PS-II in the presence of SO<sub>4</sub><sup>2-</sup> [39, 41].

After addition of higher concentrations of Cl<sup>-</sup> (>0.2 mM), an inverse relationship was observed between the signal intensities at g = 4 and at g = 2. The relative signal intensities at g = 2 calculated from the Cl<sup>-</sup>-dependent decrease of the g = 4 signal intensity matched rather well those determined experimentally (Figure 4), indicating that a direct Cl<sup>-</sup>-induced conversion occurred from the g = 4 signal to the signal at g = 2. From the comparison of the signal intensities at 0.2 mM Cl<sup>-</sup> [maximal signal intensity at g = 4 (100 %) and 80 % of the signal intensity at g = 2] and 5 mM Cl<sup>-</sup> [no g = 4 signal and maximal (100 %) signal at g = 2],

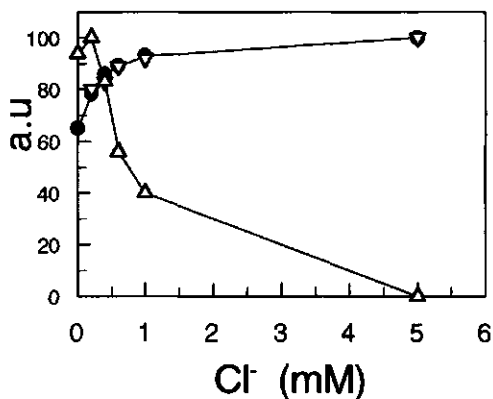


Figure 4. The intensities of ( $\Delta$ ) the  $S_2$  EPR signal at  $g = 4$  and ( $\bullet$ ) the  $S_2$  EPR signal at  $g = 2$  in PS-II membranes after  $Cl^-$ -free washes as described in Figure 2b, followed by addition on ice of increasing  $Cl^-$  concentrations to the dark-adapted samples, dark incubation on ice for 30 min. and followed by addition of PPBQ (1mM). Then the samples were frozen and illuminated at 200 K for 3 min. The  $g = 4$  signal intensity was determined as described in Figure 3. The signal intensity at  $g = 2$  was determined as the sum of the resolved hyperfine line amplitudes and the intensity of the broad signal underlying the hyperfine lines. This was done in samples following rapid thawing (5 s) and freezing in darkness of the illuminated samples which treatment resulted in the disappearance of the  $Q_A^-Fe^{2+}$  EPR signal at  $g = 1.90$  without affecting the  $S_2$  EPR signal intensity at  $g = 2$ . ( $\nabla$ ) Calculated intensities of the signal around  $g = 2$ . Instrument settings were as in Figure 2.

it is estimated that following the  $Cl^-$ -free washes about 20 % of the centers present in  $S_2$  exhibits a  $g = 4$  signal, assuming that all centers give rise to an EPR signal. This estimate of the fraction of centers giving rise to the  $S_2$   $g = 4$  signal can be considered a lower limit. If the broad signal underlying the multiline EPR signal was excluded from the quantification, a significantly larger fraction (~40 %) of centers was estimated to contribute to the  $S_2$   $g = 4$  signal.

$Cl^-$  depletion treatments in PS-II are often done in the presence of the  $SO_4^{2-}$  or  $F^-$  anions which are thought to enhance  $Cl^-$  depletion in PS-II (reviewed in Ref. 6). However, the addition of  $SO_4^{2-}$  (50 mM) or  $F^-$  (25 mM) to  $Cl^-$ -free washed PS-II at pH 6.5 had no effect on the EPR properties of  $S_2$  (not shown). These anions also did not influence the  $S_2$  EPR signals in  $Cl^-$ -free washed PS-II samples which had been partially reconstituted with  $Cl^-$  (0.6 mM). Thus it seems that under these conditions, the anions  $SO_4^{2-}$  and  $F^-$  did not compete with  $Cl^-$ .

*The effects of  $Cl^-$  depletion by treatment at pH 10.* Short treatment (30 s) of  $Cl^-$ -free washed PS-II at high pH (pH 10) resulted in extensive inhibition of oxygen evolution. The residual oxygen evolving activity during the measurement was lost relatively rapidly with a half-inhibition time of 24 s and showed an initial rate of about 15 % relative to that after reconstitution with 10 mM  $Cl^-$ . The  $Cl^-$ -reconstituted oxygen evolving activity in pH 10-treated PS-II was about 90 % relative to that of  $Cl^-$ -reconstituted,  $Cl^-$ -free washed PS-II, indicating 10 % irreversible inhibition following  $Cl^-$  depletion by pH 10 treatment, probably

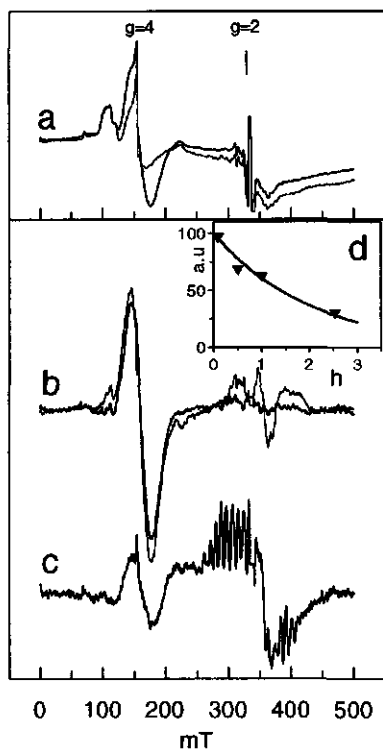


Figure 5. (a) EPR dark spectra of PS-II (thin) prior to or (thick) following pH 10/Cl<sup>-</sup>-depletion treatment recorded after dark adaptation for 5 min. on ice. (b) The EPR difference spectra of pH 10/Cl<sup>-</sup>-depleted PS-II (thick) after 5 min dark adaptation or (thin) after illumination at 200 K for 4 min. after subtraction of the dark baseline spectrum [a (thin)] of the sample prior to the pH 10 treatment. (c) Light minus dark EPR spectrum after 3 min. illumination at 200 K of dark-adapted PS-II that was pH 10/Cl<sup>-</sup>-depleted and then reconstituted with 0.2 mM Cl<sup>-</sup>. (d) Intensities of the signal around  $g = 4$  in pH 10/Cl<sup>-</sup>-depleted PS-II (▼) after increasing periods of dark-incubation on ice. The PS-II membranes were resuspended in 10 mM MES (pH 6.3) and 0.5 M sucrose. The intensities of the spectra from (b) and (c) were multiplied by 2.5 in comparison to the spectra from (a). Instrument settings were as in Figure 2.

due to a fraction of damaged centers. The initial rate of Cl<sup>-</sup>-reconstituted oxygen evolution remained approximately constant for about 2 min., in a similar fashion to that of untreated and Cl<sup>-</sup>-free washed PS-II. Furthermore, the Cl<sup>-</sup> affinity for reconstitution of oxygen evolving activity in pH 10/Cl<sup>-</sup>-depleted PS-II was relatively high with 50 % reconstitution of oxygen evolution at a Cl<sup>-</sup> concentration of about 100  $\mu$ M (not shown). This value for the Cl<sup>-</sup> binding constant is in agreement with those determined earlier in similarly treated PS-II, and is taken as an indication that the 17- and 23 kD extrinsic polypeptides are associated to most of the pH 10/Cl<sup>-</sup>-depleted PS-II centers [5,50,51]. This was confirmed by SDS-gel electrophoresis and subsequent Western blotting (not shown).

Surprisingly, after pH 10/Cl<sup>-</sup> depletion an EPR signal around  $g = 4$  was observed in the samples that were dark-adapted for 5 min. [Figure 5a (thick)] (compare to the Cl<sup>-</sup>-free washed (pH 6.3) sample [Figure 5a (thin)]). This signal, which was presumably photogenerated during the pH 10/Cl<sup>-</sup>-depletion treatment done in dim room light, was lost upon longer dark-adaptation (Figure 5d) and could be regenerated by continuous illumination at 200 K [Figure 5b (thin)] or by illumination with a single flash at room temperature (Figure

6), indicating that the  $g = 4$  signal observed after pH 10 treatment corresponds to the  $S_2$  state. However, no  $S_2$  multiline was observed before or after the illumination treatments (Figure 5a, b and Figure 6). A suppression of the  $S_2$  multiline signal also has been observed after  $Cl^-$  depletion in PS-II in the presence of various anions (see e.g. [40]). The  $S_2$   $g = 4$  signal observed in pH 10/ $Cl^-$ -depleted PS-II exhibited EPR properties similar to those of the  $S_2$   $g = 4$  signal in  $Cl^-$ -free washed PS-II (Figure 2b). However, the lifetime of the  $S_2$  state in pH 10/ $Cl^-$  depleted PS-II giving rise to the  $g = 4$  signal is clearly longer than that in  $Cl^-$ -free washed PS-II since 5 minutes of dark-adaptation on ice had little effect on the  $S_2$   $g = 4$  signal observed after pH 10/ $Cl^-$  depletion [Figure 5a (thick), Figure 5b] while in  $Cl^-$ -free washed PS-II the  $S_2$   $g = 4$  signal was absent [Figure 5a (thin)]. The half-decay time of the  $S_2$   $g = 4$  signal in pH 10/ $Cl^-$ -depleted PS-II was about 1.5 h at 0 °C (Figure 5d) and approximately 10 min. at room temperature (not shown). No  $Q_A^-Fe^{2+}$  EPR signal was present in the EPR spectrum of the short dark-adapted pH 10/ $Cl^-$ -depleted PS-II samples [Figure 5a, b (thick)]. Thus it is very unlikely that the decay of the long lived  $g = 4$  signal in pH 10/ $Cl^-$ -depleted PS-II is due to a recombination reaction with  $Q_A^-$ . In the presence of the external electron acceptor PPBQ (1 mM) the decay of the  $S_2$   $g = 4$  signal was accelerated. This is probably due to reduction of the Mn cluster by PPBQH<sub>2</sub> leading to some  $Mn^{2+}$  release, as indicated by the appearance of a 6-line signal around  $g = 2$  in the EPR spectrum, originating from hexaquomanganese (II) (not shown). The intensity of the  $S_2$   $g = 4$  signal in pH 10/ $Cl^-$ -depleted PS-II was markedly enhanced, showing an intensity of 2-3 times that observed in  $Cl^-$ -free washed PS-II (Figure 2b). From the estimate of the fraction of centers (20-40 %) in  $Cl^-$ -free washed PS-II giving rise to the  $S_2$   $g = 4$  signal (Figure 2b, Figure 4), it is estimated that the  $S_2$   $g = 4$  signal observed in pH 10/ $Cl^-$ -depleted PS-II corresponds to at least 40 % of the centers but could originate from close to 100 % of the centers.

The effects of pH 10/ $Cl^-$  depletion on the EPR properties of  $S_2$  were reversed after addition of  $Cl^-$  (for the experimental conditions, see Materials and Methods). No  $S_2$  EPR signals were observed after short dark-adaptation on ice. After illumination at 200 K of the dark-adapted  $Cl^-$  reconstituted PS-II, a normal light-induced  $S_2$  EPR spectrum was observed which is dominated by the presence of a characteristic  $S_2$  multiline signal (Figure 5c). The extent to which the  $S_2$  multiline signal intensity in pH 10/ $Cl^-$ -depleted PS-II was reconstituted with  $Cl^-$ , was comparable to the  $Cl^-$ -reconstituted level of oxygen evolving activity under these conditions, i.e., addition of 0.2 mM  $Cl^-$  after pH 10 treatment (Figure 5c) resulted in

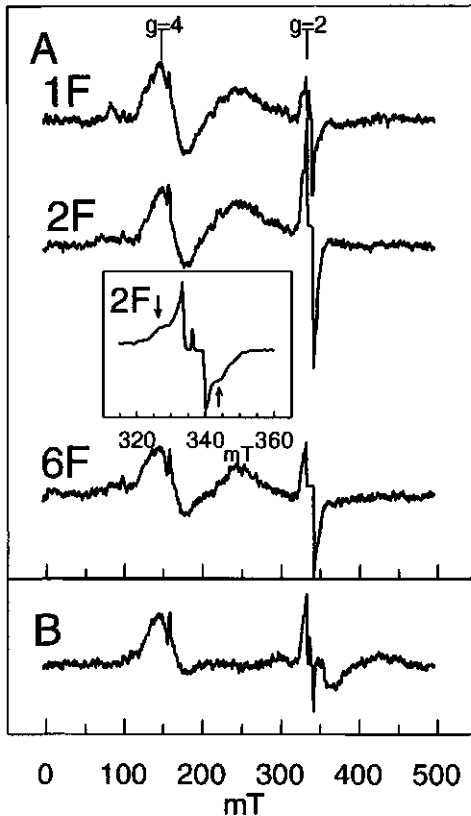


Figure 6. Light minus dark EPR spectra of pH 10/Cl<sup>-</sup>-depleted PS-II after illumination with (A) single flashes or (B) continuous illumination at 0 °C followed by rapid freezing. The inset shows the light-induced signal around  $g = 2$  generated after illumination with 2 flashes and the arrows indicate the peak to trough width of the resolved component. Before the illumination, the samples were dark-adapted at room temperature for 35 min. followed by addition of ferricyanide (50-100  $\mu$ M) and PPBQ (50-100  $\mu$ M). Instrument settings were as in Figure 2.

of this part of the signal was comparable to the  $S_3$  signal observed in Ca<sup>2+</sup>-depleted PS-II [20]. In addition, a narrower component (<10 mT) of the  $S_3$  signal was present but was unresolved due to the presence of the Tyr<sub>D</sub>• radical signal [Figure 6 (inset)]. A narrow (<10 mT)  $S_3$  signal has been observed in Cl<sup>-</sup>-depleted PS-II following treatment with SO<sub>4</sub><sup>2-</sup> [12] or F<sup>-</sup> [26]. No  $S_3$  signal could be generated following Cl<sup>-</sup> reconstitution in pH 10/Cl<sup>-</sup>-depleted PS-II (not shown) which confirmed that the ability to generate the  $S_3$  EPR signal was a Cl<sup>-</sup>

reconstitution of the  $S_2$  multiline signal and the oxygen evolving activity to about 80 % of those determined after addition of a high concentration of Cl<sup>-</sup> (20 mM).

Dark-adaptation of the pH 10/Cl<sup>-</sup>-depleted PS-II samples at room temperature for 35 min. resulted in the decay of the  $S_2$   $g = 4$  signal in most of the centers. After this dark-adaptation treatment most of the centers were in  $S_1$  since after addition of Cl<sup>-</sup> (50 mM), a normal  $S_2$  multiline signal was generated in these samples by continuous illumination at 200 K or by illumination with a single flash at room temperature, (not shown, but see e.g. Figure 5c).

Illumination of dark-adapted pH 10/Cl<sup>-</sup>-depleted PS-II with a single flash resulted in the formation of the  $S_2$   $g = 4$  signal (Figure 6A). Following illumination with two flashes, the  $S_2$   $g = 4$  signal intensity was similar to that observed after one flash. In addition, a narrow signal around  $g = 2$  was generated, corresponding to the formal  $S_3$  state (Figure 6A). Part of this signal shows a peak to trough width of about 16.4 mT [Figure 6 (inset)]. The width

depletion effect (and not the result of inadvertent  $\text{Ca}^{2+}$  depletion occurring in addition to  $\text{Cl}^-$  depletion).

Following illumination with multiple flashes (Figure 6A) or with continuous illumination at 0 °C (Figure 6B), the intensity of the  $g = 4$  signal was only slightly lower than of that formed after one flash. The EPR signal attributed to  $S_3$  was decreased after the illumination treatments but was still detected under these conditions. The significance of this decrease is unknown, however, a similar decrease in the intensity of the  $S_3$  signal was recently observed in  $\text{Ca}^{2+}$ -depleted PS-II upon multiple flash illumination [60].

The results indicate that at least a fraction of pH 10/ $\text{Cl}^-$ -depleted PS-II centers gives rise to the  $S_3$  signal after two flashes. The  $S_3$  to  $S_0$  transition in these centers seemed to be largely inhibited as is the case after  $\text{Cl}^-$  depletion of PS-II by treatment with  $\text{SO}_4^{2-}$  [12] or  $\text{F}^-$  [26]. Nevertheless, the observation that the  $S_2$   $g = 4$  signal is rather insensitive to a second flash or further illumination treatments raises the question whether the  $S_2$   $g = 4$  and  $S_3$  EPR signals originate from common or different centers. Relevant to this question is the observation (not shown) that the  $g = 4$  signal in pH 10/ $\text{Cl}^-$ -depleted PS-II, was much smaller when illumination treatments were done in the presence of high concentrations (1 mM) of PPBQ. In contrast, the  $S_3$  signal intensity was significantly less affected by PPBQ. This indicates that the centers exhibiting the  $S_2$   $g = 4$  signal were different from those in which an  $S_3$  signal was generated. The effect of a high concentration of PPBQ is tentatively attributed to the reduction of the Mn cluster in the centers exhibiting the  $g = 4$  signal, presumably due to the presence of  $\text{PPBQH}_2$ . In fact, the experiments from Figure 6 were done using low concentrations of PPBQ (50-100  $\mu\text{M}$ ) in the presence of ferricyanide (50-100  $\mu\text{M}$ ) to avoid such an effect.

*The effects of  $\text{SO}_4^{2-}$  and  $\text{F}^-$  in pH 10/ $\text{Cl}^-$ -depleted PS-II.*  $\text{Cl}^-$  depletion in PS-II is often done in the presence of the counter anions  $\text{SO}_4^{2-}$  (see e.g. [39]) or  $\text{F}^-$  (see e.g. [26]) which are thought to enhance  $\text{Cl}^-$  depletion from PS-II [6]. The  $S_2$  multiline signal intensity has been reported to diminish after  $\text{Cl}^-$  depletion of PS-II in the presence of these anions (see e.g. [26,39]). In addition, the anion  $\text{F}^-$  seems to specifically enhance the  $S_2$   $g = 4$  signal (see e.g. [40,43]). Figure 7 shows the effects of addition (at pH 7.3) of  $\text{SO}_4^{2-}$  (20 mM) or  $\text{F}^-$  (25 mM) on the EPR properties of  $S_2$  in pH 10/ $\text{Cl}^-$ -depleted PS-II, detected at pH 6.3. In comparison to the control sample (Figure 7a, see also Figure 5a, b), the anion  $\text{SO}_4^{2-}$  largely inhibited detection of the  $S_2$   $g = 4$  signal (Figure 7b). The anion  $\text{F}^-$ , however, had little effect under these conditions (Figure 7c).

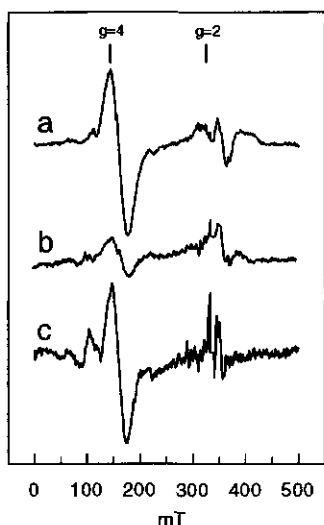


Figure 7. EPR difference spectra of PS-II after (a) pH 10/Cl<sup>-</sup> depletion (see Figure 5b) followed by (b) addition of SO<sub>4</sub><sup>2-</sup> (20 mM) or (c) addition of F<sup>-</sup> (25 mM) as described in Materials and Methods and resuspension in 10 mM MES (pH 6.3) and 0.5 M sucrose. The spectra were recorded after illuminated at 200 K for 4 min. and followed by subtraction of the dark baseline spectrum recorded prior to pH 10/Cl<sup>-</sup> depletion [see e.g. Figure 5a (thin)]. Instrument settings were as in Figure 2.

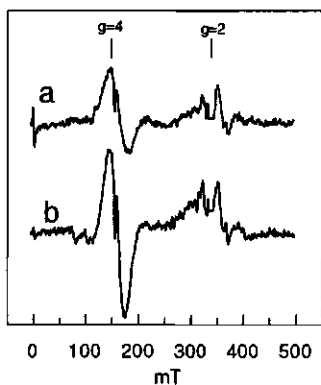


Figure 8. EPR difference spectra of pH 10/Cl<sup>-</sup>-depleted PS-II as in Figure 7 except that after the pH 10 treatment the pH was lowered to pH 7.3 instead of pH 6.3 and the resuspension solution was buffered with 10 mM HEPES (pH 7.3). (a) no additions or (b) following addition of F<sup>-</sup> (25 mM) in the dark.

Several studies in the literature on Cl<sup>-</sup>-depleted PS-II were done at pH 7.5 (see e.g. [39,44]. Figure 8 shows the effect of F<sup>-</sup> (25 mM) in pH 10/Cl<sup>-</sup>-depleted PS-II detected at pH 7.3. The S<sub>2</sub>  $g = 4$  signal of the F<sup>-</sup>-treated sample detected at pH 7.3 (Figure 8b) was similar to that detected at pH 6.3 (Figure 7a, Figure 5b). However, in absence of F<sup>-</sup> the S<sub>2</sub>  $g = 4$  signal intensity at pH 7.3 (Figure 8a) was only 50 % of that at pH 6.3. A similar decrease of the S<sub>2</sub>  $g = 4$  signal intensity was observed (not shown) after increasing the pH in the samples at pH 6.3 (see e.g. Figure 7a) by addition of 100 mM HEPES (pH 7.3). Thus, the S<sub>2</sub>  $g = 4$  signal intensity in pH 10/Cl<sup>-</sup>-depleted PS-II is pH-dependent and increases at lower pH. The F<sup>-</sup> anion affected the S<sub>2</sub> EPR properties in Cl<sup>-</sup>-depleted PS-II in a similar fashion to lowering the pH. Furthermore, this effect of F<sup>-</sup> (25 mM) also was observed (not shown) when SO<sub>4</sub><sup>2-</sup> (20 mM) was present. Thus, the effect of SO<sub>4</sub><sup>2-</sup> and increased pH on the EPR properties of S<sub>2</sub>, resulting in the suppression of the  $g = 4$  signal, was overridden by F<sup>-</sup>. Furthermore, at an increased pH, in the absence or presence of F<sup>-</sup>, the lifetime of the S<sub>2</sub>  $g = 4$  signal in pH 10/Cl<sup>-</sup>-depleted PS-II was similar to that determined at pH 6.3. The results indicate that the anions SO<sub>4</sub><sup>2-</sup> and F<sup>-</sup> have

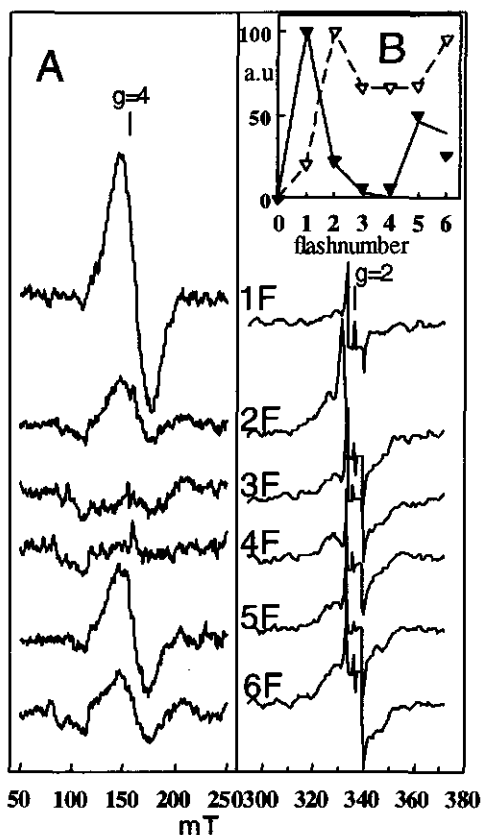


Figure 9. (A) Light minus dark spectra of pH 10/Cl<sup>-</sup>-depleted PS-II after reconstitution with F<sup>-</sup> (25 mM) and illumination with single flashes as in Figure 6 in the presence of ferricyanide (50-100  $\mu$ M) and PPBQ (50-100  $\mu$ M). (B) The intensities of ( $\blacktriangledown$ ) the  $g = 4$  signal determined as in Figure 2, and ( $--\blacktriangledown--$ ) of the signal around  $g = 2$  determined by double integration of the light-induced spectrum, plotted relative to the number of flashes. The continuous line was fitted assuming 10 %  $S_0$  and 90 %  $S_1$  before illumination, 6 % misses on the S-state transitions except for the  $S_3$  to  $S_0$  transition which was assumed to be accompanied by 45% misses (see also Discussion). The PS-II membranes were resuspended in 10 mM MES (pH 6.3), 0.5 M sucrose and 25 mM F<sup>-</sup>. Instrument settings were as in Figure 2.

distinct effects on the  $S_2$  EPR properties of pH 10/Cl<sup>-</sup>-depleted PS-II, resulting in  $S_2$  EPR properties similar to those observed after Cl<sup>-</sup> depletion in PS-II using these anions as counterions (see e.g. [40,41]).

The similarities between the  $S_2$   $g = 4$  signals observed in the absence and presence of F<sup>-</sup> in pH 10/Cl<sup>-</sup>-depleted PS-II samples led us to test if the  $S_2$   $g = 4$  signal in the presence of F<sup>-</sup> showed the same response to flash illumination as that in the absence of F<sup>-</sup> (Figure 6). The results are shown in Figure 9. After illumination of the F<sup>-</sup>-treated (25 mM), pH 10/Cl<sup>-</sup>-depleted PS-II with a single flash, an  $S_2$   $g = 4$  signal was generated similar to that in the absence of F<sup>-</sup>. After the second flash, the  $S_2$   $g = 4$  signal intensity in the F<sup>-</sup>-treated sample was significantly decreased indicating that an  $S_2$  to  $S_3$  transition occurred in most of the centers that exhibited the  $S_2$   $g = 4$  signal. In addition, a narrow signal around  $g = 2$  was generated corresponding to the formal  $S_3$  state (Figure 9), similar to that in pH 10/Cl<sup>-</sup>-depleted PS-II in the absence of F<sup>-</sup> (Figure 6). Illumination with further flashes indicated that the  $g = 4$  signal in



the F-treated sample shows a damped, flash-dependent oscillation with maximal intensities on the first and the fifth flash (Figure 9). Furthermore, although noisy and poorly resolved due to the presence of the dark-stable  $\text{Tyr}_{\text{D}}\bullet$  radical signal, the  $\text{S}_3$  signal showed a significant degree of a damped, flash-dependent oscillation with maximal intensities on the second and sixth flash (Figure 9).

The presence of oscillating EPR signals (albeit damped) in F-treated pH 10/ $\text{Cl}^-$ -depleted PS-II indicate functional enzyme turnover. This was confirmed by measurements of oxygen evolution. A study of the oxygen evolving activity versus light intensity (Figure 1) indicated that about 45 % of the centers in F-treated, pH 10/ $\text{Cl}^-$ -depleted PS-II (Figure 1, open triangles) were functional but were slowed down in the enzyme turnover by about a factor of 2 (in comparison to  $\text{Cl}^-$ -reconstituted,  $\text{Cl}^-$ -free washed PS-II: Figure 1, open circles). Thus, the results indicate that F- functionally replaced  $\text{Cl}^-$  to a large extent. The halides  $\text{I}^-$  [52] and  $\text{Br}^-$  [61] also are known to functionally replace  $\text{Cl}^-$ .

## Discussion

The results indicate that PS-II exhibits two distinct  $\text{Cl}^-$  dependent properties. These and further observations described in the Results are depicted in Figure 10. The distinct  $\text{Cl}^-$ -dependent properties of PS-II are most straightforwardly explained by considering the presence of two  $\text{Cl}^-$ -sites in PS-II, one of which is essential for oxygen evolving activity.

Some effects of salts on the functional properties of the oxygen evolving complex have been suggested to arise from conformational changes of PS-II by alterations of hydrophobic and/or electrostatic interactions on the protein surface of PS-II [62,63] (see also [64]). In general, such salt-induced effects on proteins occur at relatively high salt concentrations, ranging from tens of millimolar to molar concentrations (see e.g. [65,66]). The  $\text{Cl}^-$  dependent properties of PS-II observed at pH 6.3 could originate from such salt effects. However, reconstitution of the  $\text{S}_2$  multiline signal at the expense of the  $\text{S}_2$   $g = 4$  signal occurred at a relatively low  $\text{Cl}^-$  concentration with an apparent  $\text{Cl}^-$  affinity of  $\sim 0.8$  mM (Figure 4). Moreover, in contrast to  $\text{Cl}^-$ , the anions  $\text{SO}_4^{2-}$  (50 mM) and  $\text{F}^-$  (25 mM) added under similar conditions did not affect the  $\text{S}_2$  EPR properties in  $\text{Cl}^-$ -free washed PS-II. Thus, the  $\text{Cl}^-$ -dependent properties of PS-II at pH 6.3 (Figure 1-4) point to the presence of a  $\text{Cl}^-$ -binding site in PS-II which is not essential for oxygen evolution.

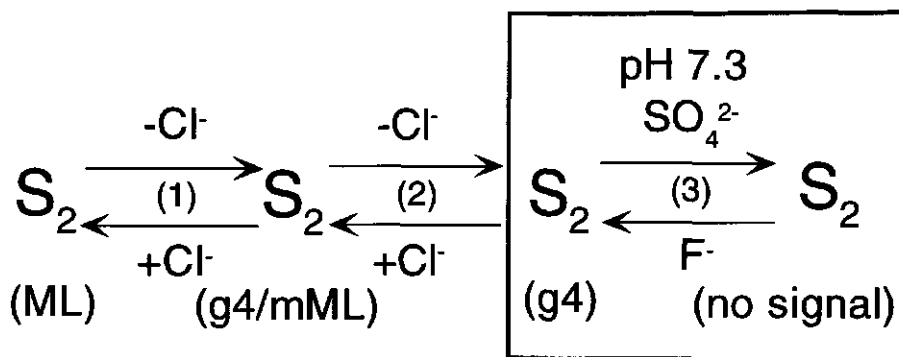


**Figure 10.** Schematic representation of the effects of  $\text{Cl}^-$  depletion treatments and the effects of anions on the EPR properties of  $\text{S}_2$  in PS-II. ML = regular multiline signal. mML = multiline signal with spectral modifications. g4= signal around  $g=4$ . Steps: (1)  $\text{Cl}^-$ -free washes of PS-II at pH 6.3-6.5/ $\text{Cl}^-$ -reconstitution (Figures 1-4). This treatment has a small effect on the enzyme kinetics. (2)  $\text{Cl}^-$  depletion of PS-II by treatment at pH 10, resulting in inhibition of oxygen evolution and a mixture of two types of centers as indicated in the box (Figures 5a,b; Figure 6; Figure 7a) which was either reversed by  $\text{Cl}^-$ -reconstitution (Figure 5c) or (3) further influenced by the pH (Figure 8a),  $\text{SO}_4^{2-}$  (Figure 7b) and  $\text{F}^-$  (Figures 7c, 8b). It is of note that in the presence of  $\text{F}^-$ , the  $\text{S}_2$   $g=4$  signal in pH 10/ $\text{Cl}^-$ -depleted PS-II originates from centers which are functionally different from those in absence of  $\text{F}^-$  (see text).

The oxygen evolving activity measured as a function of the light-intensity (Figure 1) indicated that depletion of the  $\text{Cl}^-$  at pH 6.3 which is not essential for oxygen evolution, inhibited the formation of the enzyme-substrate complex [67]. Since in this case light is considered to be the substrate, the results indicate that the removal of  $\text{Cl}^-$  at pH 6.3 lowered the quantum yield of water oxidation, reflecting the inhibition of any reversible process that is involved in charge accumulation. A slow down of electron transfer allowing charge recombination or enhanced deactivation of the higher S-states might be considered as possibilities.

The depletion of  $\text{Cl}^-$  from PS-II by high pH (pH 10) treatment resulted in only a residual oxygen evolving activity (see Results). It is considered that this reflects  $\text{Cl}^-$  depletion from the  $\text{Cl}^-$ -site in PS-II that has been studied in previous work on  $\text{Cl}^-$ -depleted PS-II [2]. This site probably corresponds to the slowly exchanging 1  $\text{Cl}^-$ /PS-II, identified by Lindberg *et al.* [68,69] that was detected from measurements of  $\text{Cl}^-$  release from  $^{36}\text{Cl}^-$  labelled PS-II at pH 6.3. The measurements by Lindberg *et al.* [69] were done after removal of the  $\text{Cl}^-$  from PS-II at pH 6.3. This pretreatment is essentially similar to the  $\text{Cl}^-$ -free washes used in this work. Thus, the other  $\text{Cl}^-$ -site, which is not obligatory for oxygen evolution (see above), would not have been detected by Lindberg *et al.* [69]. After complete release of the  $^{36}\text{Cl}^-$

from PS-II, Lindberg *et al.* (Ref. 69: Figure 5) observed significant oxygen evolving activity (30 %). The apparent lack of correlation between the slowly exchanging  $\text{Cl}^-$  and oxygen evolution implied that the  $\text{Cl}^-$  released was not required for oxygen evolution (Lindberg *et al.*, 1993). However, the observation by Lindberg *et al.* [69] of a residual oxygen evolving activity after long incubation is consistent with their earlier study [69] in PS-II isolated from spinach grown using  $^{36}\text{Cl}^-$  containing nutrients, which indicated the presence of a fraction of centers (30 %) containing  $\text{Cl}^-$  which was not exchangeable by incubation at pH 6.3. Since Lindberg *et al.* [69] used similar incubation conditions for  $^{36}\text{Cl}^-$  binding to normal PS-II membranes, it is very likely that the remaining oxygen evolving activity after complete release of  $^{36}\text{Cl}^-$  from PS-II (Ref. 69: Figure 5) corresponds to the fraction of unlabelled centers containing the non-exchangeable  $\text{Cl}^-$ . Thus, the most straightforward explanation of the results obtained by Lindberg *et al.* [68,69] is that the slowly exchanging 1  $\text{Cl}^-$  /PS-II is essential for oxygen evolving activity.

The  $S_2$   $g = 4$  signal in pH 10/ $\text{Cl}^-$ -depleted PS-II (Figure 5) was rather stable ( $t_{1/2} \approx 1.5$  h at  $0^\circ\text{C}$ ), unlike that observed in  $\text{Cl}^-$ -free washed PS-II. This may reflect a lowered oxidation potential of  $S_2$  after the pH 10/ $\text{Cl}^-$  depletion treatment. A greater stability of  $S_2$  in pH 10/ $\text{Cl}^-$ -depleted PS-II was also manifest as an upshifted emission temperature of the thermoluminescence from recombination of  $S_2Q_A^-$  and  $S_2Q_B^-$  [50,52].

The state giving rise to the  $S_2$   $g = 4$  signal in pH 10/ $\text{Cl}^-$ -depleted PS-II ( $\geq 40$  % of the centers) was rather insensitive to a second flash or further illumination treatments (Figure 6). Nevertheless, a fraction of centers exhibited a narrow signal around  $g = 2$  (Figure 6) corresponding to the formal  $S_3$  state (Figure 6). The results indicated that this fraction of centers is distinct from that exhibiting the  $S_2$   $g = 4$  signal. This implies that in the centers exhibiting the  $S_2$   $g = 4$  signal (Figure 5, Figure 6), the  $S_2$  to  $S_3$  transition was blocked. Thus the  $S_2$  state, in the fraction of centers that was able to advance to  $S_3$  probably corresponds to a state that was not detected by EPR, as is the case after  $\text{Cl}^-$  depletion of PS-II in the presence of  $\text{SO}_4^{2-}$  [12,39,41].

The results showed that the addition of the anions  $\text{SO}_4^{2-}$  and  $\text{F}^-$  to pH 10/ $\text{Cl}^-$ -depleted PS-II affected the  $S_2$   $g = 4$  signal intensity (Figure 7, Figure 8) and resulted in  $S_2$  EPR properties which were similar to those observed after  $\text{Cl}^-$  depletion in PS-II using these anions as counterions (see e.g. [40,41]). These effects and those of the pH (Figure 8) probably reflect alterations in the relative contributions of the states giving rise to an  $S_2$   $g = 4$  signal and the

'EPR-undetected'  $S_2$  state (Figure 10). Boussac and Rutherford [41] have proposed that generation of the modified, 'EPR-undetected'  $S_2$  state in Cl<sup>-</sup>-depleted PS-II is accompanied by oxidation of an amino acid residue instead of Mn oxidation, due to a Cl<sup>-</sup>-dependent redox equilibrium between the Mn cluster and a nearby amino acid residue. In the context of this model it can be speculated that this redox equilibrium is affected by the pH and the presence of other anions.

The addition of F<sup>-</sup> to pH 10/Cl<sup>-</sup>-depleted PS-II resulted in reconstitution of the oxygen evolving activity in almost 50 % of the centers. However, the enzyme turnover in the F<sup>-</sup>-reconstituted centers is significantly slowed down relative to the control sample (Figure 1), resulting in a 'residual' oxygen evolving activity (under nearly saturating light) of ~25 % relative to that after reconstitution with Cl<sup>-</sup>. Such 'residual' oxygen evolving activities in F<sup>-</sup>-reconstituted PS-II have been reported earlier [25,43,45,50]. It is quite possible that in these studies reconstitution effects of F<sup>-</sup> occurred similar to those observed in this work but were not detected since the oxygen evolving activity was not measured as a function of the light intensity.

The presence of a significant fraction of functional centers F<sup>-</sup>-reconstituted PS-II also was indicated by the flash-dependent (albeit damped) oscillation of the  $S_2$   $g = 4$  EPR signal and of the narrow EPR signal around  $g = 2$  corresponding to the formal  $S_3$  state (Figure 9). The results from fitting of the oscillating EPR signals from F<sup>-</sup>-reconstituted PS-II were consistent with those from the oxygen evolution versus light-intensity study (Figure 1) which indicated a fraction (~45 %) of oxygen evolving centers in which the enzyme turnover was slowed down and a fraction (~55 %) of inactive centers: (1) The oscillation pattern of the  $g = 4$  signal was best fit by assuming a relatively high miss factor of 40-45 % either on the  $S_3$  to  $S_0$  or on the  $S_0$  to  $S_1$  transition (Figure 9) which may suggest that the enzyme turnover is rate limiting on either of these transitions. (2) Although it is not very clear to what extent the functional and inactive centers contribute to the  $S_3$  EPR signal, reasonable fits to the flash-dependent  $S_3$  signal intensities were obtained by assuming that a significant fraction (50-60 %) of centers was functional and that the other fraction (40-50 %) of centers was blocked upon formation of  $S_3$  (not shown). Further characterization of the enzyme turnover of F<sup>-</sup>-reconstituted PS-II requires measurements of flash-dependent oxygen evolution.

$S_3$  signals are typically observed following inhibition of oxygen evolution by Ca<sup>2+</sup>-depletion treatments (e.g. [20]) or by treatments with F<sup>-</sup> [26], SO<sub>4</sub><sup>2-</sup> [12], NH<sub>3</sub> [27,28], or

acetate [29] which are thought to displace the functional  $\text{Cl}^-$  in PS-II. Recently, however, an  $\text{S}_3$  signal also has been reported in functional oxygen evolving PS-II in which  $\text{Ca}^{2+}$  and  $\text{Cl}^-$  were replaced by  $\text{Sr}^{2+}$  and  $\text{Br}^-$ , resulting in a slowing down of the enzyme turnover by a factor 4 (A. Boussac, presented at the E.S.F workshop 'Oxygen Evolution', Gif-sur-Yvette, France, November, 1994). The flash-dependent oscillation of the  $\text{S}_3$  EPR signal intensity observed in the present study in  $\text{F}^-$ -reconstituted PS-II, seems to indicate that the  $\text{S}_3$  EPR signal represents a transient intermediate involved in forward electron transfer or a sidepath component, which is oxidized in a redox equilibrium with the Mn cluster (e.g. [41]). Since  $\text{Cl}^-$  seems to be required for proton release [12,13], we speculate that the appearance of the  $\text{S}_3$  EPR signal is related to an inhibited or a slowed down deprotonation event.

Several reports have indicated that after removal of the 17- and 23 kDa extrinsic polypeptides by saltwashing, no or little  $g = 4$  signal can be generated from  $\text{S}_2$  [14,71,72]. Thus, the question arises whether the fraction (< 60 %) of centers exhibiting no signal from  $\text{S}_2$  after pH 10/ $\text{Cl}^-$  depletion treatment, lost the extrinsic polypeptides. Protein analysis by SDS-gel electrophoresis and subsequent Western blotting following  $\text{Cl}^-$ -free washes at pH 6.3, pH 10/ $\text{Cl}^-$ -depletion treatment and further incubation with  $\text{F}^-$  (25 mM) (see above), indicated the presence of the extrinsic polypeptides in nearly all the centers (not shown). Incubation of pH 10-treated PS-II with  $\text{SO}_4^{2-}$  (20 mM), however, resulted in a partial loss of the extrinsic polypeptides (not shown), i.e., 40 % loss of the 23 kDa and 70 % loss of the 17 kDa polypeptide (see also [19,69,72,73]). Thus, no correlation was observed between the  $\text{S}_2$  EPR properties in pH 10-treated PS-II and the presence/absence of the extrinsic polypeptides. However, it can not be excluded that the two types of centers in pH 10-treated PS-II exhibiting either the  $\text{S}_2$   $g = 4$  signal or no signal from  $\text{S}_2$ , reflect differences in the nature of binding of the extrinsic polypeptides to PS-II.

Figure 10 summarizes the conclusions from this work. Two  $\text{Cl}^-$  sites are considered to be present in PS-II. One of the sites is not essential for oxygen evolution and was previously ignored. This site is depleted of  $\text{Cl}^-$  by  $\text{Cl}^-$ -free washes at pH 6.3 [Figure 10, step (1)], resulting in a modified structure of the Mn cluster and a lowered quantum yield of water oxidation. A second  $\text{Cl}^-$ -site is essential for oxygen evolution and is equivalent to that studied in previous work on  $\text{Cl}^-$ -depleted PS-II. Depletion of  $\text{Cl}^-$  from this site by treatment at pH 10 [Figure 10, step (2)], results in two types of centers exhibiting either a  $g = 4$  signal or no signal from the  $\text{S}_2$  state. The  $\text{S}_2$   $g = 4$  signal shows an increased stability which may indicate

that the oxidation potential of the  $S_2$  state is lowered. The fraction of centers exhibiting the  $S_2$   $g = 4$  signal appears to be blocked on the  $S_2$  to  $S_3$  transition. A second and perhaps smaller fraction of centers exhibits no  $S_2$  EPR signal and is inhibited on the  $S_3$  to  $S_0$  transition. After formation of the formal  $S_3$  state in these centers, a narrow signal around  $g = 2$  is observed. The distribution of the two types of centers in pH 10/ $Cl^-$ -depleted PS-II is further influenced by the pH, and the anions,  $SO_4^{2-}$  and  $F^-$  [Figure 10, step (3)], resulting in EPR properties of the  $S_2$  state similar to those previously observed after  $Cl^-$  depletion of PS-II in the presence of these anions. These effects may be explained in the context of a model proposed earlier [41] by a redox equilibrium between the Mn cluster and a nearby amino acid residue, which is influenced by anions. The anion  $F^-$  is able to occupy the  $Cl^-$  site essential for oxygen evolution, resulting in reconstitution of oxygen evolving activity in a significant fraction of centers. The  $S_2$   $g = 4$  signal in  $F^-$ -reconstituted PS-II shows a damped flash-dependent oscillation and thus originates from centers which differ from those in the absence  $F^-$ .

### Acknowledgments

We thank Andreas Seidler for carrying out SDS-gel electrophoresis and Western blotting experiments and for critically reading the manuscript. We thank Peter H. Homann and Alain Boussac for their advice on experimental aspects. We thank Tjeerd J. Schaafsma for useful discussions.

### References

- 1 Kok, B., Forbush, B., & McGloin, M. (1970) *Photochem. Photobiol.* 11, 457-475.
- 2 Debus, R. J. (1992) *Biochim. Biophys. Acta* 1102, 269-352.
- 3 Rutherford, A. W., Zimmermann, J-L., & Boussac, A. (1992) in *The Photosystems: Structure, Function and Molecular Biology* (Barber, J., ed.) Chapter 5, pp 179-229, Elsevier Science Publishers, New York.
- 4 Murata, N., & Miyao, M. (1985) *Trends Biochem. Sci.* 10, 122-124.
- 5 Homann, P. H. (1988) *Photosynth. Res.* 15, 205-220.
- 6 Homann, P. H. (1987) *J. Bioenerg. Biomembranes* 19, 105-123.
- 7 Ghanotakis, D. F., Topper, J. N., Babcock, G. T. & Yocum, C. F. (1984) *FEBS Lett.* 170, 169- 173.
- 8 Ono, T., Nakayama, H., & Inoue, Y. (1988) *FEBS Lett.* 227, 147-152.
- 9 Boussac, A., & Rutherford, A. W. (1994) *Biochem. Soc. Trans.* 22, 352-358.
- 10 Boussac, A. & Rutherford, A. W. (1988) *FEBS Lett.* 236, 432-436.
- 11 Homann, P. H. (1988) *Biochim. Biophys. Acta.* 934, 1-13.
- 12 Boussac, A., Sétif, P., & Rutherford, A. W. (1992) *Biochemistry* 31, 1224-1234.

- 13 Lübbers, K., Drevenstedt, W., and Junge, W. (1993) *FEBS Lett.* 336, 304-308.
- 14 Van Vliet, P., Boussac, A., & Rutherford A.W. (1994) *Biochemistry* 33, 12998-13004.
- 15 Sandusky, P. O., & Yocum, C. F. (1984) *Biochim. Biophys. Acta* 766, 603-611.
- 16 Sandusky, P. O., & Yocum, C. F. (1986) *Biochim. Biophys. Acta* 849, 85-93.
- 17 Mei, R., & Yocum, C. F. (1993) *Photosynth. Res.* 38, 449-453.
- 18 Ghanotakis, D. F., Topper, J. N., & Yocum, C. F. (1984) *Biochim. Biophys. Acta.* 767, 524-531.
- 19 Homann, P. H. (1988) *Plant Physiol.* 88, 194-199.
- 20 Boussac, A., Zimmermann, J-L., & Rutherford, A. W. (1989) *Biochemistry* 28, 8984-8989.
- 21 Sivaraja, M., Tso, J., & Dismukes, G. C. (1989) *Biochemistry* 28, 9459-9464.
- 22 Boussac, A., Zimmermann, J-L., Rutherford, A. W., & Lavergne, J. (1990) *Nature* 347, 303-306.
- 23 Berthomieu, C. & Boussac, A., (1995) *Biochemistry* 34, 1541-1548.
- 24 Rutherford, A. W., & Boussac, A. (1992) in *Research in Photosynthesis* (Murata, N., ed.) Vol II, pp 21-27, Kluwer Academic Publishers, Dordrecht.
- 25 Gilchrist, M. L., Ball, Jr. A., Randall, D. W. & Britt, R. D. (1995) *Proc. Natl. Acad. Sci. (in press)*.
- 26 Baumgarten, J., Philo, J. S., & Dismukes, G. C. (1990) *Biochemistry* 29, 10814-10822.
- 27 Andréasson, L-E., & Lindberg, K. (1992) *Biochim. Biophys. Acta* 1100, 177-183.
- 28 Hallahan, B. J., Nugent, J. H. A., Warden, J. T., & Evans, M. C. W. (1992) *Biochemistry* 31, 4652-4573
- 29 MacLachlan, D. J., & Nugent, J. H. A. (1993) *Biochemistry* 32, 9772-9780.
- 30 Dismukes, G. C., & Siderer, Y (1981) *Proc. Natl. Acad. Sci. USA* 78, 274-278.
- 31 Brudvig, G. W., Casey, J. L., & Sauer, K. (1983) *Biochim. Biophys. Acta* 723, 366-371.
- 32 Britt, R. D., Lorigan, G. A., Sauer, K., Klein, M. P. & Zimmermann, J-L. (1992) *Biochim. Biophys. Acta* 1040, 95-101.
- 33 Astashkin, A. V., Kodera, Y., & Kawamori, A. (1994) *J. Magn. Res. B* 105, 113-119.
- 34 Smith, P. J., Åhring, K. A. & Pace, R. J. (1993) *J. Chem. Soc. Faraday Trans.* 89, 2863-2868.
- 35 Smith, P. J., & Pace, R. J. (1995), *Biochim. Biophys. Acta (in press)*.
- 36 dePaula, J. C., Innes, J. B., & Brudvig., G. W. (1985) *Biochemistry* 24, 8114-8120.
- 37 Zimmermann, J-L., & Rutherford A. W. (1986) *Biochemistry* 25, 4609-4615.
- 38 Hansson, Ö., Aasa, R., & Vänngård., T. (1987) *Biophys. J.* 51, 825-832.
- 39 Ono, T., Zimmermann, J-L., Inoue, Y., & Rutherford, A.W. (1986) *Biochim. Biophys. Acta* 851, 193-201.
- 40 Ono, T., Nakayama, H., Gleiter, H., Inoue, Y., & Kawamori, A. (1987) *Arch. Biochim. Biophys.* 256, 618-624.
- 41 Boussac, A., & Rutherford, A. W. (1994) *J. Biol. Chem.* 269, 12462-12467.
- 42 Damoder, R., Klimov, V. V., & Dismukes, G. C. (1986) *Biochim. Biophys. Acta* 848, 378-391
- 43 DeRose, V. J., Latimer, M. J., Zimmermann, J-L., Mukerji, I., Yachandra, V. K., Sauer, K., & Klein, M. P. (1995) *Chem. Phys.* 194, 443-459.
- 44 Beck, W. F., & Brudvig, G. W. (1988) *Chemica Scripta* 28A, 93-98.
- 45 Casey, J. L., & Sauer, K. (1984) *Biochim. Biophys. Acta* 767, 21-28.
- 46 Andréasson, L-E. (1990) In *Current Research in Photosynthesis* (Baltscheffsky M., ed.) Vol I, pp 785-788, Kluwer, Dordrecht.
- 47 Beck, W. F., & Brudvig, G. W. (1968) *Biochemistry* 25, 6479-6486.
- 48 Berthold, D. A., Babcock, G. T., & Yocum, C. F. (1981) *FEBS Lett.* 134, 231-234.

- 49 Ford, R. C., & Evans, M. C. W. (1983) *FEBS* 160, 159-164.
- 50 Homann, P. H. (1993) *Photosynth. Res.* 38, 395-400.
- 51 Homann, P.H. (1985) *Biochim. Biophys. Acta* 809, 311-319.
- 52 Rashid, A., & Homann, P. H. (1992) *Biochim. Biophys. Acta* 1101, 303-310.
- 53 Laemmli, U. K. (1970) *Nature* 227, 680-685.
- 54 Seidler, A. (1994) *Biochim. Biophys. Acta* 849, 73-79.
- 55 Zimmermann, J-L., & Rutherford A. W. (1984) *Biochim. Biophys. Acta* 767, 160-167.
- 56 Pace, R. J., Smith, P., Bramley, R., & Stehlik, D. (1991) *Biochim. Biophys. Acta* 1058, 161-170.
- 57 Styring, S., & Rutherford, A. W. (1988) *Biochim. Biophys. Acta* 933, 378-387.
- 58 Zimmermann, J-L., & Rutherford A. W. (1986) *Biochim. Biophys. Acta* 851, 416-423.
- 59 Diner, B. A., & Petrouleas, V. (1987) *Biochim. Biophys. Acta* 893, 138-148
- 60 Boussac, A., & Rutherford, A. W. (1995) *Biochim. Biophys. Acta*, 1230, 195-201.
- 61 Hind, G., Nakatani, H. Y., & Izawa, S. (1969) *Biochim. Biophys. Acta*. 172, 277-289.
- 62 Wydrzynski, T., Baumgart, F., MacMillan, F., Renger, G. (1990) *Photosynth. Res.* 25, 59-72.
- 63 Pauly, S., Schlopper, E., & Witt, H. T. (1992) *Biochim. Biophys. Acta* 1099, 203-210.
- 64 Kebekus, U., Messinger, J., & Renger, G. (1995) *Biochemistry* 34, 6175-6182.
- 65 von Hippel, P. H., & Schleich, T. (1969) *Accounts Chem. Res.* 9, 257-265.
- 66 Aviram, I. (1973) *Eur. J. Biochem.* 40, 631-636.
- 67 Hofstee, B. H. J. (1952) *Science* 116, 329-331.
- 68 Lindberg, K., Wydrzynski, T., Vänngård, T., & Andréasson, L-E. (1990) *FEBS Lett.* 264, 153-155.
- 69 Lindberg, K., Vänngård, T., & Andréasson, L-E. (1993) *Photosynth. Res.* 38, 401-408.
- 70 dePaula, J. C., Mark, P., Miller, A-F., Wu, B. W., & Brudvig., G. W. (1986) *Biochemistry* 25, 6487-6494.
- 71 Boussac, A. & Rutherford, A. W. (1988) *Biochemistry* 27, 3476-3483.
- 72 Beauregard, M., & Popovic, R. (1988) *J. Plant Physiol.* 133: 615-619.
- 73 Homann, P. H. (1992) *Photosynth. Res.* 33, 29-36.



## Properties of the Iodide-Reconstituted Oxygen Evolving Complex of Photosystem II studied by EPR.

Pieter van Vliet<sup>\*,†</sup>, Peter H. Homann<sup>+</sup> and A. William Rutherford<sup>†</sup>

<sup>†</sup>Section de Bioénergétique (URA CNRS 1290), Département de Biologie Cellulaire et Moléculaire, CEA Saclay, 91191 Gif-sur-Yvette, France, and Department of Molecular Physics, Agricultural University, Wageningen, The Netherlands and <sup>+</sup>Institute of Molecular Biophysics and Department of Biological Sciences, Florida State University, Tallahassee, FL.

Key Words: photosynthesis, oxygen evolution, charge accumulation states, Cl<sup>-</sup>, I<sup>-</sup>, electron paramagnetic resonance.

The properties of photosystem II (PS-II)-enriched membranes PS-II have been investigated by electron paramagnetic resonance spectroscopy (EPR) following replacement of the Cl<sup>-</sup> essential for oxygen evolution by I<sup>-</sup>. The level of oxygen evolution measured in I<sup>-</sup>-treated PS-II was nearly similar to that after Cl<sup>-</sup>-reconstitution in agreement with previous investigations in I<sup>-</sup>-activated PS-II [Rashid, A., & Homann, P. H. (1992) *Biochim. Biophys. Acta* 1101, 303-310; Homann, P. H. (1993) *Photosynth. Res.* 38, 395-400], indicating that I<sup>-</sup> is an activator of oxygen evolution. A fraction (20-50 %) of I<sup>-</sup>-activated PS-II exhibited an S<sub>2</sub> g = 4 EPR signal. Flash experiments showed that the S<sub>2</sub> g = 4 signal oscillates with a period of four in a similar fashion to that observed previously in Cl<sup>-</sup>-active PS-II. However, the S<sub>2</sub> state in I<sup>-</sup>-activated PS-II was strikingly modified in that no S<sub>2</sub> multiline signal could be generated. These results point to a majority of oxygen evolving, I<sup>-</sup>-activated centers exhibiting neither an S<sub>2</sub> g = 4 nor an S<sub>2</sub> multiline signal. The normal S<sub>2</sub> multiline EPR signal was reconstituted by addition of Cl<sup>-</sup> (25 mM). This Cl<sup>-</sup>-reconstitution effect required, however, relatively long incubation (30 min.). This is interpreted as indicating a slow anion exchange in the Cl<sup>-</sup>-site

\* To whom correspondence should be addressed. CEA Saclay, Tel: 33-1-69-08-29-40; Fax: 33-1-69-08-87-17.

essential for oxygen evolution. Addition of the solvent ethanol (4 % v/v) eliminated the I-induced modifications of S<sub>2</sub> and the normal S<sub>2</sub> EPR spectrum could be generated. However, no effects of ethanol were observed in pH 10/Cl<sup>-</sup>-depleted and F<sup>-</sup>-treated PS-II both of which exhibited an intense g = 4 signal in the S<sub>2</sub> state. These results indicate that the effects of ethanol on the S<sub>2</sub> EPR properties are modulated by the anion occupying the Cl<sup>-</sup> site essential for oxygen evolution.

## Introduction

Photosynthetic water oxidation, resulting in the formation of molecular oxygen and the release of protons, is catalyzed at the donor side of the membrane-spanning photosystem II protein complex (PS-II)<sup>1</sup>. This process is thought to occur in an enzyme cycle consisting of five intermediate oxidation states designated S<sub>0</sub> to S<sub>4</sub>, where the subscript is the number of accumulated oxidizing equivalents [1]. A cluster of probably four manganese ions plays a central role in this redox cycle. The kinetic properties of the Mn oxidation states under different experimental conditions have been characterized in detail (reviewed in Refs. 2 and 3). In addition, Ca<sup>2+</sup> and Cl<sup>-</sup> are essential for oxygen evolving activity (see e.g. Ref. 4 for a review). Three extrinsic polypeptides of 33, 23 and 17 kDa, present at the luminal side of PS-II contribute to the stability of the oxygen evolving enzyme but are not essential for oxygen evolving activity (reviewed in Ref. 5). The 33 kDa polypeptide stabilizes the Mn cluster. The 17- and 23 kDa polypeptides play a role in retention of functional Ca<sup>2+</sup> and Cl<sup>-</sup> [5,6].

In untreated PS-II, the EPR spectrum of the S<sub>2</sub> state is dominated by a characteristic multiline EPR signal at g = 2 [7]. This signal can be generated by illumination treatments allowing for a single stable charge separation, e.g., illumination with a single flash at room temperature [7], or with continuous illumination at 200 K [8]. The multiline EPR signal from S<sub>2</sub> seems to be related to functional binding of Cl<sup>-</sup> to PS-II. This is indicated by the loss of the ability to generate the S<sub>2</sub> multiline signal following inhibition of oxygen evolution by Cl<sup>-</sup> depletion in the presence of SO<sub>4</sub><sup>2-</sup> [9-12] or F<sup>-</sup> [13-16]. After inhibition of oxygen evolution

---

<sup>1</sup> Abbreviations: PS-II, the photosystem II protein complex; Tyr<sub>D</sub>, side-path electron donor of PS-II responsible for EPR signal II<sub>slow</sub>; Q<sub>A</sub>, Q<sub>B</sub>, primary and secondary quinone electron acceptors of PS-II; Chl; chlorophyll; CW, continuous wave; EPR, electron paramagnetic resonance; CAPS, 3-(cyclohexylamino)-1-propane sulphonic acid; HEPES, 4-(2-hydroxyethyl)-1-piperazineethane sulphonic acid; MES, 4-(N-morpholino)ethanesulphonic acid; PPBQ, phenyl-p-benzoquinone.

by  $\text{Cl}^-$  depletion in the presence of  $\text{SO}_4^{2-}$ , a modified  $\text{S}_2$  state was generated which was not detected by EPR and was converted to the normal  $\text{S}_2$  state by rapid addition of  $\text{Cl}^-$  in darkness, resulting in the reconstitution of the  $\text{S}_2$  multiline EPR signal [9,12].

Under certain conditions the  $\text{S}_2$  state also exhibits a signal around  $g = 4$ . The  $\text{S}_2$   $g = 4$  and  $\text{S}_2$  multiline signal probably originate from two different structural states of the oxygen evolving complex with different magnetic properties of the Mn cluster [17-19]. This has been concluded partly on the basis of EPR studies of untreated PS-II in the presence of sucrose. Under these conditions the  $\text{S}_2$   $g = 4$  signal was converted to the  $\text{S}_2$  multiline signal following addition of the cryoprotectants glycerol or ethylene glycol or the solvent ethanol [18,19]. The origin of the influences of these solutes on the  $\text{S}_2$  EPR properties is unknown but these effects seem to vary depending on the experimental conditions (see e.g. Refs. 13 and 20).

After  $\text{Cl}^-$ -depletion in PS-II by pH 10 treatment, two types of centers were observed, one type showing an intense  $\text{S}_2$   $g = 4$  signal and a second type exhibiting no EPR signal in  $\text{S}_2$  [21]. The proportion of these types of centers was influenced by the anions  $\text{SO}_4^{2-}$  or  $\text{F}^-$  resulting in EPR properties of the  $\text{S}_2$  state similar to those reported earlier following  $\text{Cl}^-$  depletion treatment of PS-II in the presence of these anions [21]. A striking observation in that study was that the addition of  $\text{F}^-$  to pH 10/ $\text{Cl}^-$ -depleted PS-II resulted in reconstitution of oxygen evolving activity in a significant fraction ( $\sim 50\%$ ) in which, however, the enzyme turnover was slowed down [21].

The addition of  $\text{I}^-$  to  $\text{Cl}^-$ -depleted PS-II has been shown to result in reconstitution of oxygen evolution to an extent only slightly diminished in comparison to that observed after addition of  $\text{Cl}^-$ , indicating that  $\text{I}^-$  is able to functionally replace the  $\text{Cl}^-$  essential for oxygen evolution [22,23]. This was also indicated by the flash-dependent oscillation of the emission temperature of the thermoluminescence from the charge recombination reaction with  $\text{Q}_\text{B}^-$  [22,23]. Nevertheless, the  $\text{S}_2$  state in  $\text{I}^-$ -reconstituted PS-II was modified in that the emission temperature of the thermoluminescence from recombination of  $\text{S}_2\text{Q}_\text{A}^-$  and  $\text{S}_2\text{Q}_\text{B}^-$  was upshifted in comparison to that in untreated and  $\text{Cl}^-$  reconstituted PS-II [22,23]. This was taken as an indication that the  $\text{S}_2$  state in  $\text{I}^-$ -reconstituted exhibits a lowered redox potential and is more stable than that in untreated PS-II [22,23].

In this report the charge accumulation properties in  $\text{I}^-$ -activated PS-II were investigated by EPR.

## Materials and methods

Photosystem II-enriched membranes were prepared according to the method of Berthold et al. [24] with the modifications of Ford and Evans [25]. The oxygen evolving activity of these membranes was  $\sim 500 \mu\text{M O}_2/\text{mg chlorophyll/h}$ . Prior to use for further treatments (see below), the PS-II membranes were stored at  $-80^\circ\text{C}$  in a buffer solution containing 25 mM MES (pH 6.5), 0.3 M sucrose and 10 mM NaCl.

$\text{Cl}^-$  depletion in PS-II was done by a short treatment at pH 10 (see below) as described by Homann [23]. The principle of the  $\text{Cl}^-$  depletion treatment is based on the idea that the 17- and 23 kDa extrinsic polypeptides are involved in retention of  $\text{Cl}^-$  in the functional site [6,26]. The short treatment at pH 10 is thought to induce a transient dissociation of the 17- and 23 kDa extrinsic polypeptides resulting in the release of  $\text{Cl}^-$  from its site [6,26]. That the pH 10 treatment results in the specific release of the  $\text{Cl}^-$  essential for oxygen evolution is indicated by the extensive,  $\text{Cl}^-$  reversible inhibition of oxygen evolution (see Results and Ref. 21), whereas the extrinsic polypeptides are associated to nearly all the centers [21].

Prior to the pH 10 treatment, the  $\text{Cl}^-$  concentration in untreated PS-II membranes was lowered by three washes (resuspension, dilution and centrifugation) in a  $\text{Cl}^-$  free buffer solution containing 5 mM MES (pH 6.3) and 0.5 M sucrose. These PS-II membranes are referred to as  $\text{Cl}^-$ -free washed PS-II. The oxygen evolving activity of the  $\text{Cl}^-$ -free washed PS-II membranes measured in the presence of  $\text{Cl}^-$  (10 mM) was about 85 % relative to that in untreated PS-II indicating a fraction (15 %) of irreversible inhibition after the  $\text{Cl}^-$ -free washes, probably due to Mn release from the functional site of PS-II as indicated by the appearance of a small 6-line signal around  $g = 2$  in the EPR spectrum originating from hexaquomanganese (II) (not shown).

Following resuspension and dilution of the  $\text{Cl}^-$ -free washed PS-II membranes to a chlorophyll concentration of 125  $\mu\text{g/ml}$  in a buffer-free solution containing 0.4 M sucrose, the pH was increased to pH 10 by addition of 15 mM (15  $\mu\text{l/ml}$  of 1.0 M) CAPS (pH 10). After 10-35 sec. of incubation at pH 10, the pH was lowered to pH 7.3 by adding 45 mM (45  $\mu\text{l/ml}$  of 1.0 M) HEPES (pH 7.3) and, unless stated otherwise, directly followed by lowering the pH to pH 6.3 by adding 45 mM (45  $\mu\text{l/ml}$  of 1.0 M) of unneutralized MES followed by 10 min.

incubation. Addition of anions (as their sodium salt) to pH 10/Cl<sup>-</sup>-depleted PS-II were done at pH 7.3, i.e. under conditions in which irreversible inhibition of oxygen evolution is minimized and yet PS-II is still sensitive to treatments that affect Cl<sup>-</sup>-dependent oxygen evolving activity [22,23]. Following 10-20 min. incubation, the pH was lowered to pH 6.3 as described above. The pH 10 treatment and addition of anions was done while stirring at 4 °C under dim room light.

I<sup>-</sup>-treatment of PS-II was done by addition of 20 mM I<sup>-</sup> following pH 10/Cl<sup>-</sup> depletion under conditions described above. Following this treatment, the I<sup>-</sup> concentration was lowered by an additional wash in a Cl<sup>-</sup>-free buffer solution containing 0.5 M sucrose and 5 mM MES (pH 6.3) to minimize possible inhibitory iodination [27,28]. The successfulness of I<sup>-</sup>-insertion in PS-II was probed by the I<sup>-</sup>-reconstituted oxygen evolution and the upshift of the thermoluminescence band related to the recombination reaction with S<sub>2</sub> [22,23].

The membranes were resuspended at 2.5-8 mg chlorophyll/ml, put in calibrated quartz EPR tubes, dark-adapted, frozen in the dark and stored in liquid nitrogen until used for EPR measurements. Further additions to these membranes were done in the EPR tube in the dark after thawing. Illumination of the samples was done following addition in darkness of the external electron acceptor PPBQ dissolved in dimethyl sulphoxide.

Continuous illumination of the samples was done, using an 800 W projector through 2 cm water and an infrared filter, in a non-silvered Dewar flask containing ethanol cooled to 198 K with solid CO<sub>2</sub> or cooled to 0 °C with liquid nitrogen. Flash illumination at room temperature was provided from an Nd-Yag laser (15 ns, 300 mJ, 532 nm).

EPR spectra were recorded at liquid helium temperatures with a Bruker ER 200 X-band spectrometer equipped with an Oxford Instruments cryostat. The relative amount of centers exhibiting Tyr<sub>D</sub><sup>•</sup> was determined on the basis of EPR measurements at unsaturating microwave powers.

Oxygen evolution was measured by using a Clark-type electrode, at 25 °C under continuous light. The measurements were done under near saturating light at a chlorophyll concentration of 20 µg/ml and 0.5 mM PPBQ was added as an external electron acceptor.

## Results

*The effects of I<sup>-</sup> in pH 10/Cl<sup>-</sup>-depleted PS-II.* The oxygen evolving activity of pH 10/Cl<sup>-</sup>-depleted PS-II was 15 % relative to that after reconstitution with Cl<sup>-</sup> (10 mM). The Cl<sup>-</sup>-reconstituted (10 mM) oxygen evolving activity was about 90 % relative to that after Cl<sup>-</sup>-free washes (see Materials and Methods) prior to pH 10/Cl<sup>-</sup>-depletion treatment. After treatment of pH 10/Cl<sup>-</sup>-depleted PS-II with I<sup>-</sup>, the oxygen evolving activity was reconstituted to 80 % of that observed after reconstitution with Cl<sup>-</sup>. In both the I<sup>-</sup> and Cl<sup>-</sup>-activated PS-II the initial rate of oxygen evolution was constant for 2 min., a feature similar to that observed in untreated PS-II. The residual oxygen evolving activity in pH 10/Cl<sup>-</sup>-depleted PS-II, however, was lost relatively rapidly during the measurement with a half inhibition time of 24 s. These results are in agreement with earlier reports on I<sup>-</sup>-activated PS-II [22,23] and indicate that I<sup>-</sup> is able to functionally replace the Cl<sup>-</sup> essential for oxygen evolution.

Figure 1 shows the EPR spectra induced by continuous illumination at 200 K of pH 10/Cl<sup>-</sup>-depleted PS-II (Figure 1a), Cl<sup>-</sup>-reconstituted PS-II (Figure 1b) and I<sup>-</sup>-activated PS-II (Figure 1c). The EPR spectrum in pH 10/Cl<sup>-</sup>-depleted PS-II showed an intense S<sub>2</sub> g = 4 signal and no S<sub>2</sub> multiline signal (Figure 1a) as reported recently [21]. After reconstitution with Cl<sup>-</sup> (20 mM), a normal S<sub>2</sub> EPR spectrum was observed giving rise to a normal S<sub>2</sub> multiline signal and a small S<sub>2</sub> g = 4 signal (Figure 1b). In contrast to Cl<sup>-</sup>-reconstituted PS-II, I<sup>-</sup>-activated PS-II showed little or no S<sub>2</sub> multiline signal and a relatively intense S<sub>2</sub> g = 4 signal (Figure 1c). The S<sub>2</sub> g = 4 signal intensity in I<sup>-</sup>-activated PS-II was only half of that observed in pH 10/Cl<sup>-</sup>-depleted PS-II.

The spectral properties (i.e. shape and g-value) of the S<sub>2</sub> g = 4 signal in I<sup>-</sup>-activated PS-II were similar to those of the S<sub>2</sub> g = 4 signal in pH 10/Cl<sup>-</sup>-depleted and untreated PS-II. The stability of the S<sub>2</sub> g = 4 signal in I<sup>-</sup>-activated PS-II was similar to that observed in untreated PS-II (t<sub>1/2</sub>=3-4 min. at room temperature in the presence of 1 mM PPBQ) (not shown). After dark-adaptation of I<sup>-</sup>-activated PS-II at 0 °C (in the absence of PPBQ) for 30 min., no S<sub>2</sub> g = 4 signal was observed. With respect to this property, I<sup>-</sup>-activated PS-II resembles untreated PS-II and is distinct from pH 10/Cl<sup>-</sup>-depleted PS-II which exhibits an S<sub>2</sub> g = 4 signal which is more stable in the dark (t<sub>1/2</sub> ~ 1.5 h at 0 °C and ~ 10 min. at room temperature, in the absence of PPBQ) [21].

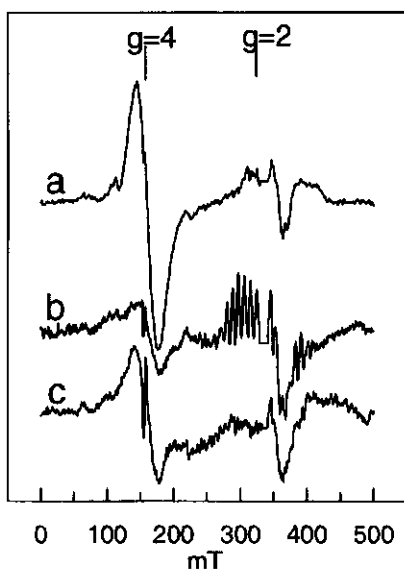


Figure 1. Light minus dark EPR spectra of PS-II membranes that were illuminated for 3 min. at 200 K following (a) pH 10/Cl<sup>-</sup>-depletion and subsequent addition of (b) 20 mM Cl<sup>-</sup> or (c) 20 mM I<sup>-</sup>. The PS-II membranes were (a) resuspended, or (b, c) washed once and resuspended in 10 mM MES (pH 6.3) and 0.5 M sucrose. The samples were illuminated in the presence of (a) 100  $\mu$ M PPBQ and 100  $\mu$ M ferricyanide or (b, c) in the presence of 1 mM PPBQ. Instrument settings: 9.42 GHz; modulation amplitude, 2.2 mT; temperature, 10 K; microwave power, 31 mW.

EPR signal at  $g \approx 3.0$  originating from the  $g_x$  component of oxidized low-spin cytochrome b<sub>559</sub> (not shown). This seems to indicate that in a significant fraction of I-activated centers (40-70 %), illumination at 200 K resulted in the oxidation of a component which was not detected by EPR.

It has recently been shown that pH 10/Cl<sup>-</sup>-depletion in PS-II results in a distribution of two types of centers, one type showing an S<sub>2</sub> g = 4 signal whereas the other exhibited no EPR signal from S<sub>2</sub> [21]. This distribution was shown to be influenced by the presence of anions, whereby SO<sub>4</sub><sup>2-</sup> appeared to suppress the S<sub>2</sub> g = 4 signal [21] resulting in an S<sub>2</sub> EPR spectrum similar to that previously observed after Cl<sup>-</sup> depletion in PS-II in the presence of SO<sub>4</sub><sup>2-</sup> [9,12].

The S<sub>2</sub> g = 4 signal in I-activated PS-II is estimated to represent 20-50 % of the centers (for estimation of the S<sub>2</sub> g = 4 signal intensity versus the amount of centers, see Ref. 21). Despite the smaller intensity of the S<sub>2</sub> g = 4 signal, following continuous illumination at 200 K of I-activated PS-II, an Q<sub>A</sub>-Fe<sup>2+</sup> EPR signal at g = 1.90 (350 mT) was generated (Figure 1c) showing an intensity similar to that generated under comparable conditions in untreated PS-II (not shown) and Cl<sup>-</sup>-reconstituted PS-II (Figure 1b). Thus the yield of stable charge separation at 200 K in I-activated PS-II seems to be similar to that of untreated and Cl<sup>-</sup>-reconstituted PS-II. Furthermore, as is the case in Cl<sup>-</sup>-reconstituted PS-II, the illumination resulted in the formation of only a small amount (5 %) of a narrow free radical signal usually attributed to Chl<sup>+</sup>, a small increase (5 %) of the Tyr<sub>D</sub><sup>•</sup> EPR signal, and a slight increase (5 %) of the

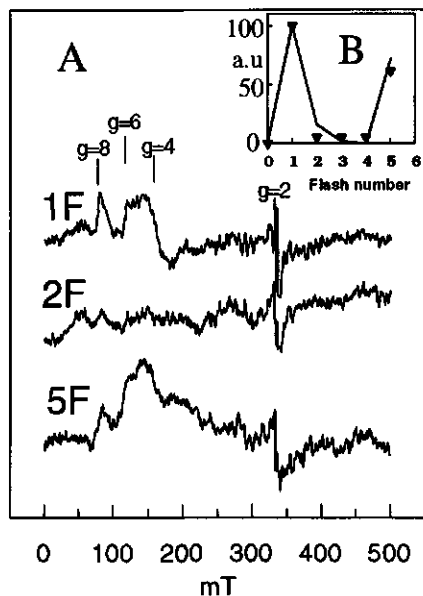


Figure 2. (A) Light minus dark EPR spectra of I-activated PS-II membranes in 5 mM MES (pH 6.3) and 0.3 M sucrose, after illumination with single flashes at room temperature in the presence of PPBQ (1 mM), followed by rapid (1s) freezing in darkness. (B) The intensities of ( $\blacktriangledown$ ) the signal at  $g = 4$  plotted relative to the number of flashes. The  $g = 4$  signal intensity was determined from the peak to trough amplitude. The continuous line was fit assuming 100 %  $S_1$  before illumination, 8 % misses and no double hits. Before addition of PPBQ (1 mM) and subsequent flash illumination, the dark-adapted samples were synchronized according to the method in [33] by illumination with a preflash followed by dark-adaptation for 15 min. at room temperature. Instrument settings were as in Figure 1.

It is reasonable to suggest that such a situation also exists in I-activated PS-II and that a significant fraction of centers in this case does not exhibit an  $S_2$  EPR signal.

Flash-illumination at room temperature of I-activated PS-II resulted in a flash-dependent oscillation of the  $S_2$   $g = 4$  signal with maximal intensities on the first and the fifth flash (Figure 2), indicating that this signal arises from centers that undergo the normal charge accumulation cycle. A similar flash-dependent oscillation of the  $S_2$   $g = 4$  signal has been observed earlier [18,29] (see also Ref. 21). The results shown in Figure 2 are consistent with the observed I-activated oxygen evolution and the flash-dependent oscillation of the thermoluminescence bands characteristic of the charge recombination reactions involving the  $S_2$  and  $S_3$  states observed earlier [22,23].

EPR signals at  $g = 8$  (82 mT) and  $g = 6$  (120 mT) are also evident in Figure 2, showing a binary oscillation with flash number in similar fashion to those observed in untreated PS-II under comparable conditions [29] (see also Ref. 21). These EPR signals have been ascribed to the oxidized non-heme iron  $Fe^{3+}$  (reviewed in Ref. 30). The oxidation of the non-heme iron has been shown to occur as a result of electron donation from  $Q_A^-$  to PPBQ resulting in the formation of the semiquinone form of PPBQ. This semiquinone, which is a good oxidant, oxidizes the non-heme iron giving rise to  $Fe^{3+}$  [29]. The intensities of the oxidized non-heme



iron EPR signals observed following flash-illumination of I<sup>-</sup>-activated PS-II, were similar to those observed in untreated PS-II under comparable conditions. These results indicate that the majority of centers in I<sup>-</sup>-activated PS-II undergoes the normal charge accumulation cycle and further indicate that a significant fraction of centers does not exhibit an S<sub>2</sub> EPR signal.

In pH 10/Cl<sup>-</sup>-depleted PS-II, a narrow EPR signal around  $g=2$ , corresponding to the formal S<sub>3</sub> state, was observed after illumination at room temperature with two flashes or by continuous illumination at 0 °C [21]. However, very little (if any) of this signal could be detected following flash illumination (Figure 2) or continuous illumination (not shown) of I<sup>-</sup>-activated PS-II, indicating that I<sup>-</sup> activation reversed the effect of pH 10/Cl<sup>-</sup> depletion on the S<sub>3</sub> EPR properties, in a similar fashion to Cl<sup>-</sup> reconstitution [21].

We showed earlier that washing of untreated PS-II in a Cl<sup>-</sup>-free buffer solution (pH 6.3) results in an altered distribution of structural states manifest as an increased S<sub>2</sub>  $g = 4$  signal at the expense of the S<sub>2</sub> multiline signal, originating from oxygen evolving centers with slightly modified enzyme kinetics [21]. In addition, these effects were rapidly reversed by readdition of Cl<sup>-</sup> and mixing (30 s). This was taken as indicating that the Cl<sup>-</sup>-free washes resulted in the loss of Cl<sup>-</sup> from a low affinity Cl<sup>-</sup>-binding site not essential for oxygen evolution [21]. Further experiments (not shown) indicated that the properties of this non-essential Cl<sup>-</sup>-site were virtually unaffected after pH 10/Cl<sup>-</sup>-depletion and subsequent Cl<sup>-</sup>-reconstitution in PS-II, since Cl<sup>-</sup>-free washes of Cl<sup>-</sup>-reconstituted PS-II, initially showing a normal S<sub>2</sub> EPR spectrum (Figure 1) [21], resulted in a similar reversible increase of the S<sub>2</sub>  $g = 4$  signal at the expense of the S<sub>2</sub> multiline signal.

We investigated the effect of such halide-free washes in I<sup>-</sup>-activated PS-II. S<sub>2</sub> EPR spectra essentially identical to that shown in Figure 1c were obtained (1) in the presence of 20 mM I<sup>-</sup> (not shown), (2) after removal of excess I<sup>-</sup> by one halide-free wash (Figure 1a) and (3) after three subsequent halide-free washes (Figure 3a). Thus, there is no indication of I<sup>-</sup>-binding equivalent to that associated with the non-essential Cl<sup>-</sup>-binding site described in Ref. 21. After addition of Cl<sup>-</sup> (25 mM) to I<sup>-</sup>-activated PS-II (after halide-free washing), the typical S<sub>2</sub> EPR spectrum observed in untreated and Cl<sup>-</sup>-reconstituted PS-II was obtained exhibiting a characteristic S<sub>2</sub> multiline signal and little S<sub>2</sub>  $g = 4$  signal (Figure 3c). However, in contrast to Cl<sup>-</sup>-free washed PS-II, this Cl<sup>-</sup>-reconstitution effect did not occur within the mixing time (Figure 3b) but required subsequent dark-incubation (30 min) (Figure 3c). This difference in

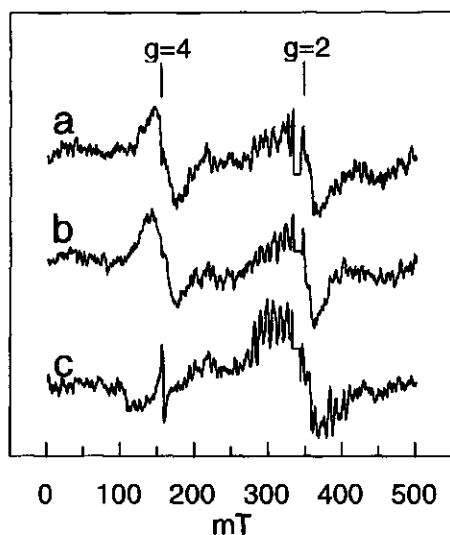


Figure 3. Light minus dark EPR spectra of I<sup>-</sup>-activated PS-II membranes that were illuminated for 3 min. at 200 K. After pH 10/Cl<sup>-</sup>-depletion and subsequent addition of I<sup>-</sup>, the PS-II membranes were washed four times in 10 mM MES (pH 6.3) and 0.5 M sucrose followed by dark incubation on ice for 30 min. and (a) followed by addition of PPBQ (1mM), freezing in the dark and illumination at 200 K. (b) As in (a) except that 25 mM Cl<sup>-</sup> was rapidly (30 s) added in the dark before freezing. (c) As in (a) except that prior to the addition of PPBQ and freezing, 25 mM Cl<sup>-</sup> was added in the dark followed by an additional 30 min. incubation on ice. Instrument settings were as in Figure 1.

the Cl<sup>-</sup>-reconstitution kinetics presumably reflects slow exchange of I<sup>-</sup> by Cl<sup>-</sup> in the site essential for oxygen evolution. Slow exchange of I<sup>-</sup> by Cl<sup>-</sup> also has been observed in thermoluminescence studies under comparable conditions [22].

*The effects of ethanol on the EPR properties of S<sub>2</sub>.* The solvent ethanol has been shown to affect the S<sub>2</sub> EPR properties in untreated PS-II resulting in the conversion of the S<sub>2</sub> g = 4 signal to the S<sub>2</sub> multiline signal [18]. It was of interest to investigate whether ethanol affects the already modified S<sub>2</sub> EPR properties in Cl<sup>-</sup>-depleted and I<sup>-</sup>-reconstituted PS-II.

Figure 4a shows that the addition of ethanol [4 % (v/v)] to Cl<sup>-</sup> free washed PS-II resulted in the suppression of the S<sub>2</sub> g = 4 signal accompanied by an increased S<sub>2</sub> multiline signal intensity. In samples of I<sup>-</sup>-activated PS-II to which ethanol (4 %) had been added, a normal S<sub>2</sub> multiline signal could be generated with an intensity similar to that observed in Cl<sup>-</sup>-reconstituted PS-II. In addition, the S<sub>2</sub> g = 4 signal was partially suppressed (Figure 4b). According to our estimate of the number of centers contributing to the S<sub>2</sub> g = 4 signal prior to ethanol addition (20-50 %) it seems clear that an important part of the ethanol-reconstituted S<sub>2</sub> multiline signal originated from the centers (> 50 %) that did not exhibit an S<sub>2</sub> EPR signal prior to ethanol addition.

In contrast, little or no effect of ethanol (4 %) on the S<sub>2</sub> EPR spectrum was observed in pH 10/Cl<sup>-</sup>-depleted PS-II and F<sup>-</sup>-treated PS-II exhibiting an intense S<sub>2</sub> g = 4 signal (Figure

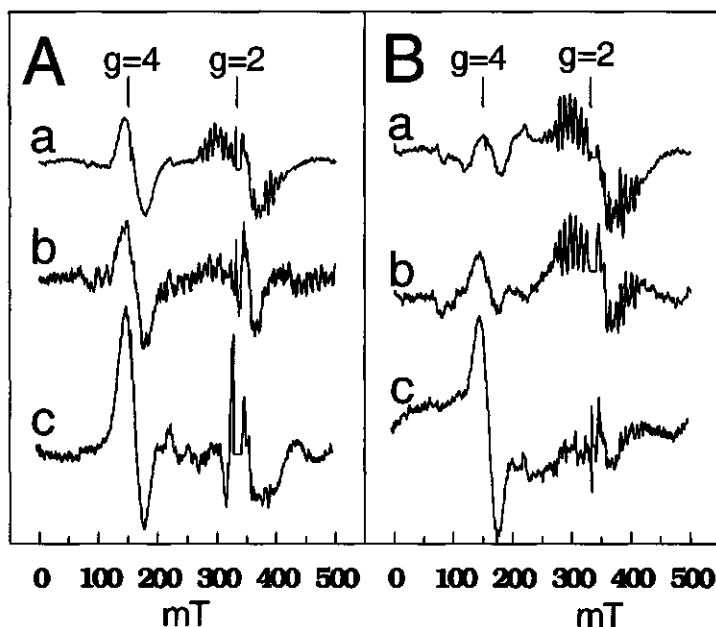


Figure 4. Light minus dark EPR spectra of PS-II membranes that were illuminated for 3 min. at 200 K following (a) Cl<sup>-</sup>-free washes in 10 mM MES (pH 6.3) and 0.5 M sucrose followed by (b, c) pH 10/Cl<sup>-</sup>-depletion treatment and subsequent addition of (b) I<sup>-</sup> (20 mM) or (c) F<sup>-</sup> (25 mM). (A) The membranes were resuspended in 10 mM MES (pH 6.3) and 0.5 M sucrose, (a, b) dark-adapted for 30 min on ice followed by addition of PPBQ (1 mM) or (c) dark-adapted for 30 min. at room temperature followed by addition of 100  $\mu$ M ferricyanide and 100  $\mu$ M PPBQ. Then the samples were frozen in the dark and illuminated at 200 K. (B) As in (A) except that prior to the addition of the electron acceptor, ethanol (4 %) was added in the dark on ice followed by an additional 30 min. dark incubation on ice. Instrument settings were as in Figure 1.

4c). These results indicate that the effect of ethanol is modulated by the anion occupying the Cl<sup>-</sup>-site essential for oxygen evolution.

### Discussion

The results showed that I<sup>-</sup> can functionally replace Cl<sup>-</sup> in the oxygen evolving complex as reported earlier [22,23]. The properties of I<sup>-</sup>-activated PS-II are comparable to those of Cl<sup>-</sup>-free washed PS-II in that both types of PS-II exhibit an enhanced S<sub>2</sub> g = 4 signal originating from oxygen evolving centers (Figures 1 and 2). In addition, in both cases the S<sub>2</sub> g = 4 signal is suppressed by ethanol addition (Figure 4). It is thought that the effects of Cl<sup>-</sup>-free washes reflect the removal of Cl<sup>-</sup> from a low affinity Cl<sup>-</sup>-site which is not essential for oxygen

evolution. Hence, a possible explanation of the observed I<sup>-</sup>-induced S<sub>2</sub> g = 4 signal is that I<sup>-</sup> may be unable to bind to the low-affinity Cl<sup>-</sup>-site which is not essential for oxygen evolution.

Nevertheless, a striking modification specific for I<sup>-</sup>-activation is that, although a characteristic S<sub>2</sub> g = 4 signal was observed, no S<sub>2</sub> multiline signal could be detected. This points to the majority of I<sup>-</sup>-activated, oxygen evolving centers exhibiting neither of the S<sub>2</sub> EPR signals. This effect of I<sup>-</sup> probably reflects minor structural modifications since it is eliminated by the presence of ethanol.

The results from the present study and the comparison with studies in the literature (see e.g. Chapter 4 and Ref. 10) point to a correlation between the EPR properties of the S<sub>2</sub> state and the size of the anion occupying the Cl<sup>-</sup>-site which is essential for oxygen evolution: Occupancy of this site with small anions (F<sup>-</sup>, OH<sup>-</sup>) results in an intense S<sub>2</sub> g = 4 signal, whereas occupancy with voluminous anions (I<sup>-</sup>, SO<sub>4</sub><sup>2-</sup>) suppresses the S<sub>2</sub> g = 4 signal in favour of the centers exhibiting no S<sub>2</sub> EPR signal.

As mentioned above, the dark-decay of the S<sub>2</sub> g=4 EPR signal and of the S<sub>2</sub> multiline EPR signal (in the presence of 4 % ethanol) in I<sup>-</sup>-activated PS-II was similar to that previously observed under similar conditions in untreated PS-II. However, the thermoluminescence of the recombination of S<sub>2</sub> with Q<sub>A</sub><sup>-</sup> or Q<sub>B</sub><sup>-</sup> indicated that I<sup>-</sup>-activated PS-II exhibits a more stable S<sub>2</sub> state [22,23]. This difference is probably due to the use of PPBQ (1 mM) in the present study to remove the electrons from the acceptor side. Under these conditions, electron donation to S<sub>2</sub> occurs via an unknown pathway which apparently is unaffected after replacement of Cl<sup>-</sup> by I<sup>-</sup>.

The results indicated that the effect of ethanol on the S<sub>2</sub> EPR properties probably is modulated by the anion occupying the Cl<sup>-</sup>-site essential for oxygen evolution (Figure 4). This presumably reflects a subtle interplay between structural effects of the anion and those of ethanol. Ethanol may induce slight conformational changes of the protein matrix. It has also been argued that the effects of ethanol may originate from ethanol binding near or to the Mn cluster itself [18]. Indeed, under certain conditions, PS-II catalyzes oxidation of alcohols resulting in the formation of aldehydes [31]. If the anion-dependent ethanol effects described in the Results indeed originate from ethanol binding near or to the catalytic site, then this may have some relevance to the role(s) of Cl<sup>-</sup> in the mechanism of water oxidation in that Cl<sup>-</sup>

modulates substrate affinity. Several suggestions in the literature on the role(s) of Cl<sup>-</sup>, are summarized in Refs 2 and 3 (see also Ref. 32).

## References

- 1 Kok, B., Forbush, B., & McGloin, M. (1970) *Photochem. Photobiol.* 11, 457-475.
- 2 Debus, R. J. (1992) *Biochim. Biophys. Acta* 1102, 269-352.
- 3 Rutherford, A. W., Zimmermann, J-L., & Boussac, A. (1992) in *The Photosystems: Structure, Function and Molecular Biology* (Barber, J., ed.) Chapter 5, pp 179-229, Elsevier Science Publishers, New York.
- 4 Boussac, A., & Rutherford, A. W. (1994) *Biochem. Soc. Trans.* 22, 352-358.
- 5 Murata, N., & Miyao, M. (1985) *Trends Biochem. Sci.* 10, 122-124.
- 6 Homann, P. H. (1988) *Photosynth. Res.* 15, 205-220.
- 7 Dismukes, G. C., & Siderer, Y (1981) *Proc. Natl. Acad. Sci. USA* 78, 274-278.
- 8 Brudvig, G. W., Casey, J. L., & Sauer, K. (1983) *Biochim. Biophys. Acta* 723, 366-371.
- 9 Ono, T., Zimmermann, J-L., Inoue, Y., & Rutherford, A.W. (1986) *Biochim. Biophys. Acta* 851, 193-201.
- 10 Ono, T., Nakayama, H., Gleiter, H., Inoue, Y., & Kawamori, A. (1987) *Arch. Biochim. Biophys.* 256, 618-624.
- 11 Boussac, A., Sétif, P., & Rutherford, A. W. (1992) *Biochemistry* 31, 1224-1234.
- 12 Boussac, A., & Rutherford, A. W. (1994) *J. Biol. Chem.* 269, 12462-12467.
- 13 Casey, J. L., & Sauer, K. (1984) *Biochim. Biophys. Acta* 767, 21-28.
- 14 Damoder, R., Klimov, V. V., & Dismukes, G. C. (1986) *Biochim. Biophys. Acta* 848, 378-391
- 15 Baumgarten, J., Philo, J. S., & Dismukes, G. C. (1990) *Biochemistry* 29, 10814-10822.
- 16 DeRose, V. J., Latimer, M. J., Zimmermann, J-L., Mukerji, I., Yachandra, V. K., Sauer, K., & Klein, M. P. (1995) *Chem. Phys.* 194, 443-459.
- 17 dePaula, J. C., Innes, J. B., & Brudvig, G. W. (1985) *Biochemistry* 24, 8114-8120.
- 18 Zimmermann, J-L., & Rutherford A. W. (1986) *Biochemistry* 25, 4609-4615.
- 19 Hansson, Ö., Aasa, R., & Vänngård., T. (1987) *Biophys. J.* 51, 825-832.
- 20 Beck, W. F., & Brudvig, G. W. (1988) *Chemica Scripta* 28A, 93-98.
- 21 Van Vliet, P., & Rutherford, A. W., (1995) *Biochemistry* (in press).
- 22 Rashid, A., & Homann, P. H. (1992) *Biochim. Biophys. Acta* 1101, 303-310.
- 23 Homann, P. H. (1993) *Photosynth. Res.* 38, 395-400.
- 24 Berthold, D. A., Babcock, G. T., & Yocum, C. F. (1981) *FEBS Lett.* 134, 231-234.
- 25 Ford, R. C., & Evans, M. C. W. (1983) *FEBS* 160, 159-164.
- 26 Homann, P.H. (1985) *Biochim. Biophys. Acta* 809, 311-319.
- 27 Ikeuchi, M., & Inoue, Y. (1988) *Plant Cell Physiol.* 29, 695-705.
- 28 Ikeuchi, M., Koike, H., & Inoue, Y. (1988) *Biochim. Biophys. Acta* 932, 160-169.
- 29 Zimmermann, J-L., & Rutherford A. W. (1986) *Biochim. Biophys. Acta* 851, 416-423.
- 30 Diner, B. A., & Petrouleas, V. (1987) *Biochim. Biophys. Acta* 893, 138-148
- 31 Frasch, W. D., Mei, R., & Sanders, M. A. (1988) *Biochemistry* 27, 3715-3719.
- 32 Van Vliet, P., Boussac, A., & Rutherford A.W. (1994) *Biochemistry* 33, 12998-13004.
- 33 Styring, S., & Rutherford, A. W. (1988) *Biochim. Biophys. Acta* 933, 378-387.

## On the magnetic properties of the Oxygen Evolving Complex of Photosystem II: EPR microwave power saturation studies of $\text{Tyr}_D^\bullet$

Pieter van Vliet<sup>\*</sup> and A. William Rutherford

*Section de Bioénergétique (URA CNRS 1290), Département de Biologie Cellulaire et Moléculaire, CEA Saclay, 91191 Gif-sur-Yvette, France, and Department of Molecular Physics, Agricultural University, Wageningen, The Netherlands.*

**Key Words:** photosynthesis, oxygen evolution, charge accumulation states,  $\text{Tyr}_D^\bullet$ , electron paramagnetic resonance.

The microwave power saturation properties of  $\text{Tyr}_D^\bullet$  in photosystem II (PS-II)-enriched membranes have been investigated by electron paramagnetic resonance spectroscopy (EPR). Dark-adaptation of PS-II at 0 °C prior to illumination affected the relaxation properties of  $S_1\text{Tyr}_D^\bullet$  as previously reported [Koulougliotis, D., Hirsh, D. J., & Brudvig, G. W., (1992) *J. Am. Chem. Soc.* 114, 8322-8323]. After 30 min. of dark-adaptation, a relatively fast-relaxing  $S_1\text{Tyr}_D^\bullet$  was observed which became slow-relaxing after 17 h dark-adaptation. This effect of dark-adaptation was accelerated by addition of 1 mM of the electron acceptor phenyl-p-benzoquinone (PPBQ). The PPBQ-induced acceleration was avoided by using low concentrations of PPBQ (50-100  $\mu\text{M}$ ) in samples that had ferricyanide (50-100  $\mu\text{M}$ ) present. This points to a reduced form of PPBQ being responsible for the conversion of the fast-relaxing to the slow-relaxing form of  $S_1$  and suggests that a redox event is involved. Upon a series of consecutive flashes, the two types of PS-II exhibiting initially either a slow-relaxing

---

<sup>\*</sup> To whom correspondence should be addressed. CEA Saclay, Tel: 33-1-6908 2940; Fax: 33-1-6908 8717.

$S_1\text{Tyr}_D\bullet$  or a fast-relaxing  $S_1\text{Tyr}_D\bullet$  prior to illumination, showed identical  $\text{Tyr}_D\bullet$  relaxation properties in  $S_2$ ,  $S_3$ ,  $S_0$  and  $S_1$  and also the spectral properties of  $S_2$  were identical. The  $S_1$  state in these samples generated after four flashes appeared to be the fast-relaxing form. When the  $S_2$  and  $S_3$  state formed in the first charge accumulation cycle were allowed to decay under conditions that the PPBQ-effect was avoided, the resulting relaxation properties of  $S_1$  were similar to those initially present prior to illumination. The results indicate the presence of a fast-relaxing and a slow-relaxing form of  $S_1$  which are interconvertible. In addition, the event responsible for the conversion of the slow-relaxing to the fast-relaxing form of  $S_1$  occurs in the first enzyme cycle at the  $S_3$  to  $S_0$  or the subsequent  $S_0$  to  $S_1$  transition. The fast- and slow-relaxing forms of  $S_1$  may correspond to respectively a paramagnetic and diamagnetic  $S_1$  state, reflecting structurally different Mn clusters as was previously proposed. Alternatively, in view of the results from this work, it is conceivable that the Mn cluster in  $S_1$  is diamagnetic and that the fast-relaxing  $\text{Tyr}_D\bullet$  in  $S_1$  is due to a nearby paramagnetic species different from the Mn cluster.

## Introduction

Photosynthetic water oxidation, resulting in the formation of molecular oxygen and proton release, is thought to occur upon photo-accumulation of four positive charges in an enzyme cycle consisting of five intermediate states designated  $S_0$  to  $S_4$ , where the subscript is the number of charges stored [1]. A cluster of presumably four manganese ions, present at the luminal side of the membrane-spanning photosystem II protein complex (PS-II)<sup>1</sup>, plays a central role in the charge accumulation cycle.  $S_4$  is thought to be a transient state which converts spontaneously to  $S_0$  accompanied by the release of oxygen.  $S_0$  is the most reduced state, and the higher oxidation states are formed by successive electron transfers to the photo-oxidized primary electron donor  $P_{680}^+$ .  $S_0$  and  $S_1$  are dark-stable states which in most PS-II materials give rise to dark populations of approximately 75 %  $S_1$  and 25 %  $S_0$  [2,3] or, after very long dark incubation, 100 %  $S_1$  [4,5].  $S_2$  and  $S_3$  are dark-unstable and decay to  $S_1$  in

---

<sup>1</sup> Abbreviations: PS-II, the photosystem II protein complex;  $P_{680}^+$ , primary electron donor in PS-II;  $\text{Tyr}_D$ , side-path electron donor of PS-II responsible for EPR signal  $\text{II}_{\text{slow}}$ ;  $Q_A$ ,  $Q_B$ , primary and secondary quinone electron acceptors of PS-II; CW, continuous wave; EPR, electron paramagnetic resonance; EDTA, (ethylenedinitrilo) tetraacetic acid; MES, 4-(N-morpholino)ethanesulphonic acid; PPBQ, phenyl-p-benzoquinone.

tens of seconds [2,3]. These decay reactions are partially the result of recombination reactions with the reduced acceptor side. In the presence of an artificial electron acceptor, which removes the electrons from the acceptor side,  $S_2$  and  $S_3$  are significantly more stable showing half-life times in the dark of 3-4 min. [6]. The kinetic properties of the oxidation states under different experimental conditions are reviewed in Refs. 7 and 8.

The magnetic properties of the oxygen evolving complex have often been investigated using EPR spectroscopy. In untreated PS-II, no signals from states other than the  $S_2$  state have been detected by conventional CW-EPR. The  $S_2$  EPR spectrum in untreated PS-II is dominated by a characteristic multiline EPR signal at  $g = 2$  [9]. This signal can be generated by illumination treatments allowing for a single stable charge separation, e.g. illumination with a single flash at room temperature [9], or with continuous illumination at 200 K [10].

In most PS-II materials, the EPR spectrum exhibits a dark-stable radical around  $g = 2$ . This radical originates from the tyrosine-160 amino acid residue in the  $D_2$  protein, denoted  $Tyr_D^\bullet$  (reviewed in Refs. 7 and 11).  $Tyr_D^\bullet$  does not change its oxidation state during enzyme turnover and is thought not to participate in steady-state electron transfer from water to  $P_{680}^+$ . Nevertheless,  $Tyr_D$  is redox-active in that the oxidized form,  $Tyr_D^\bullet$ , oxidizes  $S_0$  resulting in  $S_1Tyr_D$  [5] and the reduced form,  $Tyr_D$ , reduces  $S_2$  and  $S_3$  resulting in  $S_1Tyr_D^\bullet$  and  $S_2Tyr_D^\bullet$ , respectively [12,13].

In untreated PS-II, no signals from states other than the  $S_2$  state have been detected by conventional CW-EPR. Nevertheless, since the Mn cluster is thought to be the dominant paramagnetic relaxer of  $Tyr_D^\bullet$ , Mn redox chemistry during S-state transitions has been studied by a range of different EPR techniques using  $Tyr_D^\bullet$  as a magnetic probe (see Refs. 14-17). Investigations of the relaxation properties of  $Tyr_D^\bullet$ , using CW EPR and pulsed EPR, in samples of well-defined S-state composition using flash-illumination, indicated that the  $Tyr_D^\bullet$  species in  $S_1$  was significantly slower relaxing than in the other S-states [15,16]. Those studies suggested that the Mn cluster is paramagnetic in  $S_2$ ,  $S_3$  and  $S_0$  and diamagnetic in  $S_1$ . This was also indicated from a study on the flash-dependent magnetic susceptibility in PS-II [18].

Koulougliotis *et al.* [19] observed by pulsed EPR that the spin-lattice relaxation rate ( $T_{1^{-1}}$ ) of  $Tyr_D^\bullet$  in dark-adapted PS-II decreased with a half-time of  $t_{1/2} \approx 3.5$  h during dark-incubation. These authors interpreted their results as indicating that the  $S_1$  state slowly



converts in darkness from a paramagnetic to a diamagnetic form and related these forms to the so-called "active" and "resting" states, respectively, of the enzyme as proposed earlier [20].

In the present work we have studied the microwave power saturation of  $\text{Tyr}_D\cdot$  in the oxygen evolving complex by CW EPR. We have focussed on the interconversion between the two forms of  $S_1$  and their influence on the other S-states.

## Materials and Methods

Photosystem II-enriched membranes were prepared according to the method of Berthold *et al.* [21] with the modifications of Ford and Evans [22]. The oxygen evolving activity of these membranes was  $\approx 500 \mu\text{M O}_2/\text{mg chlorophyll/h}$ . The PS-II membranes were stored at  $-80^\circ\text{C}$  in a buffer solution containing 25 mM MES (pH 6.5), 0.3 M sucrose and 10 mM NaCl. Unless stated otherwise, the same buffer solution was used for resuspension and dilution.

The membranes were resuspended at 2-2.5 mg chlorophyll/ml, put in calibrated quartz EPR tubes, dark-adapted, frozen in the dark and stored in liquid nitrogen until used for EPR measurements.

The samples were illuminated with continuous light from an 800 W projector passed through 2 cm water and an infrared filter, in a non-silvered Dewar flask containing ethanol cooled to 198 K with solid  $\text{CO}_2$ . Flash illumination at room temperature was provided from an Nd-Yag laser (15 ns, 300 mJ, 532 nm).

EPR spectra were recorded at liquid helium temperatures with a Bruker ER 200 or ER 300 X-band spectrometer equipped with an Oxford Instruments cryostat.

Measurements of oxygen evolving activity were done using a Clark-type electrode, at  $25^\circ\text{C}$  under nearby saturating continuous light at a chlorophyll concentration of  $20 \mu\text{g/ml}$ .

## Results

Figure 1 shows the microwave power saturation properties of  $\text{Tyr}_D\cdot$  in untreated PS-II after 30 min. or 17 h dark-adaptation at  $0^\circ\text{C}$ . As expected, these samples showed no EPR signals from  $S_2$  (not shown). At low non-saturating microwave powers, both samples

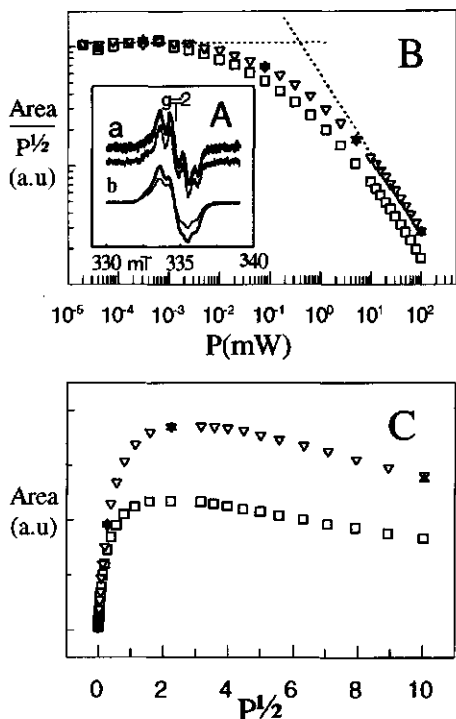


Figure 1: (A) EPR spectra of  $\text{Tyr}_{\text{D}}\bullet$  in PS-II membranes dark-adapted on ice for 30 min. (bold trace) or for 17 h (plain trace), recorded (a) at low, non-saturating microwave power ( $0.63 \mu\text{W}$ ) or (b) at high, saturating microwave power ( $5.0 \text{ mW}$ ). (B, C) Microwave power saturation of  $\text{Tyr}_{\text{D}}\bullet$  in the samples in A following 30 min. dark-adaptation ( $\nabla$ ) or 17 h dark-adaptation ( $\square$ ). The 17 h dark-adapted sample from ( $\square$ ) was thawed and illuminated for 3 min. with continuous light at  $0^\circ\text{C}$  followed by 30 min. dark-adaptation on ice and frozen in the dark ( $\blacktriangle$ ). The  $\text{Tyr}_{\text{D}}\bullet$  signal area was determined from the double integral of the signal and plotted without normalization. The microwave power for half saturation,  $P_{1/2}$ , is determined from the plots as in B by the intercept of the regression line through the points at non-saturating microwave powers and the regression line through the points at saturating microwave powers, as drawn for the open triangles. Instrument settings: 9.42 GHz; modulation amplitude, 0.22 mT; modulation frequency, 12.5 kHz; temperature, 15 K.

exhibited a similar intensity of the dark-stable  $\text{Tyr}_{\text{D}}\bullet$  EPR signal [Figure 1A (a), B], indicating an equal amount of centers containing  $\text{Tyr}_{\text{D}}\bullet$  in these samples. However, at saturating microwave powers, the intensity of  $\text{Tyr}_{\text{D}}\bullet$  after 17 h dark-adaptation was significantly smaller than that after 30 min. dark-incubation [Figure 1A (b), B]. Thus the extensive dark-adaptation resulted in a slower relaxing  $\text{Tyr}_{\text{D}}\bullet$ , which is more easily saturated by the microwave power. These CW EPR results are consistent with a pulsed EPR study of PS-II which indicated a decrease of the spin lattice relaxation rate ( $T_1^{-1}$ ) of  $\text{Tyr}_{\text{D}}\bullet$  occurring during relatively long dark-adaptation [19].

This effect of dark-adaptation could originate from the conversion of  $S_0\text{Tyr}_{\text{D}}\bullet$  to  $S_1\text{Tyr}_{\text{D}}\bullet$  in a fraction of centers [5] since in the  $S_0$  state,  $\text{Tyr}_{\text{D}}\bullet$  has been shown to be significantly faster relaxing than that observed from  $S_1$  [15]. This possibility can, however, be ruled out on the basis of the following observations. (1) The conversion of  $S_0\text{Tyr}_{\text{D}}\bullet$  to  $S_1\text{Tyr}_{\text{D}}\bullet$  would result in a proportional decrease of the  $\text{Tyr}_{\text{D}}\bullet$  signal intensity. As mentioned above, this was not observed (Figure 1). (2) Synchronization of the charge accumulation states to  $S_1$  following 17 h dark-adaptation by a preflash procedure as described previously [5,6], did not affect the

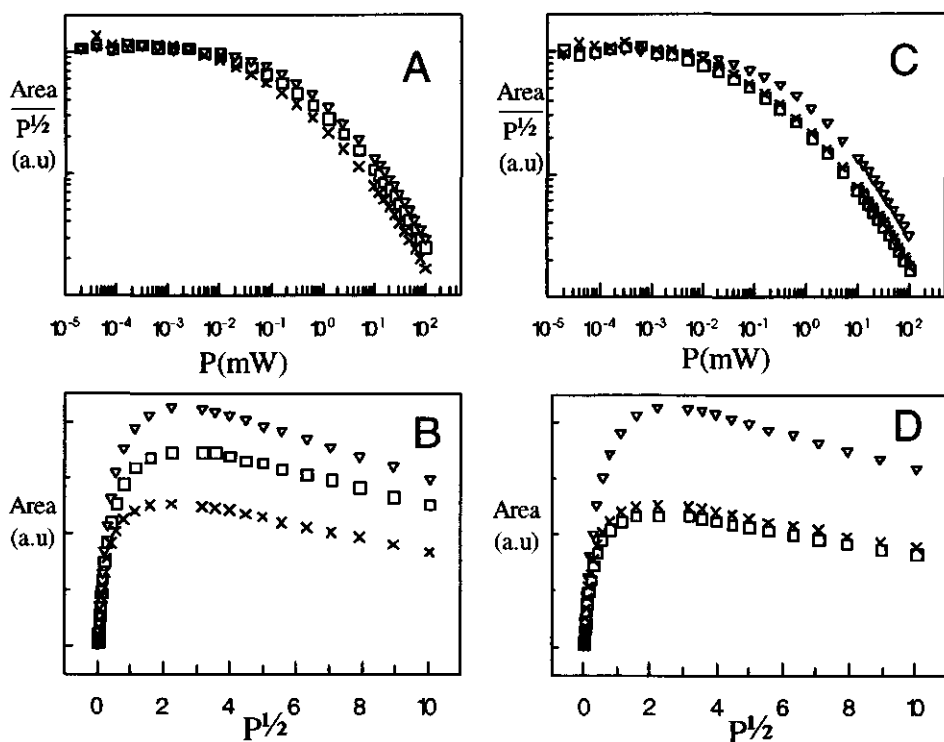


Figure 2: Microwave power saturation of  $\text{Tyr}_{\text{D}}\bullet$  (as in Figure 1), following dark-adaptation on ice (A, B) for 30 min. or (C, D) for 17 h. After dark-adaptation, the samples were given a pre-illumination treatment (see tekst) by illumination with a single flash and subsequent dark-adaptation at room temperature for 10 min. Then the samples were frozen in darkness without further additions ( $\square$ ) or after addition of 1 mM PPBQ ( $\times$ ). The PPBQ (1 mM)-containing samples were illuminated with a single flash and rapidly frozen ( $<1\text{s}$ ) in darkness ( $\nabla$ ). Instrument settings were as in Figure 1.

power saturation properties of the  $\text{Tyr}_{\text{D}}\bullet$  [compare Figure 1 (squares) with Figure 2 (crosses), giving a microwave power for half saturation ( $P_{1/2}$ ) of 0.14 mW]. Thus the slow-relaxing  $\text{Tyr}_{\text{D}}\bullet$  after extensive dark adaptation, originates from the  $\text{S}_1$  state exhibiting altered magnetic properties.

The effect of dark-adaptation, resulting in a slow-relaxing  $\text{S}_1\text{Tyr}_{\text{D}}\bullet$ , was not influenced by the presence of sucrose (0.3 M), NaCl (10 mM),  $\text{Mg}^{2+}$  (5 mM),  $\text{Mn}^{2+}$  (0.1 mM) and EDTA (5 mM) in the buffer solution.

Continuous illumination at 4 °C of the sample that had been dark-adapted for 17 h, followed by 30 min. dark-adaptation on ice, resulted in the fast-relaxing  $\text{S}_1\text{Tyr}_{\text{D}}\bullet$  (Figure 1, closed triangles). The origin of this effect of light was investigated using flash-illumination. In

PS-II membranes, an exogenous electron acceptor is required to allow efficient S-state turnover. In flash-experiments, after S-state synchronization in EPR samples by a preflash treatment, normally PPBQ is added as an electron acceptor [6]. We found that addition of 1 mM PPBQ to the sample that had been dark-adapted for 30 min. resulted in the formation of a slow-relaxing  $S_1\text{Tyr}_D^\bullet$  (Figures 2A, B), comparable that observed after 17 h dark-adaptation (Figure 1, Figures 2C, D). The solvent dimethylsulphoxide alone, which was used to dissolve the PPBQ, had no effect on the microwave saturation properties of  $\text{Tyr}_D^\bullet$  (not shown). The effect of PPBQ on the relaxation properties of  $S_1\text{Tyr}_D^\bullet$  occurred within the time required for mixing (~2 min.). The addition of PPBQ (1mM) had no effect on the slow-relaxing  $\text{Tyr}_D^\bullet$  in the sample that was dark-adapted for 17 h (Figures 2C, D). Furthermore, no significant effects were observed on the known redox components of PS-II which are detectable by EPR in their oxidized form (i.e.  $\text{cytb}^{+559}$ ,  $\text{Tyr}_D^\bullet$ ,  $\text{Chl}^+$ ,  $\text{Fe}^{3+}$  (not shown). These results indicate that PPBQ accelerated the effect of dark-adaptation on the relaxation properties of  $S_1\text{Tyr}_D^\bullet$ .

Illumination of the PPBQ (1 mM)-containing samples with a single flash or with continuous illumination at 200 K (not shown but see Figure 4), resulted in the appearance of a normal  $S_2$  multiline signal accompanied by a relaxation enhancement of  $\text{Tyr}_D^\bullet$  (Figure 2 and Figure 3), an effect that has previously been observed under similar conditions [15]. Figure 2 and Figure 3 also show that the fast-relaxing  $S_1\text{Tyr}_D^\bullet$  observed in 30 min. dark-adapted samples in the absence of PPBQ, exhibited microwave power saturation to an extent intermediate between the fast-relaxing  $S_2\text{Tyr}_D^\bullet$  and the slow-relaxing  $S_1\text{Tyr}_D^\bullet$  observed after 17h dark-adaptation or after addition of PPBQ (1 mM).

The effect of PPBQ on the relaxation properties of  $S_1\text{Tyr}_D^\bullet$  was essentially avoided by adding a relatively low concentration (50-100  $\mu\text{M}$ ) of PPBQ to samples that already contained 50-100  $\mu\text{M}$  ferricyanide. This points to a *reduced* form of PPBQ being responsible for the PPBQ-effect described above. By using a low concentration (50-100  $\mu\text{M}$ ) of PPBQ in the presence of ferricyanide (50-100  $\mu\text{M}$ ), it was possible to study efficient charge accumulation without interference of PPBQ.

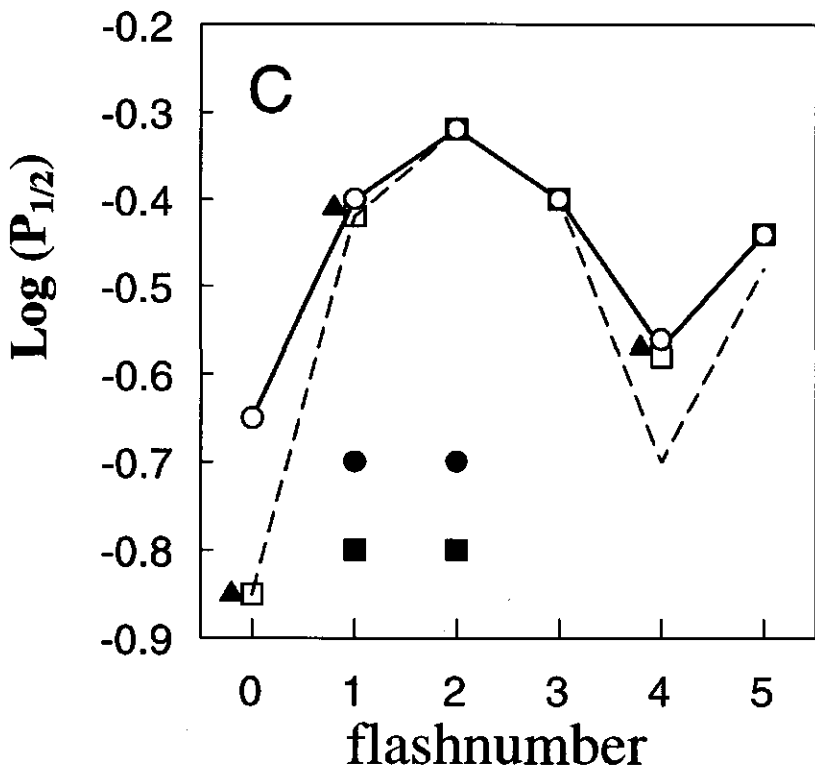
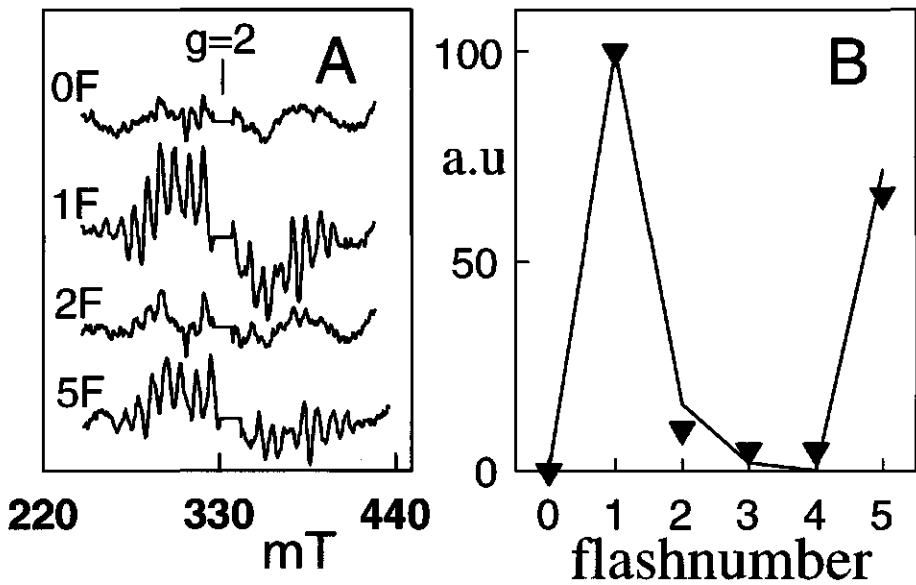


Figure 3 (see page on the left): (A) EPR spectra of PS-II membranes recorded after dark-adaptation followed by a preflash treatment and addition of 50-100  $\mu\text{M}$  ferricyanide and 50-100  $\mu\text{M}$  PPBQ (0F) and subsequent flash-illumination (1F, 2F, 5F). After the flash-illumination the samples were rapidly (<1s) frozen in darkness. The spectra shown were obtained in samples that had been dark-adapted for 17 h on ice. Similar spectra were obtained in samples after 30 min. dark-adaptation on ice (not shown). (B) The multiline signal intensities ( $\blacktriangledown$ ) were determined as the sum of the resolved hyperfine line amplitudes. The continuous line was fitted assuming 100 %  $S_1$  prior to illumination and 8 % misses. (C) The microwave power saturation of  $\text{Ty}_{\text{D}}\bullet$  of the samples from the spectra in A (O) or similarly treated samples except that these were dark-adapted for 17 h ( $\square$ ). ( $\blacktriangle$ ) was as (O) except that 1 mM PPBQ was added in the absence of ferricyanide. ( $\bullet$ ,  $\blacksquare$ ) The samples from (O,  $\square$ ) thawed after illumination with the indicated number of flashes, dark-adapted for 30 min at room temperature and frozen in darkness. The  $P_{1/2}$ -values of  $\text{Ty}_{\text{D}}\bullet$  in the  $S_0$ ,  $S_1$ ,  $S_2$ , and  $S_3$  oxidation states were determined as described in the text and were as follows.  $S_1$  after 30 min. dark-adaptation:  $P_{1/2} = 224 \mu\text{W}$ ;  $S_1$  after 17 h dark-adaptation:  $P_{1/2} = 140 \mu\text{W}$ ;  $S_2$ ,  $S_3$  and  $S_0$ :  $P_{1/2} = 440 \mu\text{W}$ ,  $510 \mu\text{W}$  and  $390 \mu\text{W}$ , respectively. The continuous and dashed lines were fitted to the datapoints as described in the text [15] by including respectively the  $P_{1/2}$ -value of  $S_1\text{Ty}_{\text{D}}\bullet$  after 30 min. dark-adaptation or the  $P_{1/2}$ -value of  $S_1\text{Ty}_{\text{D}}\bullet$  after 17 h dark-adaptation. Instrument settings were as in Figure 1.

Figure 3A shows that flash illumination of PS-II EPR samples after 17 h of dark-adaptation resulted in a flash-dependent oscillation of the multiline signal with maximal intensities on the first and the fifth flash (Figures 3A, B). This also was the case in samples that, prior to the illumination, had been dark-adapted for 30 min (not shown). A similar flash-dependent oscillation of the  $S_2$  multiline signal has been reported previously [9,23].

As seen previously [15], the  $P_{1/2}$ -values after generation of  $S_2$ ,  $S_3$  and  $S_0$  were larger than those in the presence of  $S_1$  (Figure 3C). In addition, these were independent on the relaxation properties of  $S_1\text{Ty}_{\text{D}}\bullet$  initially present prior to the flash series.

The samples that were illuminated with one or two flashes were subsequently dark-adapted for 30 min. at room temperature to allow the decay of  $S_2$  and  $S_3$  back to  $S_1$ . Figure 3C shows that the  $\text{Ty}_{\text{D}}\bullet$  in the sample that was dark-adapted for 17 h prior to the illumination, was significantly slower relaxing than that in the sample that was dark-adapted for 30 min. prior to the illumination. These results indicate that during the period of dark-incubation, the  $S_2$  and  $S_3$  states returned to the magnetic form of  $S_1$  that was initially present prior to the illumination. This is consistent with the observation mentioned above that the pre-illumination with a single flash had no effect on the  $S_1\text{Ty}_{\text{D}}\bullet$  saturation properties.

After illumination of dark-adapted PS-II with four flashes, the  $S_1$  state is expected to be regenerated in approximately 72 % of the centers, taking the misses into account [ $-8$  % misses per flash (Figures 3A, B)]. Figure 3C shows that illumination of the 17 h dark-adapted and the 30 min. dark-adapted sample with four flashes results in almost identical  $P_{1/2}$ -values of

Tyr<sub>D</sub>•. This indicates that the difference in the relaxation properties of S<sub>1</sub>Tyr<sub>D</sub>• between the 17 h dark-adapted and the 30 min. dark-adapted sample seen prior to the flash series, is lost upon enzyme turnover.

To compare the relaxation properties of Tyr<sub>D</sub>• in the S<sub>1</sub> state after four flashes with those of S<sub>1</sub>Tyr<sub>D</sub>• prior to the illumination, a fitting procedure was applied as described previously [15]. The P<sub>1/2</sub>-value of Tyr<sub>D</sub>• in each of the S-states was determined using the following expression [15],

$$I = k \sum_{i=S_0}^{i=S_3} [C_i P^{0.5} / (1 + P/P_{1/2,i})^{0.5b}] \quad (1)$$

where  $I$  is the sum of the EPR signal intensities at each of the oxidation states ( $i=S_0-S_3$ ),  $k$  is an apparatus-dependent constant,  $C_i$  is the fraction of each oxidation state,  $P$  is the microwave power in milliwatts,  $P_{1/2}$  is the microwave power for half-saturation and  $b$  is the inhomogeneity parameter. The oscillation pattern of the S<sub>2</sub> multiline signal intensity as in the Figures 3A and 3B was used to determine the fractions ( $C_i$ ) of each of the S-states after a given number of flashes. The P<sub>1/2</sub>-value after the preflash treatment was presumed to originate from 100 % S<sub>1</sub>Tyr<sub>D</sub>•. The P<sub>1/2</sub>-value of S<sub>2</sub>Tyr<sub>D</sub>• was determined from the experimentally determined P<sub>1/2</sub>-value after one flash and correction for the residual fraction of S<sub>1</sub>, using (1) and the P<sub>1/2</sub>-value of S<sub>1</sub>Tyr<sub>D</sub>•, and so on. The determined P<sub>1/2</sub>-values for each of the S-states and the determined flash-dependent S-state composition were then used in (1) to calculate the experimental P<sub>1/2</sub>-values at each flash number.

Figure 3C (solid line) shows that a good fit to the data points is obtained by including the P<sub>1/2</sub>-value of the fast-relaxing S<sub>1</sub>Tyr<sub>D</sub>• determined after 30 min. dark-adaptation. However, by including the P<sub>1/2</sub>-value of the slow-relaxing S<sub>1</sub>Tyr<sub>D</sub>• determined after 17 h dark-adaptation, the predicted P<sub>1/2</sub>-value (dashed line) on the fourth flash is significantly lower than that measured. These results indicate that after illumination with four flashes, the slow-relaxing S<sub>1</sub>Tyr<sub>D</sub>• is converted to the fast-relaxing form. When the slow-relaxing S<sub>1</sub>Tyr<sub>D</sub>• prior to illumination was formed by the addition of 1 mM PPBQ (Figure 3C, closed triangles), the flash-induced changes in the P<sub>1/2</sub>-values of Tyr<sub>D</sub>• were identical to those in samples in which the slow-relaxing S<sub>1</sub>Tyr<sub>D</sub>• prior to illumination was formed by 17 h dark-adaptation.

## Discussion

Figure 4 shows a schematic representation of the results and conclusions from this work. The results showed that  $S_1\text{Tyr}_D^\bullet$  converts from a fast-relaxing form to a slow-relaxing form during dark-adaptation. This is consistent with the results of a pulsed EPR study which indicated that the dipolar spin-lattice relaxation rate constant ( $T_1^{-1}$ ) of  $\text{Tyr}_D^\bullet$  in dark-adapted PS-II decreased during dark-incubation with a half time of about 3.5 h [19]. In that study, it was also shown that  $T_1$  of the slowly relaxing form of  $\text{Tyr}_D^\bullet$  which is observed after long dark-adaptation of untreated PS-II was similar to that of  $\text{Tyr}_D^\bullet$  after Mn depletion in PS-II. From this comparison, Koulougliotis *et al.* [19] concluded that the slow-relaxing  $\text{Tyr}_D^\bullet$  in untreated PS-II after long dark-adaptation, reflects the presence of a diamagnetic  $S_1$  state. In addition, the fast-relaxing  $\text{Tyr}_D^\bullet$  in dark-adapted PS-II was proposed to reflect the presence of a paramagnetic form of  $S_1$  [19]. By synchronization of the S-states in  $S_1$ , we have in this work ruled out the possibility that the fast-relaxing  $\text{Tyr}_D^\bullet$  in dark-adapted PS-II is due to a contribution from  $S_0$  which is known to be a more rapid relaxer of  $\text{Tyr}_D^\bullet$  [15] and, in addition, is known to be involved in a redox reaction with  $\text{Tyr}_D^\bullet$  which occurs on a time scale of hours and results in the conversion of  $S_0\text{Tyr}_D^\bullet$  to  $S_1\text{Tyr}_D^\bullet$  [15].

Flash-experiments (Figure 3) showed that the relaxation properties of  $\text{Tyr}_D^\bullet$  are dependent on the S-state present as previously reported [15], with  $S_2$ ,  $S_3$  and  $S_0$  being relatively rapid relaxers and  $S_1$  being the slowest. The fast-relaxing  $S_1\text{Tyr}_D^\bullet$  showed a  $P_{1/2}$ -value between that of the fast-relaxing  $S_2\text{Tyr}_D^\bullet$  and that of the slow-relaxing  $S_1\text{Tyr}_D^\bullet$  (see also Figure 4).

The  $S_1$  state generated after four flashes appeared to be the fast-relaxing form, even when the slow-relaxing form of  $S_1$  was present (Figures 3 and 4). This indicates that the conversion from the slow- to fast-relaxing form occurs during the first enzyme turnover. The conversion of the slow-relaxing ("resting") form of  $S_1$  to the fast-relaxing ("active") form during enzyme turnover was an intrinsic assumption in previous proposals [19,20]. In the present work it is shown that the  $S_2$  and  $S_3$  state formed in the first cycle decay to the magnetic form of  $S_1$  initially present prior to illumination (Figures 3 and 4). Thus, the event responsible for the conversion from the slow- to fast-relaxing  $S_1\text{Tyr}_D^\bullet$  occurs on the  $S_3$  to  $S_0$  transition or on the subsequent  $S_0$  to  $S_1$  transition.



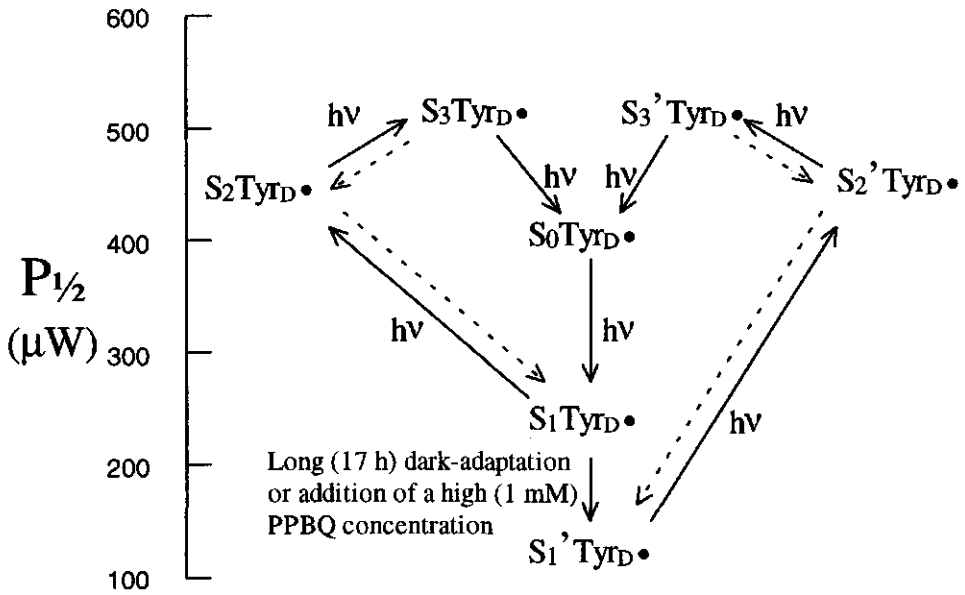


Figure 4. Schematic representation of the microwave saturation behaviour of Tyr<sub>D</sub>• after generation of the various oxidation states of the oxygen evolving complex under a range of experimental conditions described in the Results. S<sub>1</sub>'Tyr<sub>D</sub>•, S<sub>2</sub>'Tyr<sub>D</sub>• and S<sub>3</sub>'Tyr<sub>D</sub>• represent the oxidation states formed in PS-II samples after long dark-adaptation (17 h on ice) or after addition of millimolar concentrations of PPBQ. It is assumed that the event responsible for the conversion from the slowly relaxing form of S<sub>1</sub>Tyr<sub>D</sub>• (S<sub>1</sub>'Tyr<sub>D</sub>•) to the fast-relaxing S<sub>1</sub>Tyr<sub>D</sub>• occurs on the S<sub>3</sub> to S<sub>0</sub> transition. However, it can not be excluded that the subsequent S<sub>0</sub> to S<sub>1</sub> transition is involved (see text).

Addition of millimolar concentrations of the exogenous electron acceptor PPBQ resulted in a relatively rapid conversion (on the timescale of minutes) of the fast-relaxing S<sub>1</sub>Tyr<sub>D</sub>• to the slow-relaxing S<sub>1</sub>'Tyr<sub>D</sub>• (Figure 2B). The effect of PPBQ-addition and the effect of flash-illumination discussed above explains the observation by Styring and Rutherford [15] that illumination of PS-II membranes with four flashes resulted in a significantly faster relaxing S<sub>1</sub>Tyr<sub>D</sub>• than predicted on the basis of: (a) the known S-state composition and (b) the  $P_{1/2}$ -values of Tyr<sub>D</sub>• determined from the different S-states, which presumably included the  $P_{1/2}$ -value of the slow-relaxing S<sub>1</sub>Tyr<sub>D</sub>• since the measurements were done after addition of millimolar concentrations of PPBQ. Styring and Rutherford [15] also investigated the charge accumulation properties of PS-II in thylakoid membranes, in the absence of an exogenous electron acceptor. In this case, the measured  $P_{1/2}$ -value of Tyr<sub>D</sub>• on

the fourth flash matched the predicted value [15]. Thus, it is possible that under these conditions a fast-relaxing  $S_1$  state was present in the dark-adapted thylakoid membranes.

The conversion from the fast-relaxing (paramagnetic) to the slow-relaxing (diamagnetic)  $S_1$  state has been attributed to structural changes occurring in the Mn cluster, resulting in modifications of the exchange couplings between the Mn ions [19]. However, a surprising observation was that the exogenous electron acceptor PPBQ accelerated the conversion of the fast-relaxing (paramagnetic) to the slow-relaxing (diamagnetic)  $S_1$ Tyr<sub>D</sub>• (Figure 2B). Since this effect was avoided at low PPBQ concentrations in the presence of the oxidant ferricyanide, it seems that a redox event is involved. The putative redox change associated with the observed PPBQ-effect might be explained in the context of the model by Koulougliotis et al. [19] in an ad hoc way by linking structural changes in the Mn cluster to a redox event. This explanation, however, becomes unlikely if this redox event is obligatory associated with the conversion from the slow-relaxing (diamagnetic) to the fast-relaxing (paramagnetic)  $S_1$  state in forward electron transfer, since the results did not indicate the occurrence of an additional oxidation event in the charge accumulation cycle. In addition, neither the relaxation properties of the  $S_2$ ,  $S_3$  and  $S_0$  states nor the spectral properties of the  $S_2$  state showed any manifestation of the putative structural changes associated with the conversion of the fast-relaxing to slow-relaxing  $S_1$  state. We therefore consider an alternative explanation for the magnetically different forms of  $S_1$ , i.e., that the Mn cluster in  $S_1$  is diamagnetic and that a magnetic species different from the Mn cluster is responsible for the rapid relaxation of Tyr<sub>D</sub>• in  $S_1$ . This suggestion, however, seems to contrast with the report of a broad gaussian shaped signal of the  $S_1$  state detected by parallel mode EPR under some conditions, which was attributed to an  $S = 1$  spin state [24]. This EPR signal was argued to originate from the Mn cluster, although other possibilities were not ruled out [24]. Nevertheless, one possible candidate of the paramagnetic species other than the Mn cluster that may give rise to an enhanced relaxation of Tyr<sub>D</sub>• in  $S_1$  as observed in the present work, could be bound molecular oxygen, the product of water oxidation.

### Acknowledgment

We thank Tjeerd J. Schaafsma for critically reading the manuscript and useful discussions.

## References

- 1 Kok, B., Forbush, B., & McGloin, M. (1970) *Photochem. Photobiol.* 11, 457-475.
- 2 Forbush, B., Bessel, K., & McGloin, M. P. (1971) *Photochem. Photobiol.* 14, 307-321.
- 3 Joliot, P., Joliot, A., Bouges, B., & Barbieri, G. (1971) *Photochem. Photobiol.* 14, 287-305.
- 4 Vermaas, W. F. J., Renger, G., & Dohnt, G. (1984) *Biochim. Biophys. Acta* 764, 194-202.
- 5 Styring, S., & Rutherford, A. W. (1987) *Biochemistry* 26, 2401-2405.
- 6 Styring, S., & Rutherford, A. W. (1988) *Biochim. Biophys. Acta* 933, 378-387.
- 7 Debus, R. J. (1992) *Biochim. Biophys. Acta* 1102, 269-352.
- 8 Rutherford, A. W., Zimmermann, J-L., & Boussac, A. (1992) in *The Photosystems: Structure, Function and Molecular Biology* (Barber, J., ed.) Chapter 5, pp 179-229, Elsevier Science Publishers, New York.
- 9 Dismukes, G. C., & Siderer, Y. (1981) *Proc. Natl. Acad. Sci. USA* 78, 274-278.
- 10 Brudvig, G. W., Casey, J. L., & Sauer, K. (1983) *Biochim. Biophys. Acta* 723, 366-371.
- 11 Babcock, G. T., Barry, B. A., Debus, R. J., Hoganson, C. W., Atamian, M., McIntosh, L., Sithole, I., & Yocum, C. F. (1989) *Biochemistry* 28, 9557-9565.
- 12 Babcock, G. T., & Sauer, K. (1973) *Biochim. Biophys. Acta* 325, 483-503.
- 13 Velthuys, B. R., & Visser, J. W. M. (1975) *FEBS Lett.* 55, 109-112.
- 14 De Groot, A., Plijter, J. J., Evelo, R., Babcock, G. T. & Hoff, A. J. (1986) *Biochim. Biophys. Acta* 848, 8-15.
- 15 Styring, S., & Rutherford, A. W. (1988) *Biochemistry* 27, 4915-4923.
- 16 Evelo, R. G., Styring, S., Rutherford, A. W., & Hoff, A. J. (1989) *Biochim. Biophys. Acta* 973, 428-442.
- 17 Kodera, Y., Takura, K., & Kawamori, A. (1992) *Biochim. Biophys. Acta* 1101, 23-32.
- 18 Sivaraja, M., Philo, J. S., Lary, J., & Dismukes, G. C. (1989) *J. Am. Chem. Soc.* 111, 3221-3225.
- 19 Koulougliotis, D., Hirsh, D. J., & Brudvig, G. W., (1992) *J. Am. Chem. Soc.* 114, 8322-8323.
- 20 Beck, W. F., dePaula, J. C., & Brudvig, G. W. (1985) *Biochemistry* 24, 3035-3043.
- 21 Berthold, D. A., Babcock, G. T., & Yocum, C. F. (1981) *FEBS Lett.* 134, 231-234.
- 22 Ford, R. C., & Evans, M. C. W. (1983) *FEBS* 160, 159-164.
- 23 Zimmermann, J-L., & Rutherford A. W. (1984) *Biochim. Biophys. Acta* 767, 160-167.
- 24 Dexheimer, S. L., & Klein, M. P. (1992) *J. Am. Chem. Soc.* 114, 2821-2826.

**On the Magnetic properties of the Chloride-Depleted Oxygen Evolving Complex of Photosystem II: EPR microwave power saturation studies of Tyr<sub>D</sub>• in the S<sub>2</sub> oxidation state**

Pieter van Vliet, Sun Un and A. William Rutherford.

*Section de Bioénergétique (URA CNRS 1290), Département de Biologie Cellulaire et Moléculaire, CEA Saclay, 91191 Gif-sur-Yvette, France, and Department of Molecular Physics, Agricultural University, Wageningen, The Netherlands.*

**Key Words:** photosynthesis, oxygen evolution, charge accumulation states, Tyr<sub>D</sub>•, electron paramagnetic resonance.

**Introduction**

Photosynthetic water oxidation, resulting in the formation of molecular oxygen and proton release, is thought to occur upon photo-accumulation of four positive charges in an enzyme cycle consisting of five intermediate states designated S<sub>0</sub> to S<sub>4</sub>, where the subscript is the number of charges stored [1]. A cluster of presumably four manganese ions, present at the luminal side of the membrane-spanning photosystem II protein complex (PS-II)<sup>1</sup>, plays a central role in the charge accumulation cycle. Also Cl<sup>-</sup> and Ca<sup>2+</sup> are essential (reviewed Refs. 2 and 3).

In untreated PS-II, the EPR spectrum of the S<sub>2</sub> state is dominated by a characteristic multiline EPR signal at g = 2 [4]. This signal is attributed to a ground state spin S = 1/2 probably arising from a mixed valence tetrameric Mn cluster (see [5] and references therein).

---

<sup>1</sup> Abbreviations: PS-II, the photosystem II protein complex, primary electron donor in PS-II; Tyr<sub>D</sub>, side-path electron donor of PS-II responsible for EPR signal II<sub>slow</sub>; Q<sub>A</sub>, Q<sub>B</sub>, primary and secondary quinone electron acceptors of PS-II; CW, continuous wave; EPR, electron paramagnetic resonance; MES, 4-(N-morpholino) ethanesulphonic acid; PPBQ, phenyl-p-benzoquinone.

The formation of the  $S_2$  multiline signal has been shown to be accompanied by a relaxation enhancement of  $\text{Tyr}_D^\bullet$  [6-9] (see also Chapter 6; Van Vliet et al., in preparation). This effect originates from the magnetic dipolar interaction between  $\text{Tyr}_D^\bullet$  and the Mn cluster which in the  $S_2$  state is a faster relaxation center than in  $S_1$  [6-9].

The Mn cluster can also exhibit an  $S_2$   $g = 4$  EPR signal which is thought to correspond to a structural state of PS-II different from that giving rise to the  $S_2$  multiline EPR signal [10-13]. The  $S_2$   $g = 4$  signal is less well characterized than the  $S_2$  multiline signal and may arise either from a spin  $S = 3/2$  or  $S = 5/2$  ground or excited state of the mixed valence Mn cluster (see e.g. Refs. 13-15). The nature of the  $S_2$   $g = 4$  signal seems to depend on the pretreatment of the enzyme [16].

Until now, the influence of the state giving rise to the  $S_2$   $g = 4$  on the microwave power saturation properties of  $\text{Tyr}_D^\bullet$  has not been addressed. In the present work the microwave power saturation of  $\text{Tyr}_D^\bullet$  in PS-II is investigated under  $\text{Cl}^-$ -depletion conditions as described in Ref. 17, giving rise to an enhanced  $S_2$   $g = 4$  signal.

## Materials and Methods

Photosystem II-enriched membranes were prepared according to the method of Berthold et al. [18] with the modifications of Ford and Evans [19]. The oxygen evolving activity of these membranes was  $\approx 500 \mu\text{M O}_2/\text{mg chlorophyll/h}$ . Prior to use for further treatments, the PS-II membranes were stored at  $-80^\circ\text{C}$  in a buffer solution containing 25 mM MES (pH 6.5), 0.3 M sucrose and 10 mM NaCl.

PS-II membranes were depleted of  $\text{Cl}^-$  either by three  $\text{Cl}^-$ -free washes (resuspension, dilution and centrifugation) in 0.5 M sucrose and 10 mM MES (pH 6.3) or by subsequent short (30 s) treatment at pH 10 according to Homann [20,21] (see also Ref. 17).

In some experiments, where indicated, PS-II membranes were washed in a  $\text{Cl}^-$ -free buffer solution as described above except that the pH was adjusted to pH 6.5. No differences were observed between the effects of the washes at pH 6.3 or the washes at pH 6.5. The PS-II membranes that were repetitively washed in  $\text{Cl}^-$ -free buffer solutions at pH 6.3 or pH 6.5, will be referred to as  $\text{Cl}^-$ -free washed PS-II.

The membranes were resuspended at 8-12 mg chlorophyll/ml, put in calibrated quartz EPR tubes, dark-adapted, frozen in the dark and stored in liquid nitrogen until used for EPR measurements.

The samples were illuminated with continuous light from an 800 W projector passed through 2 cm water and an infrared filter, in a non-silvered Dewar flask containing ethanol cooled to 198 K with solid CO<sub>2</sub>.

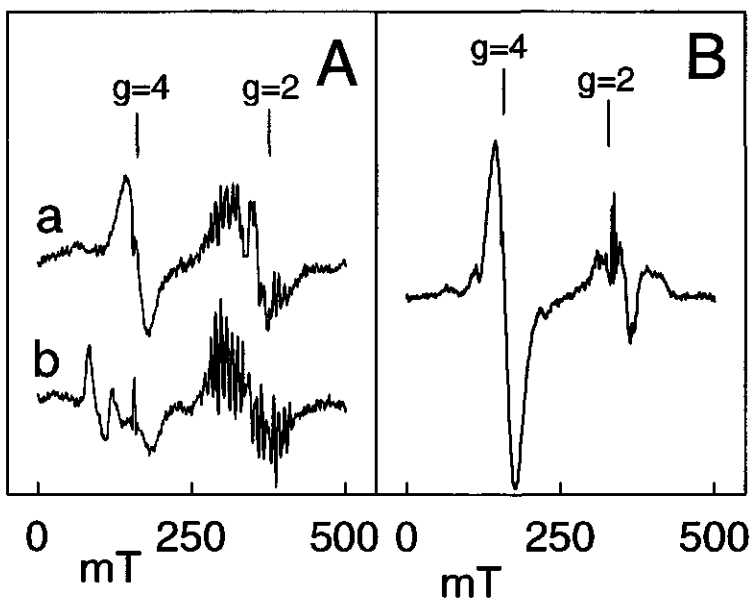
EPR spectra were recorded at liquid helium temperatures with a Bruker ER 200 or ER 300 X-band spectrometer equipped with an Oxford Instruments cryostat.

Measurements of oxygen evolution were done using a Clark-type electrode, at 25 °C under nearby saturating continuous light at a chlorophyll concentration of 20 µg/ml.

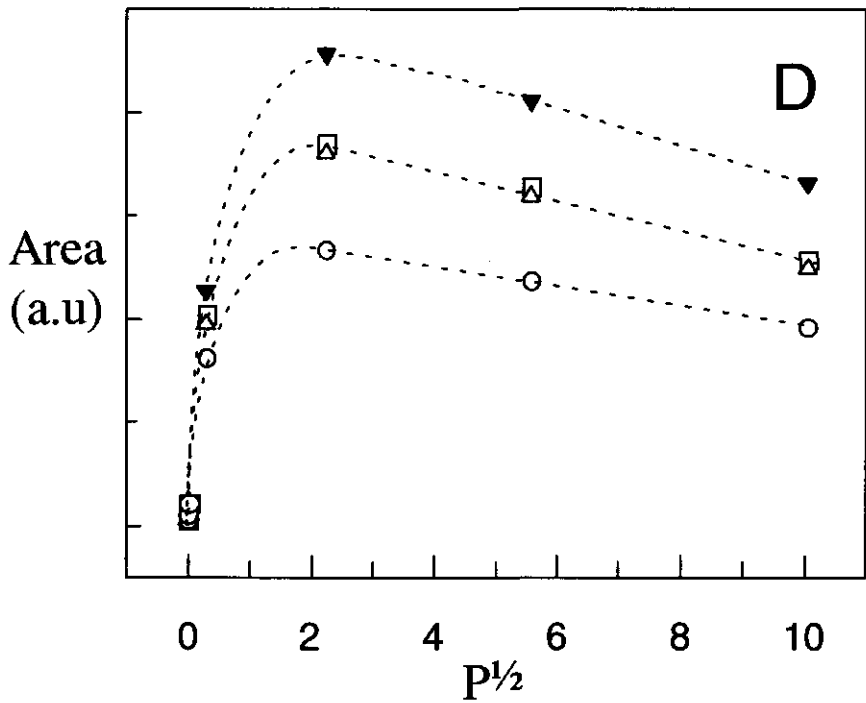
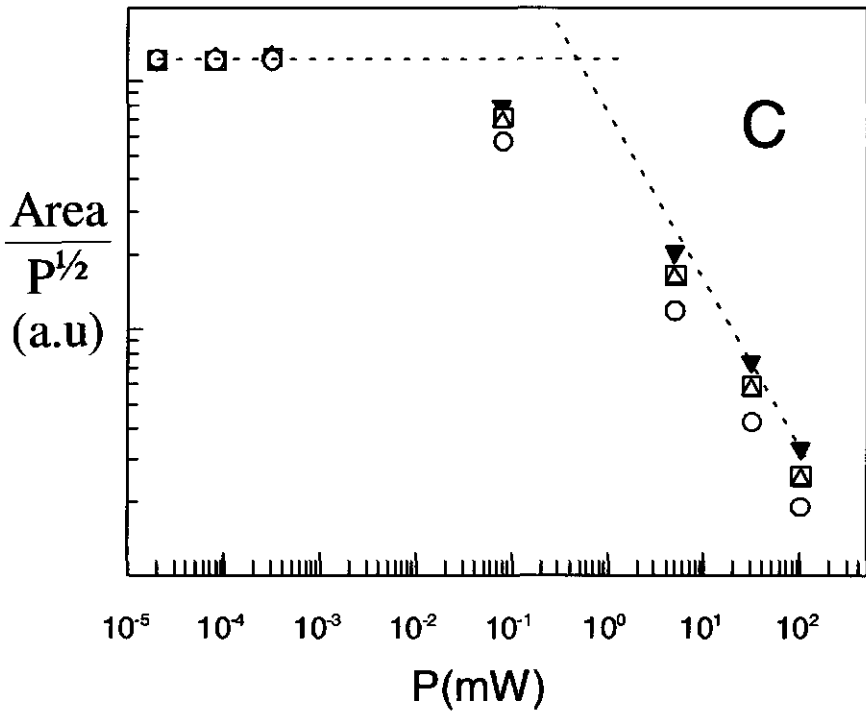
## Results

Figure 1A (a) shows that washes of PS-II membranes in Cl<sup>-</sup>-free buffer solutions (pH 6.3-6.5) which is generally done to minimize Cl<sup>-</sup> contamination during subsequent inhibitory Cl<sup>-</sup>-depletion treatments, affect the EPR properties of the S<sub>2</sub> state. The S<sub>2</sub> EPR spectrum in Cl<sup>-</sup>-free washed PS-II, generated by continuous illumination at 200 K, showed an enhanced S<sub>2</sub> g = 4 EPR signal at the expense of the S<sub>2</sub> multiline EPR signal as previously reported [17]. This altered distribution of structural states has been shown to originate from oxygen evolving centers in which the quantum yield of water oxidation is slightly diminished, and is considered to reflect the presence of a Cl<sup>-</sup>-site in PS-II which is not essential for oxygen evolution [17]. The multiline signal following the Cl<sup>-</sup>-free washes has been estimated to correspond to ~ 30 % of the centers whereas a broad signal underlying the S<sub>2</sub> multiline signal (e.g. Ref. 22), was apparently unaffected by the Cl<sup>-</sup>-free washes [17]. Rapid addition of Cl<sup>-</sup> (50 mM) in darkness to the S<sub>2</sub> state (in the presence of 1 mM PPBQ) (Figure 1A (a)), a method that has previously been used to investigate the S<sub>2</sub> state in Cl<sup>-</sup>-depleted PS-II [23,24], reversed the effects of Cl<sup>-</sup>-free washes (Figure 1A (b) and Ref. 17), resulting in the disappearance of the S<sub>2</sub> g = 4 signal and reconstitution of the S<sub>2</sub> multiline signal.

In dark-adapted (30 min. on ice), Cl<sup>-</sup>-free washed PS-II to which PPBQ (1 mM) had been added prior to illumination, a slowly relaxing Tyr<sub>D</sub>• was observed (Figure 1C, D; circles) showing a microwave power for half-saturation (P<sub>1/2</sub>) of 0.14 mW, similar to that seen in



**Figure 1.** EPR spectra of the  $S_2$  oxidation state in PS-II. (A) PS-II membranes Cl-free washed by two washes in 5 mM MES (pH 6.5) and 0.1 M sucrose followed by two washes and resuspension in 5 mM MES (pH 6.5). (a) Light-induced spectrum of Cl-free washed PS-II after 3 min. illumination at 200 K following 30 min. dark-adaptation on ice and subsequent addition of 1 mM PPBQ. (b) The sample from spectrum a was thawed and  $Cl^-$  (50 mM) was added rapidly (30 s) in darkness and refrozen. (B) EPR difference spectrum of pH 10/ $Cl^-$ -depleted PS-II after 4 min. illumination at 200 K and subtraction of the dark-baseline spectrum prior to pH 10/ $Cl^-$  depletion. the PS-II membranes were resuspended in 10 mM MES (pH 6.3) and 0.5 M sucrose followed by 1 h dark-adaptation on ice prior to illumination. (C, D) (see page on the right) Microwave power saturation of  $Tyr_D^\bullet$ . (O) The sample from A prior to and ( $\square$ ) after illumination at 200 K illumination resulting in spectrum a. ( $\blacktriangledown$ ) The sample from spectrum A (b). ( $\Delta$ ) The sample from spectrum B. To eliminate differences in the  $Tyr_D^\bullet$  signal intensities due to differences in the chlorophyll concentration between the samples from A and B, the data were normalized on the basis of the  $Tyr_D^\bullet$  signal intensities at unsaturating microwave powers. No significant changes of the  $Tyr_D^\bullet$  signal intensities at unsaturating microwave powers were observed in the sample from A after the  $Cl^-$  addition. The microwave power for half saturation ( $P_{1/2}$ ) was determined from the plots as in panel C by the intercept of the regression line through the points at non-saturating microwave powers and the regression line through the points at saturating microwave powers, as drawn for the closed triangles. Instrument settings: (A, B) 9.42 GHz; modulation amplitude, 2.2 mT; modulation frequency, 100 kHz; temperature, 10 K; microwave power, 31 mW. (C, D) 9.42 GHz; modulation amplitude, 0.22 mT; ; modulation frequency, 12.5 kHz; temperature, 15 K.





untreated PS-II under similar conditions (not shown, but see Ref. 7; Van Vliet et al., in preparation (Chapter 6)). Generation of the  $S_2$  EPR spectrum by continuous illumination at 200 K shown in Figure 1A (a), resulted in a relaxation enhancement of  $Tyr_D\cdot$  (Figure 1C, D; squares). This effect is qualitatively similar to that seen previously in untreated PS-II [7]. However, the rapid addition of  $Cl^-$  to the  $S_2$  state in  $Cl^-$ -free washed PS-II, resulting in the conversion of the  $g = 4$  signal to the multiline signal (Figure 1A (b)), was accompanied by a further relaxation enhancement of  $Tyr_D\cdot$  (Figure 1C, D; closed triangles). This resulted in microwave saturation properties  $Tyr_D\cdot$  ( $P_{1/2} = 0.44$  mW) similar to those of  $S_2Tyr_D\cdot$  in untreated PS-II (not shown, but see Ref. 7 and Van Vliet et al., in preparation (Chapter 6)). Similar microwave saturation properties of  $S_2Tyr_D\cdot$  were obtained when the  $S_2$  state was generated after addition of  $Cl^-$  (50 mM) to dark-adapted  $Cl^-$ -free washed PS-II (not shown).

The results indicate that  $Tyr_D\cdot$  in the  $S_2$  in  $Cl^-$ -free washed PS-II is relaxation enhanced but to a lesser extent than when  $Cl^-$  is present. This could reflect the observed decrease (to 30 %) of the  $S_2$  multiline signal intensity after  $Cl^-$ -free washes.

The influence on the relaxation of  $Tyr_D\cdot$  by the spin state of the Mn cluster giving rise to the  $S_2$   $g = 4$  EPR was investigated following short treatment (30 s) of  $Cl^-$ -free washed PS-II at pH 10. This treatment resulted in inhibition of oxygen evolution (to 15 %) which was largely reconstituted (to 90 % of that of  $Cl^-$ -reconstituted/ $Cl^-$ -free washed PS-II) by readdition of 10 mM  $Cl^-$ , indicating that  $Cl^-$  was removed from the  $Cl^-$ -site essential for oxygen evolution, in agreement with earlier work [17,20,21]. The  $S_2$  EPR spectrum of pH 10/ $Cl^-$ -depleted PS-II exhibited an intense  $S_2$   $g = 4$  EPR signal, whereas no  $S_2$  multiline signal could be generated (Figure 1B and see Ref. 17). The  $S_2$   $g = 4$  EPR signal has been estimated to correspond to 40-100 % of the centers [17].

Figures 1C and 1D (open triangles) show that in the presence of the  $S_2$   $g=4$  EPR signal in pH 10/ $Cl^-$ -depleted PS-II,  $Tyr_D\cdot$  was significantly faster relaxing ( $P_{1/2} = 0.23$  mW) than in the  $S_1$  state ( $P_{1/2} = 0.14$  mW, compare with Figures 1A (b) and 1C, D; circles).

## Discussion

The  $T_1$  of the slow-relaxing  $S_1\text{Tyr}_D\cdot$  in untreated PS-II was shown to be comparable to that of  $\text{Tyr}_D\cdot$  after Mn depletion in PS-II [25]. This was taken as an indication that the slow-relaxing  $S_1\text{Tyr}_D\cdot$  reflects the presence of a diamagnetic Mn cluster in the  $S_1$  state [25] (see also Refs. 7 and 8). Upon formation of the  $S_2$  multiline signal, a relaxation enhancement of  $\text{Tyr}_D\cdot$  was observed which is thought to arise from the magnetic interaction of  $\text{Tyr}_D\cdot$  with the  $S=1/2$  spin state of the Mn cluster [6-9]. It is shown in the present work that  $\text{Tyr}_D\cdot$  also is relaxation enhanced, albeit to a lesser extent, by the spin state of the Mn cluster in pH 10/Cl-depleted PS-II which gives rise to an intense  $S_2$   $g=4$  signal.

The relaxation enhancement of  $\text{Tyr}_D\cdot$  is thought to reflect a decreased spin-lattice relaxation time of  $\text{Tyr}_D\cdot$  originating from the dipolar interaction between  $\text{Tyr}_D\cdot$  and the Mn cluster [6-9,26], whereas no exchange interaction is thought to be involved since  $\text{Tyr}_D\cdot$  is thought to be relatively distant, i.e. at 30 Å [8,30] from the Mn cluster. In view of these considerations the spin-lattice relaxation time of  $\text{Tyr}_D\cdot$  ( $T_{1(D)}$ ) can be expressed as follows [26-29]:

$$\frac{1}{T_{1(D)}} = \frac{\gamma^2 \hbar^2 S(S+1) (A/6 + 3B + 3C/2)}{4\pi^2 r^6} \quad (1)$$

where,  $\hbar$  is the constant of Planck,  $\gamma$  is the gyromagnetic ratio,  $S$  is the spin state of the Mn cluster and  $r$  is the distance between the dipoles. The constants A-C are defined as follows:

$$A = \frac{T_{2(Mn)} (1 - 3\cos^2\theta)^2}{1 + \omega_{(D)}^2 (1 - g_{(Mn)}/g_{(D)})^2 T_{2(Mn)}^2} \quad (2)$$

$$B = \frac{T_{1(Mn)} \sin^2\theta \cos^2\theta}{1 + \omega_{(D)}^2 T_{1(Mn)}^2} \quad (3)$$

$$C = \frac{T_{2(Mn)} \sin^4\theta}{1 + \omega_{(D)}^2 (1 + g_{(Mn)}/g_{(D)})^2 T_{2(Mn)}^2} \quad (4)$$

Where  $\omega$  is the resonance frequency,  $g$  is the  $g$ -value of the given spin system,  $\theta$  is the angle between the magnetic field and the interspin vector,  $T_2$ , is the spin-spin relaxation time and the subscripts (D) and (Mn) refer to  $\text{Tyr}_D^\bullet$  and Mn cluster, respectively. Equation (1) is valid for  $T_{2(\text{Mn})} \ll T_{1(D)}$  which condition is fulfilled for our case (see e.g. [26]).

Under the conditions of the present study, term  $A$  in equation (1) is dominating. Thus,  $T_{1(D)}$  is essentially determined by  $T_{2(\text{Mn})}$ , the difference between the  $g$ -values of the two spin systems, the distance between the spin systems and the spin states.

Using the dipolar model described above and including (1) a magnetic field of 0.3 T, (2) a Mn cluster-to- $\text{Tyr}_D^\bullet$  distance of 30 Å [8,30] and (3) a  $T_1$ -value of the Mn cluster of 0.1  $\mu\text{s}$  [31],  $T_{1(D)}$  was calculated as a function of  $T_{2(\text{Mn})}$  with  $S = 1/2$  at  $g = 2$  for  $\text{Tyr}_D^\bullet$ . With respect to the spin state,  $S$ , of the Mn cluster in the  $S_2$  state, the following possibilities were considered. (a) an  $S = 1/2$  spin state contributing to  $g = 2$ , giving rise to the  $S_2$  multiline EPR signal. (b) an  $S = 3/2$  spin state giving rise to a contribution of spins to  $g=4$  and  $g = 2$  (see e.g. Ref. 15) and (c) an  $S = 5/2$  spin state from which all the spins contribute to  $g = 4$  (see e.g. Ref. 14).

For the slow-relaxing  $\text{Tyr}_D^\bullet$  in  $S_1$ , in which the Mn cluster is thought to be diamagnetic [25], a  $T_1$ -value of approximately 6 ms has been determined, using saturation-recovery experiments by pulsed EPR [25] (see also Ref. 8). When the Mn cluster exhibits an  $S_2$  multiline signal, the  $T_1$  of  $S_2\text{Tyr}_D^\bullet$  was predicted to be significantly smaller, as expected. At higher spin states ( $S > 1/2$ ) of the Mn cluster contributing to  $g = 2$ , the relaxation of  $\text{Tyr}_D^\bullet$  would be enhanced relative to that in the presence of an  $S = 1/2$  spin state of the Mn cluster.

Assuming that the spins contributing to the  $S_2$   $g=4$  signal would significantly enhance the relaxation of  $\text{Tyr}_D^\bullet$ , i.e.,  $T_{1(D)} \ll 6$  ms, a  $T_2$ -value of  $\ll 1$  ns for the Mn cluster was calculated. This value is unrealistic since at such small  $T_2$ -values no EPR signal from the Mn cluster would be detectable. It is therefore considered that the spins contributing to the  $S_2$  EPR signal at  $g = 4$  are magnetically decoupled from  $\text{Tyr}_D^\bullet$  due to the mismatch between the  $g$ -values of the two spin systems. Hence, no relaxation enhancement of  $\text{Tyr}_D^\bullet$  is expected in this case.

Nevertheless, Figure 1 shows that in the presence of the  $S_2$   $g=4$  EPR signal in pH 10/Cl<sup>-</sup>-depleted PS-II, Tyr<sub>D</sub><sup>•</sup> was significantly faster relaxing than in the slow-relaxing  $S_1$  state. These results suggest that the  $S_2$   $g = 4$  signal originates from an  $S = 3/2$  spin system which is expected to give rise to a contribution of spins around  $g = 2$  (see e.g. Ref. 15).

Philouze et al. [32] have pointed out that the spin state of the Mn cluster responsible for the  $S_2$   $g = 4$  signal reveals information on the spin coupling chain topology of the Mn cluster. These authors compared the structural and magnetic properties of the tetranuclear Mn compound  $[\text{Mn}^{\text{IV}}_4\text{O}_6(\text{bpy})_6]^{4+}$  with the proposed dimer-of-dimer configuration of the Mn cluster of PS-II [33]. On the basis of analysis of the possible exchange couplings between the individual Mn ions of the Mn cluster and the resulting spin states, Philouze et al. [32] concluded that an  $S = 3/2$  spin ground state being the origin of the  $S_2$   $g = 4$  signal implies that the two terminal Mn ions are magnetically coupled. This then would point to the presence of an efficient coupling group between the two terminal Mn ions.

### Acknowledgments

We thank Tjeerd J. Schaafsma for critically reading the manuscript and useful discussions. We also thank Yannis Deligiannakis for useful discussions.

### References

- 1 Kok, B., Forbush, B., & McGloin, M. (1970) *Photochem. Photobiol.* 11, 457-475.
- 2 Debus, R. J. (1992) *Biochim. Biophys. Acta* 1102, 269-352.
- 3 Rutherford, A. W., Zimmermann, J-L., & Boussac, A. (1992) in *The Photosystems: Structure, Function and Molecular Biology* (Barber, J., ed.) Chapter 5, pp 179-229, Elsevier Science Publishers, New York.
- 4 Dismukes, G. C., & Siderer, Y. (1981) *Proc. Natl. Acad. Sci. USA* 78, 274-278.
- 5 Britt, R. D., Lorigan, G. A., Sauer, K., Klein, M. P. & Zimmermann, J-L. (1992) *Biochim. Biophys. Acta* 1040, 95-101.
- 6 De Groot, A., Plijter, J. J., Evelo, R., Babcock, G. T. & Hoff, A. J. (1986) *Biochim. Biophys. Acta* 848, 8-15.
- 7 Styring, S., & Rutherford, A. W. (1988) *Biochemistry* 27, 4915-4923.
- 8 Evelo, R. G., Styring, S., Rutherford, A. W., & Hoff A. J. (1989) *Biochim. Biophys. Acta* 973, 428-442.
- 9 Kodera, Y., Takura, K., & Kawamori, A. (1992) *Biochim. Biophys. Acta* 1101, 23-32.
- 10 dePaula, J. C., Innes, J. B., & Brudvig, G. W. (1985) *Biochemistry* 24, 8114-8120.
- 11 Zimmermann, J-L., & Rutherford A. W. (1986) *Biochemistry* 25, 4609-4615.

- 12 Hansson, Ö., Aasa, R., & Vänngård., T. (1987) *Biophys. J.* 51, 825-832.
- 13 Kim, D. H., Britt, R. D., Klein, M. P., & Sauer, K. (1992) *Biochemistry* 31, 541-547.
- 14 Astashkin, A. V., Kodera, Y., & Kawamori, A. (1994) *J. Magn. Res. B* 105, 113-119.
- 15 Smith, P. J., Åhring, K. A. & Pace, R. J. (1993) *J. Chem. Soc. Faraday Trans. 89*, 2863-2868.
- 16 Smith, P. J., & Pace, R. J. (1995), *Biochim. Biophys. Acta* (in press).
- 17 Van Vliet, P., & Rutherford, A. W. (1995) *Biochemistry* (in press).
- 18 Berthold, D. A., Babcock, G. T., & Yocum, C. F. (1981) *FEBS Lett.* 134, 231-234.
- 19 Ford, R. C., & Evans, M. C. W. (1983) *FEBS* 160, 159-164.
- 20 Homann, P.H. (1985) *Biochim. Biophys. Acta* 809, 311-319.
- 21 Homann, P. H. (1993) *Photosynth. Res.* 38, 395-400.
- 22 Pace, R. J., Smith, P., Bramley, R., & Stehlik, D. (1991) *Biochim. Biophys. Acta* 1058, 161-170.
- 23 Ono, T., Zimmermann, J-L., Inoue, Y., & Rutherford, A.W. (1986) *Biochim. Biophys. Acta* 851, 193-201.
- 24 Boussac, A., & Rutherford, A. W. (1994) *J. Biol. Chem.* 269, 12462-12467.
- 25 Koulougliotis, D., Hirsh, D. J., & Brudvig, G. W., (1992) *J. Am. Chem. Soc.* 114, 8322-8323.
- 26 Hirsch D. J., Beck, W. F., Innes, J. B., & Brudvig, G. W. (1992) *Biochemistry* 31, 532-541.
- 27 Bloembergen, N. (1948) *Physica* 15, 386-426.
- 28 Abragam, A. (1961) *The principles of Nuclear Magnetism*, pp 295-319.
- 29 Goodman, G., & Leigh Jr., J. S. (1985) *Biochemistry* 24, 2310-2317.
- 30 Un, S., Brunel, L-C, Brill, T. M., Zimmermann, J-L., & Rutherford, A. W. (1994) *Proc. Natl. Acad. Sci.* 91, 5262-5266.
- 31 Lorigan, G. A., & Britt, R. D. (1994) *Biochemistry* 33, 12072-12076.
- 32 Philouze, C., Blondin, G., Girerd, J-J., Guilhem, J., Pascard, C., & Lexa, D. (1994) *J. Am. Chem. Soc.* 116, 8557-8565.
- 33 Sauer, K., Yachandra, V. K., Britt, R. D., & Klein, M. P. (1992) in *Manganese Redox Enzymes* (Pecoraro, V. L., ed.), pp 141-175, VCH, New York.

## Summary

This Thesis presents the results of a study by electron paramagnetic resonance (EPR) and measurements of oxygen evolution of the Oxygen Evolving Complex of Photosystem II (PS-II) in PS-II enriched membranes from spinach.

The experimental part of this Thesis is preceded by a general introduction (Chapter 1) and a brief overview and rationale of methods and techniques used (Chapter 2).

Chapter 3 describes an EPR study of PS-II after  $\text{Ca}^{2+}$  depletion and subsequent  $\text{Cl}^-$  depletion. The anions  $\text{Ca}^{2+}$  and  $\text{Cl}^-$  are essential for oxygen evolution. After  $\text{Ca}^{2+}$  depletion in PS-II in the presence the  $\text{Ca}^{2+}$  chelator ethylene glycol bis ( $\beta$ -aminoethyl ether)-N,N,N',N'-tetraacetic acid (EGTA), the  $\text{S}_2$  state exhibits a modified multiline signal which is stable in the dark. It is found that the modification of  $\text{S}_2$  is due to binding of EGTA to PS-II which occurs after removal of  $\text{Ca}^{2+}$ . The pH buffer 4-(N-morpholino)ethanesulphonic acid (MES) modified the  $\text{S}_2$  state in a similar fashion to EGTA as indicated by the EPR spectrum. EGTA and MES possibly bind with their anionic oxo-groups nearby or at the Mn cluster itself. It is also found that the EGTA binding-affinity is lowered by subsequent  $\text{Cl}^-$  depletion in EGTA-treated/ $\text{Ca}^{2+}$ -depleted PS-II. After  $\text{Cl}^-$  depletion in the presence of millimolar EGTA concentrations, the  $\text{S}_2$  state remains modified by bound EGTA. However, the  $\text{S}_2$  state is not detected by EPR due to an additional modification of  $\text{S}_2$  induced by  $\text{Cl}^-$  depletion. Addition of  $\text{Cl}^-$  in darkness reversed this  $\text{Cl}^-$ -depletion effect and resulted in the reconstitution of the EGTA-modified multiline EPR signal. Also the  $\text{S}_3$  state is reversibly modified after  $\text{Cl}^-$  depletion in  $\text{Ca}^{2+}$ -depleted PS-II, resulting in a narrowing of the  $\text{S}_3$  EPR signal. The  $\text{Cl}^-$ -dependent EPR properties of the  $\text{S}_2$  and  $\text{S}_3$  state in  $\text{Ca}^{2+}$ -depleted PS-II indicate that the  $\text{Cl}^-$  which is essential for oxygen evolution, remains functionally bound after  $\text{Ca}^{2+}$ -depletion. The observed effects of  $\text{Ca}^{2+}$  and  $\text{Cl}^-$  depletion in PS-II may be relevant to the proposed role(s) of  $\text{Ca}^{2+}$  and  $\text{Cl}^-$  in controlling substrate binding in the charge accumulation cycle.

Chapter 4 presents an EPR study of the charge accumulation properties after  $\text{Cl}^-$  depletion in PS-II whereas  $\text{Ca}^{2+}$  remains present in PS-II. The light-intensity dependence of oxygen evolution is measured to study enzyme kinetics. The results indicate the presence of two  $\text{Cl}^-$ -binding sites in PS-II. One of the sites is not essential for oxygen evolution and has not been previously reported in the literature. This site is depleted of  $\text{Cl}^-$  by washes of PS-II

membranes in Cl<sup>-</sup>-free buffer solutions at pH 6.3. This Cl<sup>-</sup>-depletion treatment results in a small decrease of the quantum yield of water oxidation and an increase of the S<sub>2</sub> g = 4 EPR signal intensity at the expense of the S<sub>2</sub> multiline EPR signal. The second site is essential for oxygen evolution and is equivalent to that studied in previous work on Cl<sup>-</sup>-depleted PS-II. This site is depleted of Cl<sup>-</sup> by short incubation of diluted Cl<sup>-</sup>-free washed PS-II membrane suspensions at pH 10. After this treatment no S<sub>2</sub> multiline signal can be generated and an intense S<sub>2</sub> g = 4 EPR signal is observed corresponding to 40-100 % of the centers. The S<sub>2</sub> g = 4 signal is relatively stable in the dark. This probably indicates a lowered oxidation potential of S<sub>2</sub>. These centers are unable to undergo further charge accumulation. A fraction of the centers, different from that corresponding to the S<sub>2</sub> g = 4 signal, does not exhibit an S<sub>2</sub> EPR signal and is able to advance to the S<sub>3</sub> state, giving rise to a narrow EPR signal around g = 2. The SO<sub>4</sub><sup>2-</sup> and F<sup>-</sup> anions, which have previously been used to facilitate Cl<sup>-</sup>-depletion, have specific effects in pH 10/Cl<sup>-</sup>-depleted PS-II and give rise to S<sub>2</sub> EPR properties that previously have been observed after Cl<sup>-</sup>-depletion treatments in the presence of these anions. Addition of F<sup>-</sup> to pH 10/Cl<sup>-</sup>-depleted PS-II results in reconstitution of oxygen evolution in ~ 45 % of the centers in which, however, the enzyme turnover is slowed down.

Chapter 5 presents an EPR study of I<sup>-</sup>-activated PS-II. The oxygen evolving activity of I<sup>-</sup>-activated PS-II is nearly similar to that after Cl<sup>-</sup> reconstitution. A fraction of I<sup>-</sup>-activated centers exhibits a characteristic S<sub>2</sub> g = 4 EPR signal. However, a second and significant fraction of active centers exhibits no S<sub>2</sub> EPR signal. The comparison with the effects of other anions described in Chapter 4 and in the literature, points to a correlation between the S<sub>2</sub> EPR properties and the size of the anion that occupies the Cl<sup>-</sup>-site essential for oxygen evolution. The effects of I<sup>-</sup> on the properties of S<sub>2</sub> presumably reflect subtle structural changes of the Mn cluster since the I<sup>-</sup>-induced modifications of S<sub>2</sub> are eliminated by addition of ethanol, resulting in the reconstitution of the normal S<sub>2</sub> multiline signal. However, no effects of ethanol are observed in pH 10/Cl<sup>-</sup>-depleted and F<sup>-</sup>-treated PS-II, both of which exhibit an intense g = 4 signal in the S<sub>2</sub> state (Chapter 4). This appears to indicate that the effects of ethanol on the S<sub>2</sub> EPR properties are modulated by the anion occupying the Cl<sup>-</sup> site essential for oxygen evolution. If the observed ethanol effects would originate from ethanol binding to PS-II the results may be relevant for the role of Cl<sup>-</sup> in the mechanism of water oxidation, and may indicate that Cl<sup>-</sup> modulates the substrate affinity.

In Chapter 6 the microwave power saturation of  $\text{Tyr}_D^\bullet$  in untreated PS-II is investigated to reveal information on the magnetic properties of the oxygen evolving complex in the different oxidation states. The  $S_1$  state is not detected by conventional EPR. Nevertheless, by using  $\text{Tyr}_D^\bullet$  as a magnetic probe, two magnetically distinct forms of  $S_1$  are detected which are interconvertible. After 30 min. dark-adaptation ( $0^\circ\text{C}$ ) a rapidly relaxing  $S_1\text{Tyr}_D^\bullet$  is observed which is converted to a slowly relaxing form upon 17 h dark-adaptation ( $0^\circ\text{C}$ ), in agreement with a pulsed EPR study in the literature. This conversion is accelerated by phenyl-p-benzoquinone (PPBQ) used as an electron acceptor. This effect of PPBQ is presumably induced by the reduced form of PPBQ ( $\text{PPBQH}_2$ ) since it is avoided by addition of relatively low concentrations of PPBQ to samples to which ferricyanide was added to maintain PPBQ in the oxidized form. It is shown that the slowly relaxing  $S_1$  state becomes rapidly relaxing on the first enzyme cycle. The event responsible for this conversion occurs on the  $S_3$  to  $S_0$  transition or on the  $S_0$  to  $S_1$  transition. It has been previously proposed that the rapidly and slowly relaxing forms of  $S_1$  correspond to a paramagnetic and diamagnetic  $S_1$  state, respectively, reflecting structurally different Mn clusters. However, in view of the results from this work, it may be considered that the Mn cluster in  $S_1$  is diamagnetic and that the rapidly relaxing  $\text{Tyr}_D^\bullet$  in  $S_1$  is due to a nearby paramagnetic species different from the Mn cluster.

Chapter 7 presents a microwave power saturation study of  $\text{Tyr}_D^\bullet$  in PS-II after Cl-depletion as described in Chapter 4. The spin state of the Mn cluster in Cl-depleted PS-II giving rise to an  $S_2$   $g=4$  signal, significantly enhances the microwave power saturation of  $\text{Tyr}_D^\bullet$ . However, on the basis of a mathematical model for the dipolar interaction between two spin systems, it is considered that the spins contributing to the  $S_2$   $g=4$  EPR signal are magnetically decoupled from  $\text{Tyr}_D^\bullet$ , due the mismatch between the  $g$ -values of the two spin systems. These results suggest that the  $S_2$   $g = 4$  signal originates from an  $S = 3/2$  spin state of the Mn cluster which also gives rise to a contribution of spins at  $g = 2$ .



## Samenvatting

Dit proefschrift presenteert de resultaten van een studie met behulp van elektron paramagnetische resonantie (EPR) en metingen van de zuurstofontwikkeling van het zuurstofontwikkeldend complex in fotosysteem II (PS-II) in PS-II rijke membranen van spinazie.

Het experimentele gedeelte van dit proefschrift (Hoofdstukken 3 t/m 7), wordt vooraf gegaan door een algemene inleiding (Hoofdstuk 1) en een kort overzicht en verklaring van de gebruikte methoden en technieken (Hoofdstuk 2).

Hoofdstuk 3 beschrijft een EPR studie van PS-II na  $\text{Ca}^{2+}$  extractie gevolgd door  $\text{Cl}^-$  extractie. De aanwezigheid van  $\text{Ca}^{2+}$  en  $\text{Cl}^-$  in PS-II is essentieel voor de zuurstofontwikkeling. Na  $\text{Ca}^{2+}$  extractie van PS-II in de aanwezigheid van de  $\text{Ca}^{2+}$  binder ethyleen glycol bis ( $\beta$ -aminoethyl ether)-N,N,N',N'-tetraacetaat (EGTA) is de  $\text{S}_2$  oxydatie toestand stabiel in het donker en vertoont een gemodificeerd multilijn EPR signaal. Er is gevonden dat de modificatie van  $\text{S}_2$  veroorzaakt wordt door binding van EGTA aan PS-II na verwijdering van  $\text{Ca}^{2+}$ . De pH buffer 4-(N-morfoline) ethylsulfonaat (MES) modificeert  $\text{S}_2$  op dezelfde wijze als EGTA zoals blijkt uit het EPR spectrum. EGTA en MES binden waarschijnlijk met de negatief geladen oxo-groepen dichtbij of aan het Mn cluster zelf. Ook is gevonden dat de EGTA bindingsaffiniteit vermindert door  $\text{Cl}^-$  extractie. Na  $\text{Cl}^-$  extractie in EGTA-behandelde/ $\text{Ca}^{2+}$ -deficiënte PS-II in de aanwezigheid van millimolaire EGTA concentraties, blijft  $\text{S}_2$  gemodificeerd door gebonden EGTA. De  $\text{S}_2$  toestand wordt echter niet met EPR gedetecteerd vanwege een extra modificatie van  $\text{S}_2$ , geïnduceerd door  $\text{Cl}^-$  extractie. Toevoeging van  $\text{Cl}^-$  in het donker heft dit  $\text{Cl}^-$ -extractie effect op en resulteert in de reconstitutie van het EGTA-gemodificeerde  $\text{S}_2$  multilijn EPR signaal. Ook de  $\text{S}_3$  toestand is reversibel gemodificeerd na  $\text{Cl}^-$  extractie in  $\text{Ca}^{2+}$ -deficiënte PS-II, resulterend in een smaller  $\text{S}_3$  EPR signaal. De  $\text{Cl}^-$ -afhankelijke EPR eigenschappen van  $\text{S}_2$  en  $\text{S}_3$  in  $\text{Ca}^{2+}$ -deficiënte PS-II duiden erop dat het  $\text{Cl}^-$  ion essentieel voor de zuurstofontwikkeling, gebonden blijft na  $\text{Ca}^{2+}$  extractie. De waargenomen  $\text{Ca}^{2+}$ - en  $\text{Cl}^-$ -extractie effecten kunnen relevant zijn voor de mogelijke rol van  $\text{Ca}^{2+}$  en  $\text{Cl}^-$  in de regulering van substraat binding in de ladings-accumulerende cyclus.

Hoofdstuk 4 rapporteert de resultaten van een EPR studie van de ladings-accumulerende cyclus na  $\text{Cl}^-$  extractie van PS-II in aanwezigheid van  $\text{Ca}^{2+}$  in PS-II. De lichtintensiteit-afhankelijke zuurstofontwikkeling is gemeten ter bestudering van de enzym kinetiek. De resultaten duiden op de aanwezigheid van twee  $\text{Cl}^-$ -bindingsplaatsen. Eén van deze bindingsplaatsen is niet essentieel voor zuurstofontwikkeling en is tot nu toe niet gerapporteerd in de literatuur.  $\text{Cl}^-$  wordt verwijderd van deze bindingsplaats door PS-II membranen te wassen in  $\text{Cl}^-$ -vrije buffer oplossingen bij pH 6.3. Dit resulteert in een kleine vermindering van de quantum opbrengst van water oxydatie en een toename van de  $S_2$   $g = 4$  EPR signaal intensiteit ten koste van het  $S_2$  multilijn signaal. De tweede  $\text{Cl}^-$ -bindingsplaats is essentieel voor zuurstofontwikkeling en is equivalent met die gerapporteerd in eerder werk.  $\text{Cl}^-$  wordt verwijderd van deze bindingsplaats door verdunde,  $\text{Cl}^-$ -vrije PS-II membraan suspensies kort te incuberen bij pH 10. Na deze  $\text{Cl}^-$ -extractie kan geen  $S_2$  multilijn EPR signaal worden gegenereerd en wordt een intens  $S_2$   $g = 4$  EPR signaal waargenomen dat overeenkomt met 40-100 % van de centra. Het  $S_2$   $g = 4$  EPR signaal is relatief stabiel in het donker. Dit duidt waarschijnlijk op een verlaagde oxydatie potentiaal van de  $S_2$  toestand. Deze centra kunnen geen verdere oxydatie overgangen ondergaan. Een fractie van de centra, verschillend van de fractie die overeenkomt met het  $S_2$   $g = 4$  signaal, vertoont geen  $S_2$  EPR signaal en kan overgaan naar de  $S_3$  toestand resulterend in een smal EPR signaal bij  $g = 2$ . De  $\text{SO}_4^{2-}$  and  $\text{F}^-$  anionen, die vaak worden gebruikt om  $\text{Cl}^-$ -extractie te vergemakkelijken, hebben specifieke effecten in pH 10/ $\text{Cl}^-$ -geëxtraheerde PS-II, resulterend in EPR eigenschappen van  $S_2$ , vergelijkbaar met die eerder waargenomen na  $\text{Cl}^-$ -extractie methoden in PS-II in de aanwezigheid van deze anionen. Tevens resulteert het toevoegen van  $\text{F}^-$  aan pH 10/ $\text{Cl}^-$ -geëxtraheerde PS-II in reactivering van de zuurstofontwikkeling in ~ 45 % van de centra. De enzym cyclus is daarin echter trager.

Hoofdstuk 5 presenteert een EPR studie van I-geactiveerde PS-II. De zuurstofontwikkeling van I-geactiveerde PS-II is vrijwel gelijk aan die na activering met  $\text{Cl}^-$ . Een fractie van de I-geactiveerde centra vertoont een karakteristiek  $S_2$   $g = 4$  EPR signaal. Een tweede en significante fractie van de actieve centra vertoont echter geen  $S_2$  EPR signaal. De vergelijking met de effecten van andere ionen beschreven in Hoofdstuk 4 en in de literatuur duidt op een correlatie tussen de  $S_2$  EPR eigenschappen en het volume van het anion dat de  $\text{Cl}^-$ -bindingsplaats, essentieel voor de zuurstofontwikkeling, bezet. De effecten

van I<sup>-</sup> op de S<sub>2</sub> EPR eigenschappen weerspiegelen waarschijnlijk subtiële structurele veranderingen van het Mn cluster aangezien de I<sup>-</sup>-geïnduceerde modificaties van S<sub>2</sub> teniet worden gedaan door toevoeging van ethanol, resulterend in de reconstitutie van het normale S<sub>2</sub> multilijn EPR signaal. Er worden echter geen effecten van ethanol waargenomen in pH 10/Cl<sup>-</sup>-geëxtraheerde PS-II en F<sup>-</sup>-behandelde PS-II die beide een intens S<sub>2</sub> g = 4 EPR signaal vertonen (Hoofdstuk 4). Dit duidt erop dat de effecten van ethanol op de S<sub>2</sub> EPR eigenschappen, gemoduleerd worden door het anion dat de Cl<sup>-</sup>-bindingsplaats, essentieel voor de zuurstofontwikkeling, bezet. Wanneer de waargenomen effecten van ethanol het gevolg zouden zijn van ethanol-binding aan PS-II, zouden de resultaten relevant kunnen zijn voor de rol van Cl<sup>-</sup> in het mechanisme van water oxydatie en erop kunnen duiden dat Cl<sup>-</sup> de substraat affiniteit beïnvloedt.

In Hoofdstuk 6 is in onbehandelde PS-II de microgolfermogen-afhankelijke verzadiging van het Tyr<sub>D</sub>• EPR signaal bestudeerd om informatie te krijgen over de magnetische eigenschappen van het zuurstofontwikkeld complex in de verschillende oxydatie toestanden. De S<sub>1</sub> toestand wordt niet gedetecteerd met conventionele EPR. Niettemin, gebruik makend van Tyr<sub>D</sub>• als een magnetische probe, zijn twee magnetisch verschillende vormen van S<sub>1</sub> waargenomen die in elkaar kunnen overgaan. Na 30 min. donker-adapteren (0 °C) is een snel-relaxerend S<sub>1</sub>Tyr<sub>D</sub>• radicaal waargenomen dat in een langzaam-relaxerende vorm overgaat na 17 h donker-adapteren (0 °C), in overeenstemming met een puls-EPR studie in de literatuur. De elektron acceptor fenyl-p-benzochinon (PPBQ) versnelt deze overgang. Dit effect wordt waarschijnlijk geïnduceerd door de gereduceerde vorm van PPBQ aangezien het kan worden vermeden door lage PPBQ concentraties toe te voegen aan samples waaraan ferricyanide is toegevoegd om PPBQ in de geoxydeerde vorm te houden. Er is aangetoond dat de langzaam-relaxerende S<sub>1</sub> toestand overgaat in de snel-relaxerende vorm in de eerste enzym cyclus. Het proces verantwoordelijk voor deze conversie vindt plaats in de S<sub>3</sub> naar S<sub>0</sub> overgang of in de S<sub>0</sub> naar S<sub>1</sub> overgang. Eerder is in de literatuur verondersteld dat de snel- en langzaam-relaxerende vormen van S<sub>1</sub> zouden overeen komen met respectievelijk een paramagnetische en een diamagnetische S<sub>1</sub> toestand welke structureel verschillende Mn clusters weerspiegelen. Echter, de resultaten van deze studie zouden erop kunnen wijzen dat het Mn cluster in S<sub>1</sub> diamagnetisch is en dat de snel-relaxerende Tyr<sub>D</sub>• in

$S_1$  veroorzaakt wordt door een naburige paramagnetische component, verschillend van het Mn cluster.

Hoofdstuk 7 presenteert een studie van de microgolfvermogen-afhankelijke verzadiging van het Tyr<sub>D</sub>• radicaal in PS-II na Cl<sup>-</sup> extractie zoals beschreven in Hoofdstuk 4. De spin toestand van het Mn cluster verantwoordelijk voor het  $S_2$   $g = 4$  EPR signaal, versnelt aanzienlijk de relaxatie van Tyr<sub>D</sub>•. Echter op basis van een mathematisch model voor de dipolaire interactie tussen twee spin systemen wordt verondersteld dat de spins, die bijdragen aan het  $S_2$   $g = 4$  EPR signaal, magnetisch ontkoppeld zijn van Tyr<sub>D</sub>• vanwege het verschil tussen de  $g$ -waarden van de twee spin systemen. De resultaten suggereren dat het  $S_2$   $g = 4$  EPR signaal afkomstig is van een  $S = 3/2$  spin toestand van het Mn cluster die tevens aanleiding geeft tot een bijdrage van spins bij  $g = 2$ .

## **Curriculum Vitae**

Pieter van Vliet is geboren op 7 juli 1965 te Monster. In 1985 deed hij eindexamen V.W.O. op de Rijksscholengemeenschap te Brielle. Hij studeerde moleculaire wetenschappen aan de Landbouw Universiteit te Wageningen van 1985 tot 1991. Zijn afstudeervakken waren Fysische Plantenfysiologie en Moleculaire Fysica en de praktijktijd bracht hij voor de vakgroep Moleculaire Fysica door in de Section de Bioénergétique, Département de Biologie Cellulaire et Moléculaire, CEA Saclay in Frankrijk.

Na zijn studie vervulde hij de vervangende dienst op het instituut voor Agrotechnologisch Onderzoek (ATO) te Wageningen. Het promotie-onderzoek vond plaats in de Section de Bioénergétique, Département de Biologie Cellulaire et Moléculaire, CEA Saclay in Frankrijk, in de periode 1992-1995.

Momenteel is hij post-doc in de Department of Life Sciences, King's College, te Londen.